NOTICE

The quality of this microform is heavily dependent upon the quality of the original thesis submitted for microfilming. Every effort has been made to ensure the highest quality of reproduction possible.

If pages are missing, contact the university which granted the degree.

Some pages may have indistinct print especially if the original pages were typed with a poor typewriter ribbon or if the university sent us an inferior photocopy.

Previously copyrighted materials (journal articles, published tests, etc.) are not filmed.

Reproduction in full or in part of this microform is governed by the Canadian Copyright Act, R.S.C. 1970, c. C-30.

AVIS

La qualité de cette microforme dépend grandement de la qualité de la thèse soumise au microfilmage. Nous avons tout fait pour assurer une qualité supérieure de reproduction.

S'il manque des pages, veuillez communiquer avec l'université qui a conféré le grade.

La qualité d'impression de certaines pages peut laisser à désirer, surtout si les pages originales ont été dactylographiées à l'aide d'un ruban usé ou si l'université nous a fait parvenir une photocopie de qualité inférieure.

Les documents qui font déjà l'objet d'un droit d'auteur (articles de revue, tests publiés, etc.) ne sont pas microfilmés.

La reproduction, même partielle, de cette microforme est soumise à la Loi canadienne sur le droit d'auteur, SRC 1970, c. C-30.

BEHAVIOR OF REINFORCED CONCRETE COLUMNS CONFINED WITH WELDED WIRE FABRIC

by

Salim R. Razvi

A thesis
Submitted under the supervision of
Dr. M. Saatcioglu
in partial fulfillment
of the requirements for the degree of
Master of Applied sciences

Department of Civil Engineering
Faculty of Engineering
University of Ottawa
January 7, 1988

ISBN 0-315-46843-2

Abstract

Concrete when subjected to lateral pressure exhibits increase in strength and ductility. In case of reinforced concrete columns, lateral pressure can be provided by transverse reinforcement. At a high axial strain level, transverse strain in concrete increases due to progressive internal cracking. In the presence of lateral reinforcement, the expansion tendency of concrete is resisted by restraining pressure applied by the reinforcement. This limits further internal cracking in the concrete and improves its ability to sustain higher stresses and strains. The main variables affecting the shape of the stress–strain relationship for confined concrete are: lateral pressure applied by steel, spacing of ties, longitudinal steel distribution, concrete strength and rate of loading.

In this investigation, thirty four small scale columns were tested under monotonic axial compression. The objective of the research program was to study concrete confinement by a cage which consisted of hoops and/or closely spaced reinforcement in both longitudinal and transverse directions in the form of Welded Wire Fabric. The main variables studied in this program were: tie spacing and amount of lateral reinforcement, tie hooks, location and size of WWF in the reinforcement cage, and possibility of using WWF as lateral reinforcement without the ties.

The test data were evaluated. The axial load axial strain relationships for columns, and core concrete were studied. Significant improvement in

strength and ductility was observed when WWF was used along with ties with 135 degree hooks or ties with 90 degree hooks welded at the ends. An analytical procedure was developed to determine stress-strain relationship of concrete confined with Welded Wire Fabriç. Comparisons between the experimental and analytical behaviors were found to be good.

Acknowledgements

The author wishes to express his sincere appreciation to Dr. M. Saatcioglu for his guidance, advice and financial support throughout this research project.

I also wish to thank Mr. Z. Wasiewicz, Mr. C. Pilette and Mr. H. Hachem for their help during the experimental part of this project. Thanks are also due to the technical staff of Civil Engineering Department for their assistance.

Contents

List of Figures

List of Tables

Notations

A_b	=	area of bound concrete under compression.
A_c	=	area of concrete under compression.
A_{co}	=	area of the core bounded by the centerline of the outer tie.
A_g	=	gross area of column cross section.
A_{gage}	=	cross sectional area of a wire in WWF.
A_s	=	area of longitudinal steel.
A_s'	=	area of longitudinal wires in WWF
A_s''	=	area of tie steel.
A_{sh}	=	total cross sectional area of ties including cross ties.
a_s	=	cross sectional area of spiral or hoop.
B	=	width of concrete core.
b''	=	width of confined core measured to outside of hoops.
C	=	center to center distance between longitudinal bars.
c	=	center to center distance between longitudinal wires in WWF.
d	=	diameter of core concrete.
d_e	=	equivalent diameter.
E_c	=	modulus of elasticity of plain concrete.
f, f_c	=	concrete stress.
f_{cc}	=	strength of confined concrete.
f_{cp}, f_p	=	strength of concrete in plain specimen.
f_c'	=	ultimate strength of plain concrete obtained from standard cylinder test.

f''	=	yield strength of WWF.
f_r	=	confinement index.
f'_s	=	useful stress in lateral steel.
f_y	=	yield strength of longitudinal steel.
f_{yh}, f'_y	=	yield strength of lateral tie.
f_{ywwf}	=	yield strength of WWF.
f_0	=	peak stress of concrete.
F_4	=	stress in steel corresponding to 4% strain.
H	=	short side dimension of the core.
K	=	ratio of strength of confined concrete to the strength of plain concrete.
kd	=	depth of neutral axis from extreme compression fiber.
$(kd)_0$	=	depth of neutral axis in Sargin's tests (125 mm).
K_s	=	ratio of strength of confined concrete to the strength of plain concrete in the specimens of similar size and shape.
K_{3c}	=	ratio of maximum stress in the confined core concrete to cylinder stress.
K_{3o}	=	ratio of maximum stress in the plain concrete to cylinder stress.
L	=	total length of ties at tie level
m	=	number of regression coefficient.
N	=	number of data points.
n	=	number of spacing between longitudinal bars.
p''	=	ratio of volume of hoops to volume of concrete core measured to outside of hoops.
P_{add}	=	extra load carrying capacity of the concrete due to confinement.
P_{cmax}	=	maximum load carried by concrete.
P_{col}	=	total load carried by column.

P_{conc} = load carried by concrete.

P_o = theoretical capacity of column.

P_{oc} = theoritical capacity of column concrete.

P_{occ} = theoritical capacity of core concrete.

P_{st} = load carried by longitudinal steel.

P_{test} = maximum load carried by column as observed in test.

P_{oc} = theoritical capacity of column concrete.

q'' = parameter reflects the effectiveness of transverse reinforcement in concrete confinement.

s = tie spacing.

s_o = longitudinal spacing at which lateral reinforcement is not effective in confining the concrete.

WWF = welded wire fabric.

ϵ, ϵ_c = average longitudinal strain in concrete.

ϵ_{ce}, ϵ_{s1}, ϵ_1 = minimum average longitudinal strain corresponding to the maximum stress in concrete.

ϵ_{cf} = longitudinal strain of confined concrete corresponding to 0.8 of peak stress on the falling branch of the curve.

ϵ_{cs}, ϵ_{s2}, ϵ_2 = maximum average longitudinal strain corresponding to the maximum stress in concrete.

ϵ_{co} = average longitudinal strain in column corresponding to maximum load carried by the column.

ϵ_{c85} = average longitudinal strain in column corresponding to 0.85 of maximum load carried by the column on the falling branch of load-strain curve.

ϵ_o, ϵ_{oo}	=	strain corresponding to maximum stress in plain concrete.
ϵ_{oc}	=	strain corresponding to maximum stress in confined concrete.
ϵ_p	=	strain corresponding to peak stress in concrete.
ϵ_s	=	strain in longitudinal steel.
ϵ_{s85}, ϵ_{85}	=	average longitudinal strain of confined concrete corresponding to 0.85 of peak stress on the falling branch of the curve.
ϵ_{20c}	=	longitudinal strain of confined concrete corresponding to 0.20 of peak stress on the falling branch of the curve.
ϵ_{50u}	=	longitudinal strain of unconfined concrete corresponding to 0.50 of peak stress on the falling branch of the curve.
ϵ_{50c}, ϵ_{50}	=	longitudinal strain of confined concrete corresponding to 0.50 of peak stress on the falling branch of the curve.
ϵ_{50h}	=	$\epsilon_{50c} - \epsilon_{50u}$
δ P	=	drop in load carried by column between ϵ_{co} and $(\epsilon_{co} + 2\%)$.
λ	=	ratio of area of effectively confined concrete to the core area at tie level.
λ^*	=	ratio of area of effectively confined concrete to the core area at critical section midway between the ties.
σ_e	=	standard error.
ρ_{core}	=	ratio of area of longitudinal steel to core area of column.
ρ_{gross}	=	ratio of area of longitudinal steel to gross area of column.
ρ_s	=	ratio of volume of tie steel to volume of concrete core measured center to center of outer tie.
ρ_s'	=	ratio of volume of lateral wires in WWF to volume of concrete core.

Chapter 1

Introduction

1.1 General

During the last decade, structural engineers have been paying more attention to the behavior of structures subjected to earthquake excitation. A natural outgrowth of the life threatening and property damaging earthquakes is to conduct further research to establish safe and reliable design techniques for structures situated in seismically active regions.

The importance of ductility and associated energy absorption capacity of a structure in resisting earthquakes has long been recognized. The need for ductility was emphasized in recent years in light of the damages sustained by ductile buildings subjected to severe earthquakes. The previous research has shown that the required ductility can be attained relatively easily if the member behaves essentially in the flexure mode. Therefore, in earthquake resistant frame structures, the moment capacity of columns at a joint are made higher than the adjoining beams. The rationale behind this restriction is to ensure that plastic hinges, which absorb earthquake induced energy, occur in the flexure dominant beams rather than the axially compressed columns. However, this restriction may not be sufficient to prevent column hinging. Recent earthquakes showed that hinging of columns might take place even if they were designed following the strong column weak beam concept [12]. Moreover, it is difficult to prevent column hinging at the base of a multistory structure.

Compression failure in reinforced concrete members is a brittle failure. It is evident that special design and detailing techniques must be employed to improve ductility of a column, which is a compression member. Previous research has demonstrated that confinement of column concrete improves ductility very significantly.

1.2 Research Needs

In order to have columns capable of behaving in a ductile manner, it is essential to understand the behavior of concrete in columns at high compressive strain levels, higher than that corresponding to peak compressive strength. It has been well established that the strength and ductility of concrete increase when subjected to lateral pressure [11]. The lateral pressure in the case of reinforced concrete columns can be provided by lateral reinforcement. Concrete under high axial compression develops transverse strains due to progressive internal cracking. In the presence of lateral reinforcement it starts applying pressure on the steel which in turn applies reactive pressure on the concrete [11]. This limits further internal cracking in the concrete and improves its ability to sustain higher stresses and strains.

The main factors affecting concrete confined by reinforcement, as concluded by various researchers, are as follows:

1. Confining pressure applied by lateral reinforcement. This pressure is a function of two parameters:
   - The ratio of volume of lateral steel to the volume of core concrete.
   - The yield strength of lateral reinforcement.
2. Spacing of transverse reinforcement.
3. Distribution of longitudinal steel.
4. Tie configuration.
5. Concrete strength.
6. Rate of loading.
7. Amount of longitudinal reinforcement.

Researchers recently showed that both longitudinal and transverse reinforcement are effective in confining concrete if they are designed to satisfy specific requirements[2]. Therefore it is reasonable to assume that concrete confinement will be increased if the concrete is placed in a cage which consists of closely spaced reinforcement in both longitudinal and transverse directions. Welded Wire Fabric (WWF) appears to satisfy this requirement. However, no attempt has been made in the past to investigate the effect of Welded Wire Fabric on concrete confinement.

Welded Wire Fabric has the following favorable features for concrete confinement :

1. Spacing is small between transverse reinforcement. Researchers found that reduction in spacing between transverse reinforcements results in higher strength and ductility, even if the same amount of transverse steel is used.
2. Welded Wire Fabric provides longitudinal reinforcement which is effective in concrete confinement.
3. The longitudinal reinforcement is well distributed around the core perimeter.
4. The unsupported length of longitudinal reinforcement is small.

There is a clear need for research in this area.

1.3 Objective and Scope

The objective of the research program reported here is to study the effect of Welded Wire Fabric reinforcement on the behavior of square reinforced concrete columns. The objective includes establishment of a relationship between Welded Wire Fabric and concrete confinement.

The scope consists of experimental and analytical investigations of column response. The experimental program includes testing of thirty four small scale square columns (160 x 160 x 460 mm). Columns were tested under monotonic axial compression. Testing was performed in the concrete laboratory of the University of Ottawa.

To study the effectiveness of Welded Wire Fabric on concrete confinement, the following cases were considered in this program :

1. WWF placed between longitudinal steel and welded ties with 90° hooks.
2. WWF placed inside longitudinal steel and welded ties with 90° hooks.
3. WWF placed inside longitudinal steel and ties with 135° hooks.
4. WWF placed between longitudinal steel and ties with 90° hooks.
5. WWF and longitudinal steel without any ties. Three types of Welded Wire Fabric connections were considered:

- Welded at overlaps.
- Mechanically connected.
- Connected with wires.

6. Columns with different size welded wire fabric.

To quantify the findings of the aforementioned cases the following key variables were used:

- Concrete strength.
- Amount of longitudinal steel.
- Tie spacing
- Tie hooks (135° versus 90°)

The analytical program includes evaluation of test data and establishment of concrete stress strain relationship for columns confined by WWF.

1.4 Previous Research

A number of experimental and analytical research has been conducted in the past to investigate confinement of concrete by rectilinear ties. A comprehensive bibliography of this work has been compiled by Sheikh [1] in 1978.

Most of the previous researchers tested small scale specimens with four corner longitudinal bars and simple tie configurations. The researchers prior to 1975 ignored the effect of longitudinal steel distribution around the core perimeter and the resulting tie configuration [1]. The main variables considered in these tests were :

- Ratio of lateral steel volume to the volume of concrete core.
- Lateral steel spacing.
- Size of lateral reinforcement.

Other variables, considered in some of the previous investigations include:

- Concrete strength and type.
- Cross section shape and dimensions.
- Characteristics of lateral steel (yield strength and heat treatment).
- Rate of loading.
- Response to eccentric loading.
- Response to cyclic loading.

Work done with reference to the above mentioned variables can be found elsewhere [2,3,5,8,9,10].

Following are the main conclusions drawn from the tests conducted until 1977, that has relevance to the current project:

1. Stiffness of concrete does not change as a result of the use of rectangular lateral ties.

2. The effect of ties on concrete core strength seems to be controversial issue among many researchers. The reason for the disagreement might be due to the fact that in most of these tests, the ratio of concrete core area to the gross area of the specimen was small. After spalling of concrete cover the capacity of the confined core would not exceed the capacity of unconfined specimen based on gross concrete area [7].

3. Ductility increases significantly by reducing tie spacing and increasing amount of lateral reinforcement.

4. The behavior of large scale columns is different than equivalent small scale columns.

5. Longitudinal steel improves the efficiency of confinement provided by lateral steel.

The analytical models, proposed by different researchers, were based on specific test results [1], and limited in their scope of application. A comprehensive discussion of various models have been made by Sheikh[6] in 1982.

The effect of longitudinal column reinforcement on concrete confinement was discussed by Paulay [11] in 1975 and Vallenas, Bertero and Popov [16] in 1977. However, it was not until 1978 when Sheikh and Uzumeri demonstrated the substantial improvement achieved in column strength and ductility by distributing the longitudinal steel around the core perimeter and providing a support for each bar by means of cross ties and/ or hoops [2]. At the University of Toronto, Sheikh and Uzumeri tested twenty four columns with 305 x 305 x 2000 mm dimensions under monotonic axial compression [1,2]. Column reinforcement included four different tie configurations and eight to sixteen longitudinal bars. The following main variables were considered in their tests :

- Distribution and amount of longitudinal steel around the core perimeter.
- Volumetric ratio, spacing and characteristics of lateral steel.

The following conclusions were made based on the test program [2] :

- The strength of concrete increased up to 70% when confined with rectangular ties and well distributed longitudinal steel. Significant improvement in ductility was observed.
- Well distributed longitudinal steel and resulting tie configurations increased both strength and ductility. Enhancement of strength and

ductility was observed when tie spacing was reduced, even if the same volumetric ratio was used.

- Strength and ductility were improved by increasing the amount of lateral steel. The incremental improvement was less than the incremental increase in lateral steel content.

- The amount of longitudinal steel, within the range of 1.7% to 3.7%, had small effect on concrete confinement.

In 1982, B. D. Scott, R. Park and M. Priestley, tested twenty five columns having 450 x 450 x 1200 mm dimensions, at the University of Canterbury in New Zealand [3]. Each column contained either eight or twelve longitudinal steel bars. The tests were conducted under high and low strain rates. Among the variables considered, the effect of longitudinal steel distribution on enhancement of concrete strength and ductility, was also examined. The following conclusions were reported:

- Properly confined concrete showed significant improvement in compressive strength.

- Increasing number of longitudinal reinforcing bars, while maintaining a constant longitudinal reinforcement area, showed improved confinement. This was manifested by reducing the longitudinal bars spacing.

- Increasing the amount of lateral reinforcement increased the peak stress for concrete core and decreased the slope of the falling branch of the stress–strain relationship for concrete core. Increasing spacing of lateral reinforcement resulted in reduction of confinement efficiency for the same amount of lateral reinforcement.

In 1985, Fafitis and Shah developed simple equations to predict the stress–strain relationship of confined concrete [5]. Although they recognized the importance of tie spacing, distribution of longitudinal steel and the resulting tie configuration was not included in their equation.

In 1987, Ozcebe and Saatcioglu reported results of column tests conducted under constant axial load and lateral load reversals [4]. One of the variables studied was the effectiveness of longitudinal reinforcement in confining the core concrete under bending moment reversals. They concluded that longitudinal bars could improve the confinement efficiency under inelastic load cycles only if they were properly supported by lateral reinforcement.

It can be concluded from the results of previous research, that both longitudinal and lateral reinforcement are effective in confining the core concrete. Reduction in longitudinal and lateral reinforcement spacings increases concrete confinement, due to the increase in the area of effectively confined concrete core. In the light of this conclusion WWF was used in this research program as confinement reinforcement.

Chapter 2

Experimental program

2.1 General

The experimental program was designed to investigate the effectiveness of Welded Wire Fabric in confining reinforced concrete columns. It included testing of thirty four small scale square columns, under monotonic axial compression. Although the tests were made under monotonic axial compression, the results could be useful to predict the behavior of the same columns under cyclic loading. Researchers showed that the envelop curve of the axial load versus strain under cyclic loading is almost the same as that obtained from monotonic compression[17].

Details of the test specimens, test set up, instrumentation and test proce-

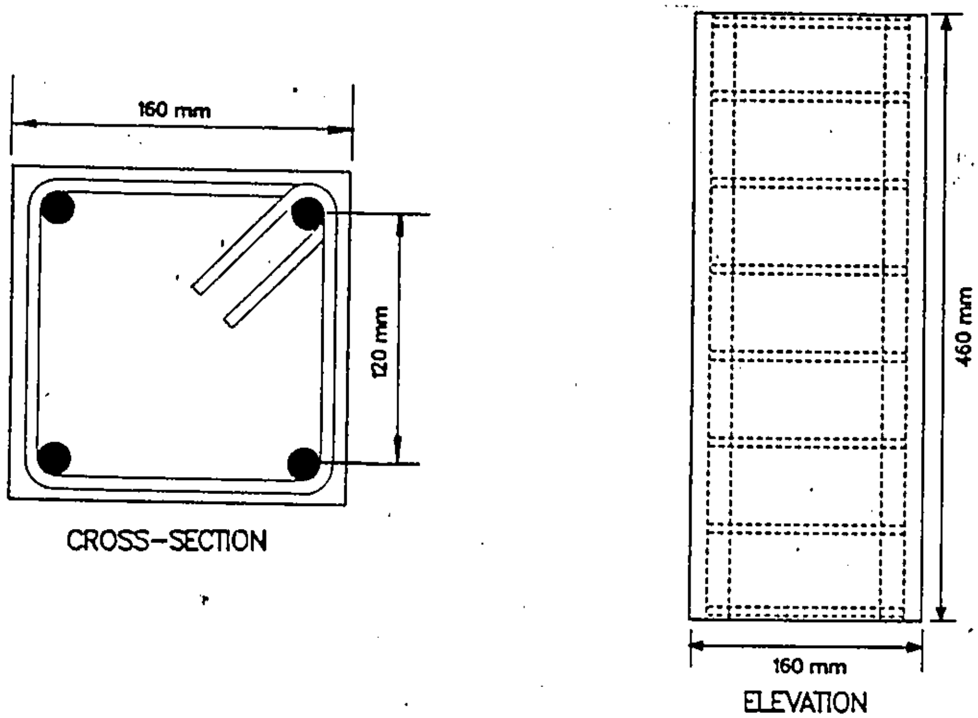

Figure 2.1: Geometry of a typical test specimen

dure are described in this chapter. In addition, the material properties and reinforcement arrangements are also reported.

2.2 Test specimens

The test specimens were cast vertically in three sets. The first set contained ten columns, the second and third sets contained twelve columns each. All columns were 160 x 160 x 460 mm. Figure 2.1 illustrates overall geometry of the specimens. Different reinforcement configurations were considered in the test program. The specimens were labelled on the basis of their reinforcement configurations, and concrete strength. Therefore specimens 1 through 18 represent eighteen different reinforcement arrangement and/or concrete strength. Two specimens were tested for each reinforcement configuration with the exception of columns 17(a) and 18(a). The subscript (a) and (b) assigned to each test specimen distinguish the specimens in a given pair. This applies to all the columns except columns 17(a) and 18(a) in set number three.

All columns contained four longitudinal bars, one at each corner, spaced 120 mm center to center. The longitudinal bars were either 16 mm diameter (No.15) or 11.3 mm diameter (No.10). The ties used were 6.53 mm diameter plain bars with hooks extending ten times the bar diameter. The provided percentage of longitudinal steel was 1.562 for specimens with No.10 bars and 3.125 for specimens with No.15 bars. Reinforcement details for each column are presented in Figures 2.2 and 2.6. Tables 2.1 to 2.3 provide a summary of all test specimens and their properties.

Each set was cast from the same batch of concrete. A number of cylinders were cast along with each set, to determine the properties of unconfined concrete. After casting columns and cylinders, they were covered with burlaps and plastic sheets for two days. Curing of specimens continued till the required strength was reached.

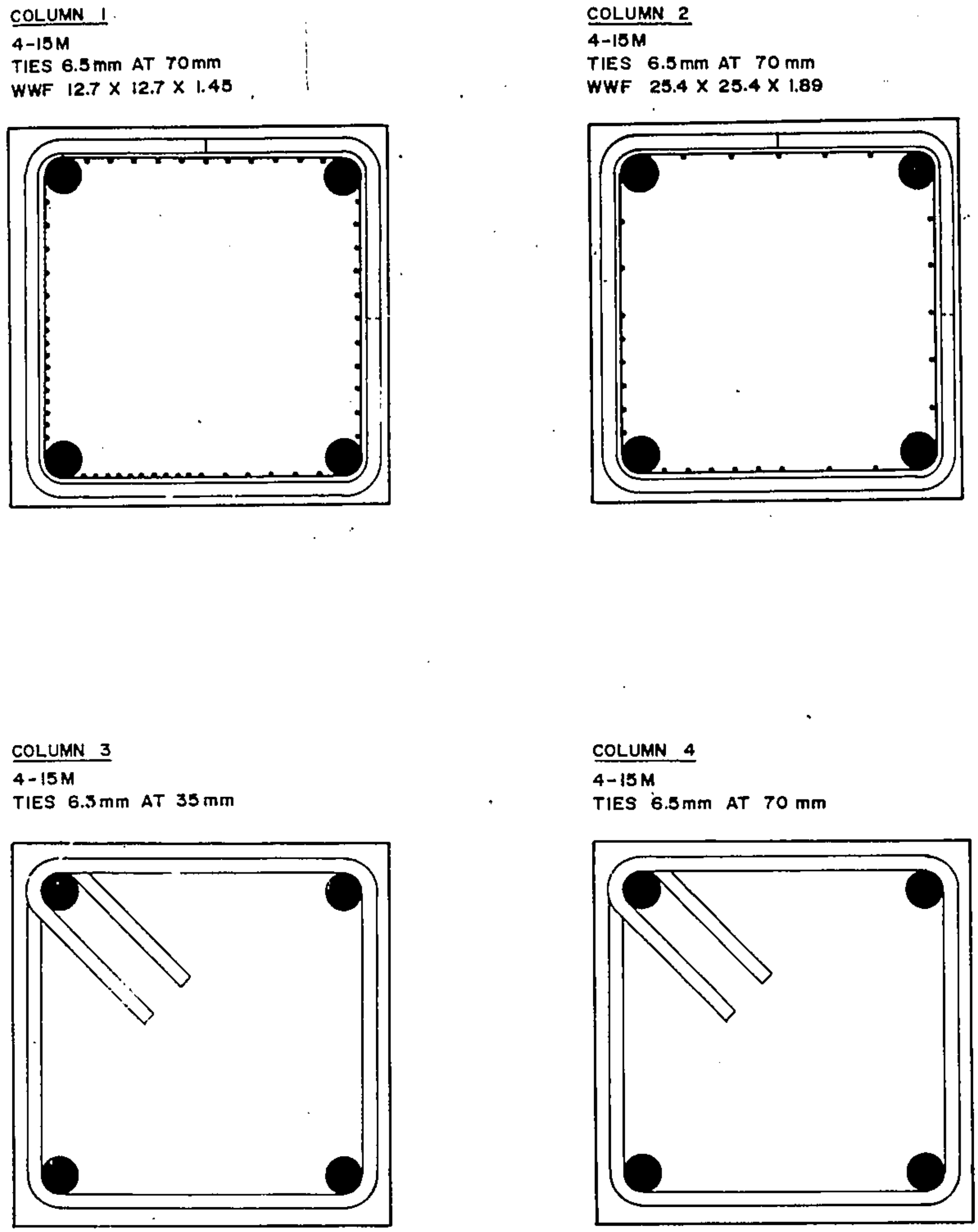

Figure 2.2: Reinforcement detail of column pairs 1 - 4

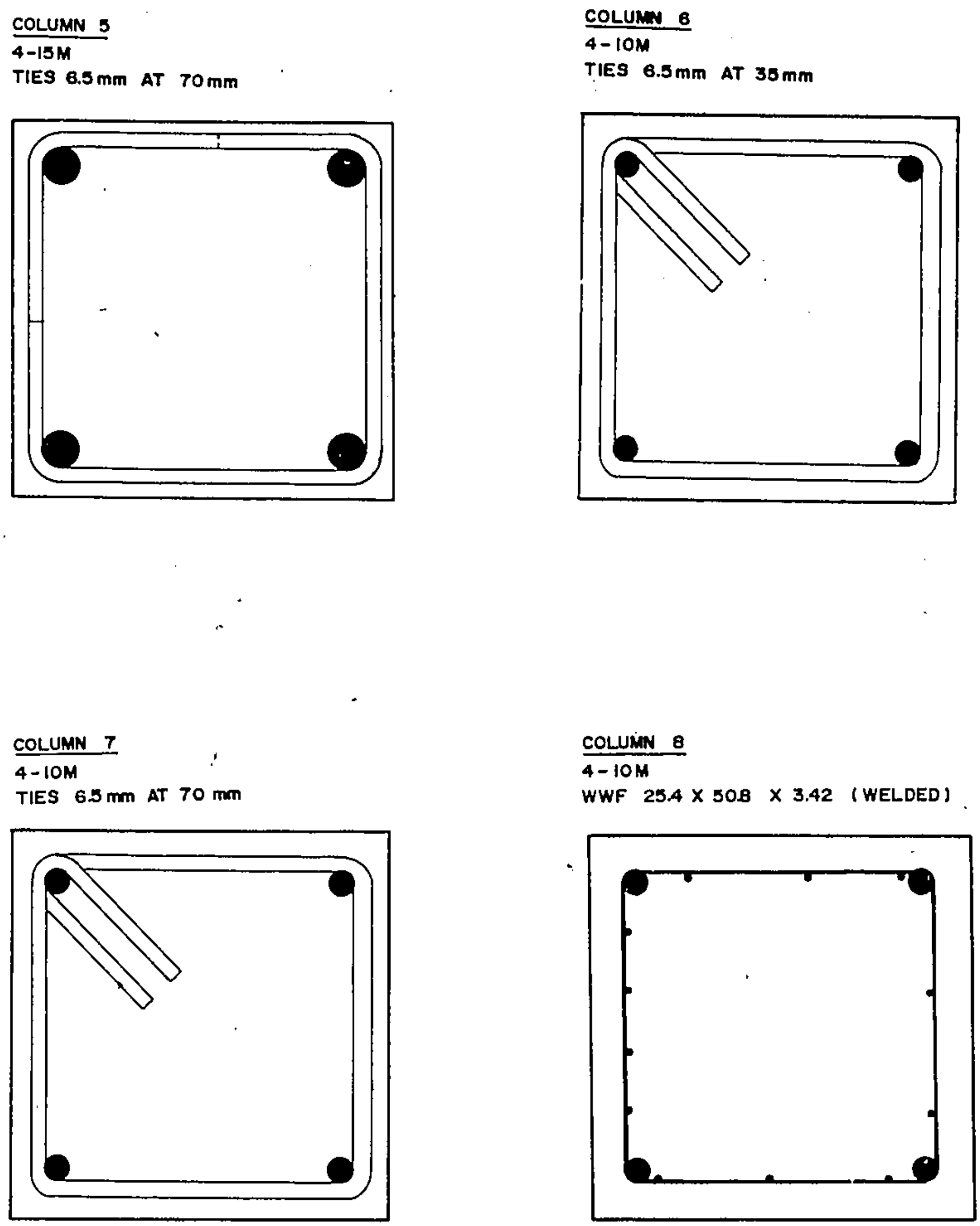

Figure 2.3: Reinforcement detail of column pairs 5 - 8

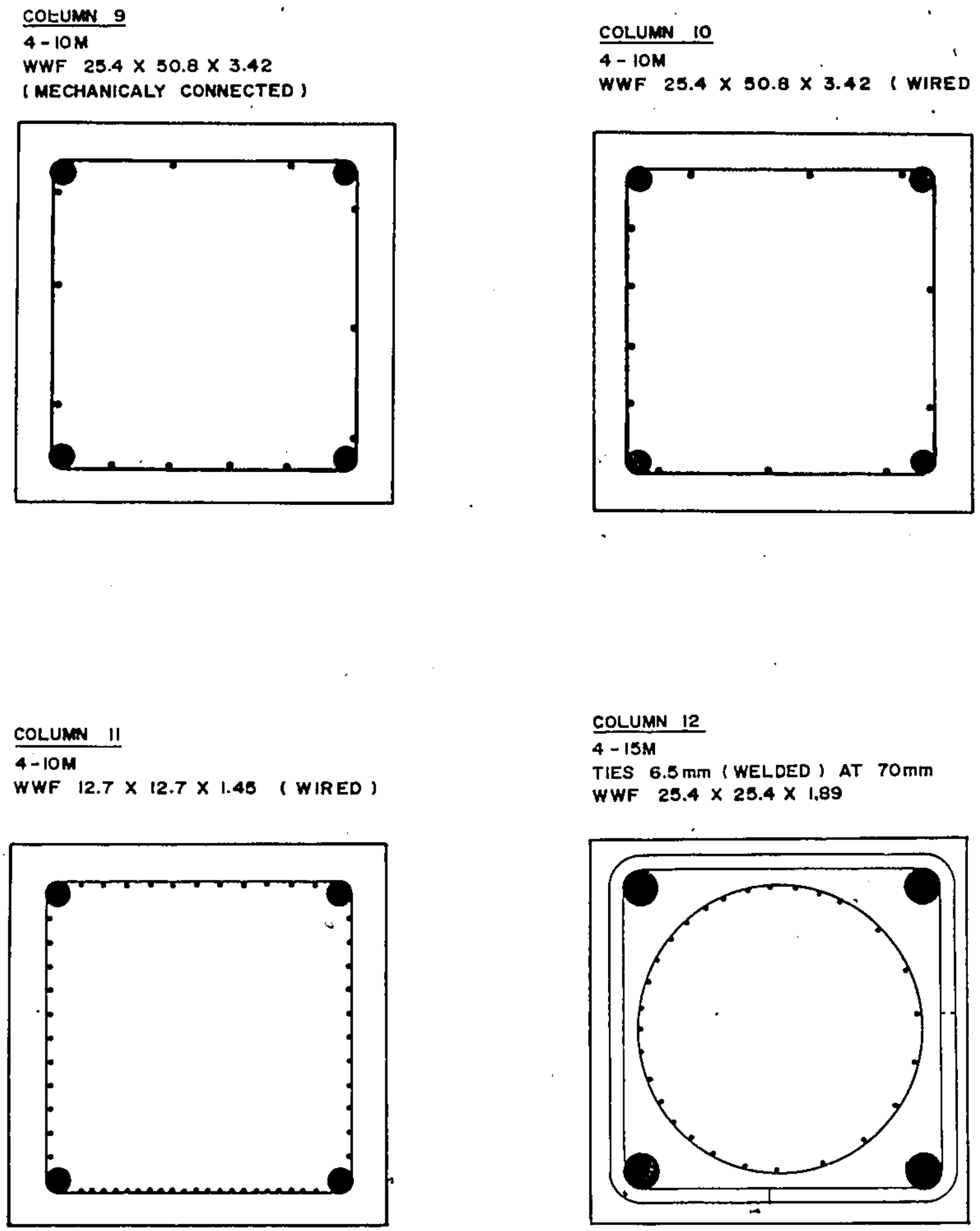

Figure 2.4: Reinforcement detail of column pairs 9 - 12

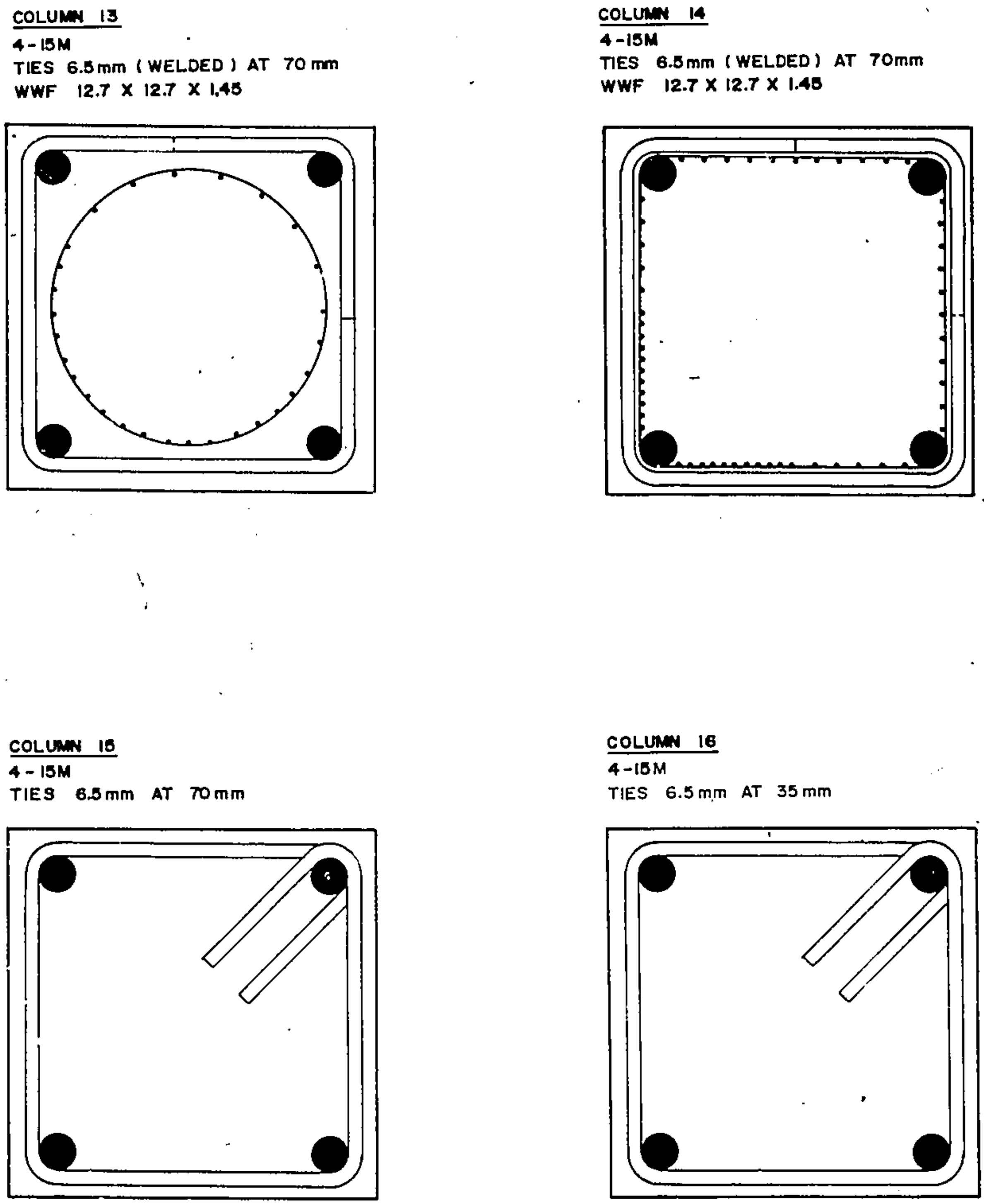

Figure 2.5: Reinforcement detail of column pairs 13 - 16

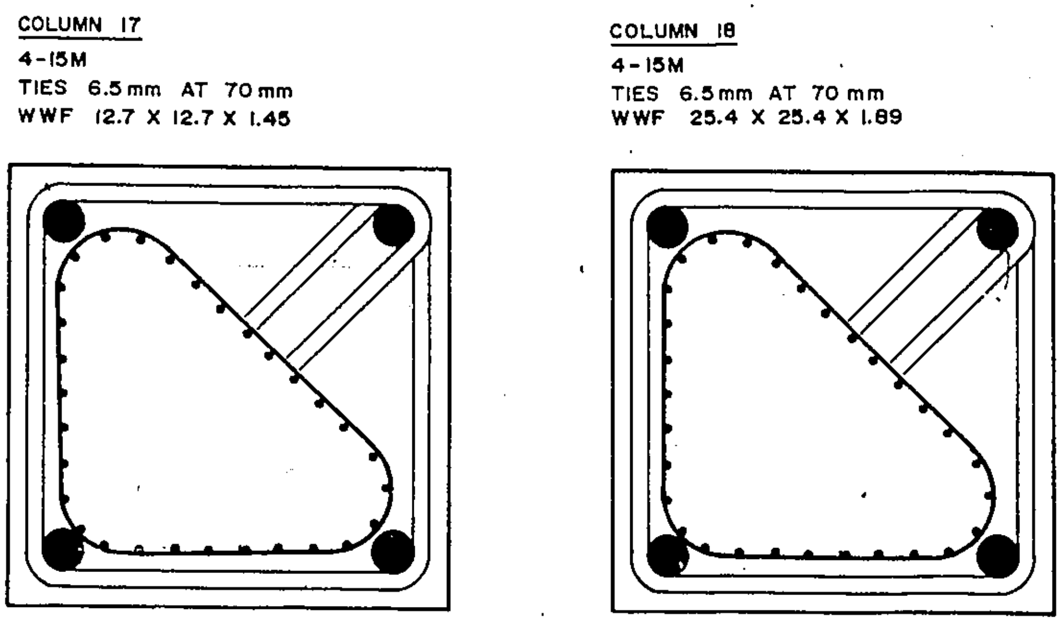

Figure 2.6: Reinforcement detail of columns 17(a) and 18(a)

2.3 Material Properties

2.3.1 Concrete

Three batches of concrete were used to cast the specimens. Column pairs 1 to 5, 6 to 11 and 12 to 18 were cast from batches 1, 2 and 3 respectively.

Following are the concrete specifications for each batch:

1. Batch 1

   - Concrete was mixed in lab.
   - Mix design 1 :2.5 :4 (cement:sand:aggregate)

Column No.	1	2	3	4	5
Longitudinal steel	4No.15				
$f_y(MPa)$	470				
$\rho_{gross}(\%)$	3.125				
$\rho_{core}(\%)$	3.938				
$f'_c\ (MPa)$	32				
Lateral ties					
Bar Size(mm)	6.53				
$f'_y(MPa)$	373				
Spacing[1]	d/2	d/2	d/4	d/2	d/2
$\rho_s(\%)$	1.34	1.34	2.68	1.34	1.34
Hook	90°	90°	135°	135°	90°
Welded wire fabric					
Spacing (mm)	12.7 x 12.7	25.4 x 25.4	N.A.	N.A.	N.A.
Gage	16	14			
$f_{ywwf}(MPa)$	300	375			
$\rho'_s(\%)$	0.35	0.30			
Length(mm)	600	600			

Table 2.1: Details for specimens in set 1

[1]effective depth (d) = 140 mm

Column No.	6	7	8	9	10	11
Longitudinal steel	4No.10					
$f_y(MPa)$	480					
$\rho_{gross}(\%)$	1.562					
$\rho_{core}(\%)$	2.105					
$f'_c\ (MPa)$	39					
Lateral ties						
Bar size(mm)	6.53	6.53				
$f'_y(MPa)$	373	373				
Spacing[1]	d/4	d/2	N.A.	N.A.	N.A.	N.A.
$\rho_s(\%)$	2.78	1.39				
Hook	135°	135°				
Welded wire fabric						
Spacing (mm)	N.A.	N.A.	25.4 x 50.8	25.4 x 50.8	25.4 x 50.8	12.7 x 12.7
Gage			10	10	10	16
$f_{ywwf}(MPa)$			500	500	500	300
$\rho'_s(\%)$			1.071	1.071	1.071	0.391
Length(mm)			600	600	600	600

Table 2.2: Details for specimens in set 2

[1]effective depth (d) = 140 mm

Column No.	12	13	14	15	16	17	18
Longitudinal steel	4No.15						
$f_y(MPa)$	470						
$\rho_{gross}(\%)$	3.125						
$\rho_{core}(\%)$	3.938						
$f'_c\ (MPa)$	29						
Lateral ties Bar Size(mm)	6.53						
$f'_y(MPa)$	373						
Spacing [1]	d/2	d/2	d/2	d/2	d/4	d/2	d/2
$\rho_s(\%)$	1.34	1.34	1.34	1.34	2.68	1.34	1.34
Hook	90°	90°	90°	135°	135°	135°	135°
Welded wire fabric							
Spacing (mm)	25.4x25.4	12.7x12.7	12.7x12.7	N.A.	N.A.	12.7x12.7	25.4x25.4
Gage	14	16	16			16	14
$f_{ywwf}(MPa)$	375	300	300			300	375
$\rho'_s(\%)$	0.30	0.35	0.35			0.35	0.30
Length(mm)	600	600	600			600	600

Table 2.3: Details for specimens in set 3

[1]effective depth (d) = 140 mm

- Type 10 Normal Portland Cement was used.
- Slump: 90 mm
- W/C = 0.72
- Concrete strength = 32 MPa (on the day of column tests)

2. Batch 2

   - Ready mix concrete was used.
   - Type 20 High Early Strength Cement was used.
   - Slump: 100 mm
   - Concrete strength = 39 MPa (on the day of column tests)

3. Batch 3

   - Concrete was mixed in lab.
   - Mix design 1 :2.5 :4 (cement:sand:aggregate)
   - Type 10, Normal Portland Cement was used.
   - W/C = 1.0
   - Slump: 100 mm.
   - Strength = 29 MPa (on the day of column tests)

To insure that concrete was able to pass through the smallest spacing of wire mesh, which was 12.7 mm, a maximum aggregate size of 10 mm was used in all columns. The concrete was vibrated very well, and high water-cement ratio was used to avoid any possible placement problems.

Type number	Spacing(mm)	Gage	$A_{gage}(mm^2)$	$f_{ywwf}(Mpa)$
1	12.7 x 12.7	16	1.65	300
2	25.4 x 25.4	14	2.826	375
3	25.4 x 50.8	10	9.160	500

Table 2.4: Details for welded wire fabric

Stress–strain relationship obtained from cylinder tests for each batch of concrete are shown in Figure 2.7. It should be noted, that the strain is based on 300 mm gage length in all cylinders.

2.3.2 Steel

Deformed reinforcing bars with 11.3 mm diameter (No.10) and 16 mm diameter (No.15) were used as longitudinal steel for the columns. Plain bars with 6.53 mm diameter bars were used as lateral ties. The stress-strain relationship for each type of reinforcement is given in Figure 2.8.

2.3.3 Welded wire fabric

Three different types of welded wire fabric were used. Table 2.4 summarizes the properties of these types. Few samples of WWF were tested for each type of WWF. Figure 2.9 shows the stress–strain relationship for WWF.

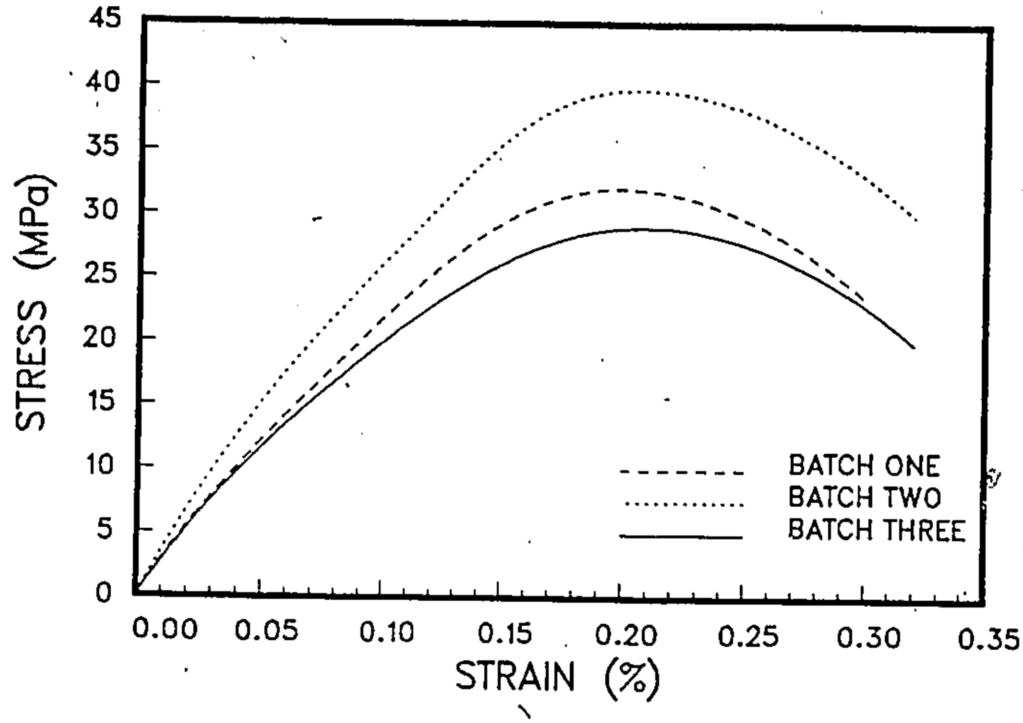

Figure 2.7: Stress-strain relationship for plain concrete

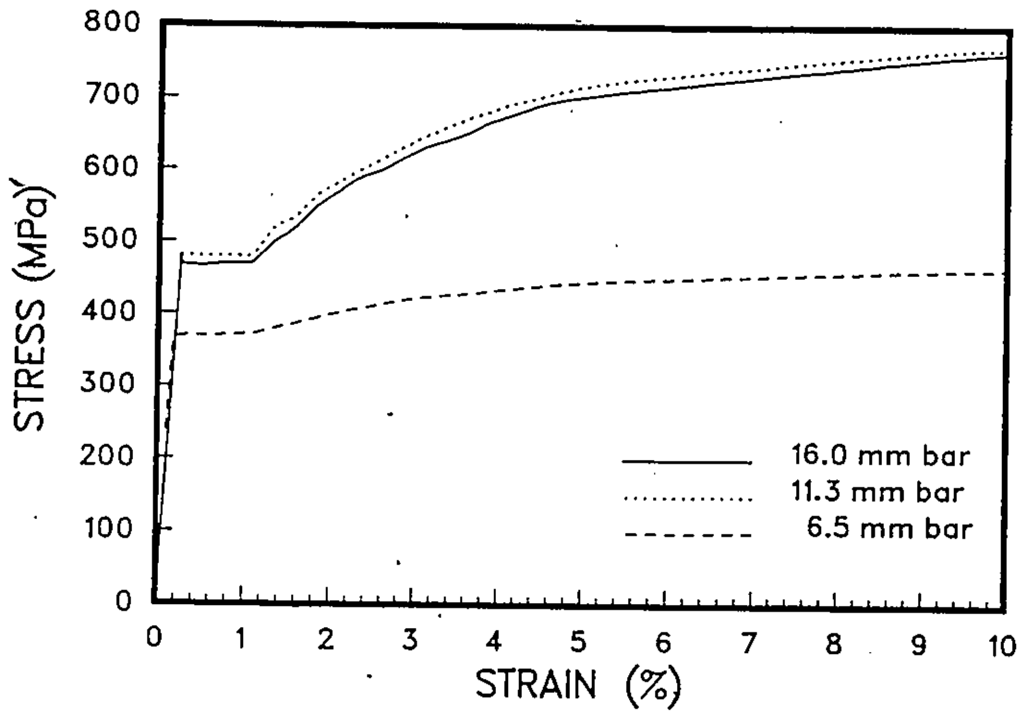

Figure 2.8: Stress–strain relationship for steel

No clear yield point was observed. The yield strength was assumed to be 67% of the ultimate strength.

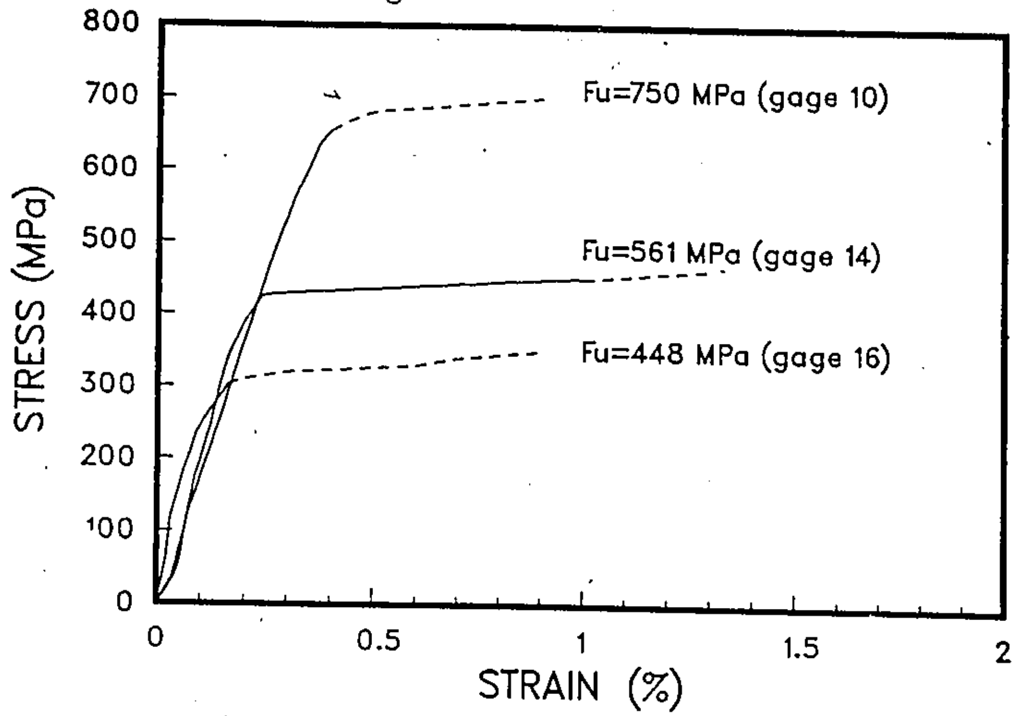

Figure 2.9: Stress–strain relationship for WWF

2.4 Test Setup

All the columns were tested using a Forney concrete compression testing machine with a 1335 kN load capacity. The overall test setup is illustrated in Figure 2.10. The columns were externally confined in the top and bottom regions, where the load was applied, by means of steel brackets. Each bracket consisted of four pieces of steel angles that were bolted together.

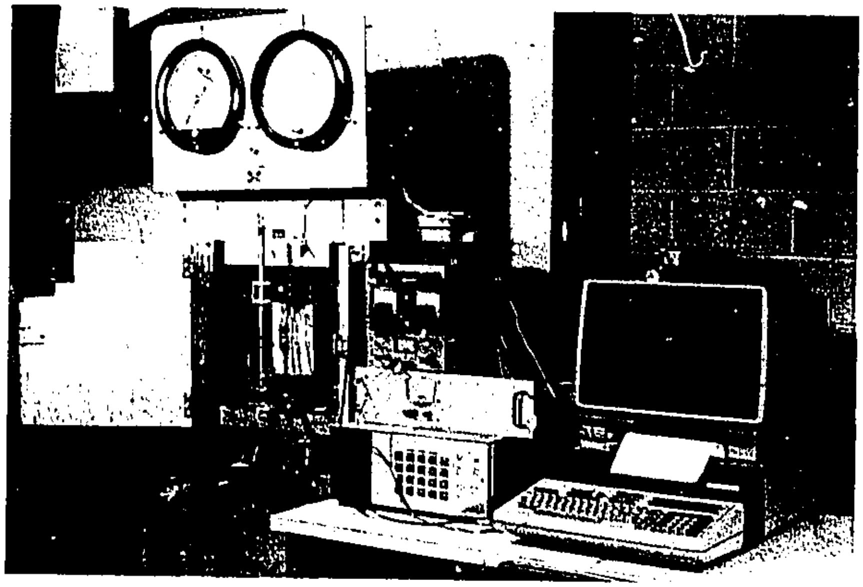

Figure 2.10: Overall test setup

Figure 2.11 illustrates the end region of a test specimen.

A thin layer of cement paste was placed at the top of the specimen whenever it was necessary to make it smooth and level. In addition, pieces of plywood were provided at the top and bottom of the specimens to ensure uniform distribution of load. Ball joints could not be used due to the limitation of clear space between the heads of the testing machine. Shims were used at column ends to ensure concentric loading. The location and thickness of the shims were decided through a trial- and - error procedure and by loading and unloading the columns in the elastic range, prior to the actual testing. During this process, the axial strain measured on each side was monitored until they produced approximately the same reading.

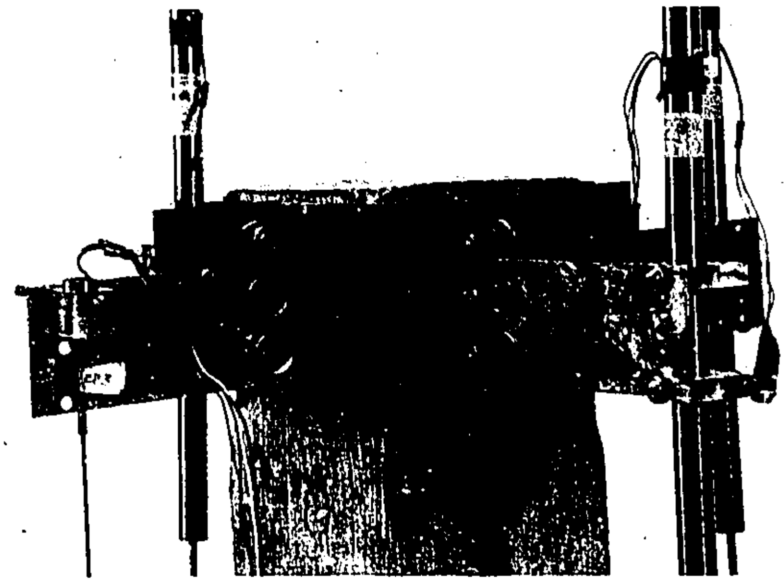

Figure 2.11: Confinement arrangement for top and bottom of the specimen

2.5 Instrumentation

Axial deformations of columns in the longitudinal direction were measured using linear variable differential transformers (LVDTs). Three LVDTs with 150 mm stroke and one LVDT with 10 mm stroke were used, one on each face. The LVDTs were held by plastic clamps which were attached to aluminum plates (165 x 70 x 2 mm). The aluminum plates were connected to columns by the help of the steel angles used for confinement of the extreme top and bottom regions of columns. Figure 2.12 shows the instrumentation and typical arrangement of the LVDTs.

LVDT readings were used to compute the average strain of the test region. The gage length used for this purpose was the portion between the externally confined end regions, i.e., 240 mm. It is to be noted that, in the

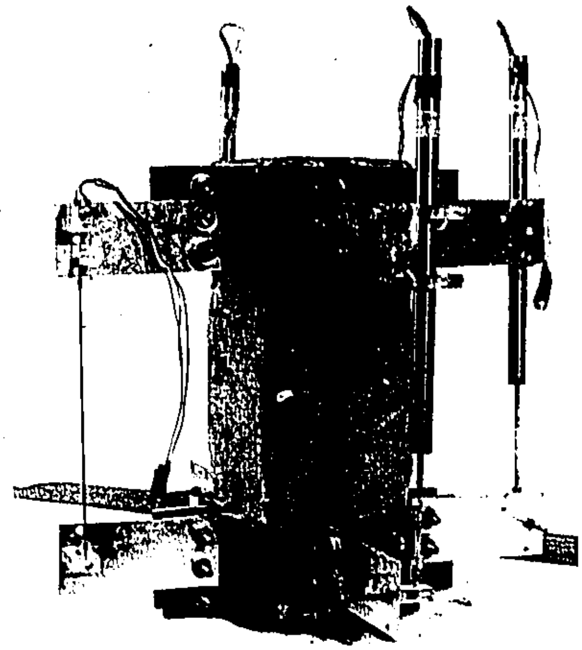

Figure 2.12: Typical arrangement for LVDTs

low strain range (i.e. less than 0.005), the gage length was assumed to be 350 mm, which was the distance from center of top angles to the center of bottom angles, to account for the movement of concrete under the steel angles. Beyond 0.005 strain, the deformation at the top and bottom of the column was assumed to be negligible due to the confinement provided by the steel angles. The total shortening recorded by LVDTs was assumed to take place in the test region.

Strains in ties were measured using electric strain gages. The central tie had four strain gages, while the ties above and below had two strain gages each. Hence a total of eight strain gages were used in one column of each pair. Strain gages were placed in the center of the outer face of the ties, as shown in Figure 2.13.

Steel strains and axial deformations of columns were recorded from the

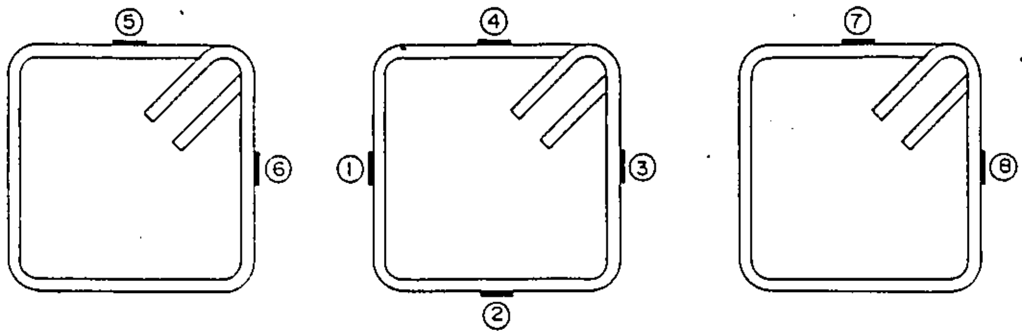

Figure 2.13: Strain gage locations

strain gages and LVDTs by an HP Data Acquisition System which consisted of Desktop Computer (HP 9845 B) and Control Unit (HP 3497 A). However, the load was recorded manually because there was no room in the testing machine to provide an additional load cell.

It is to be noted that the instrumentation used for some of the specimens in the first test was different than the arrangement just discussed. In columns 1(a) and 2(a) two pins were inserted into each face of the column, one at the top and the other at the bottom, to support the LVDTs as shown in Figure 2.14. Later it was found that the aluminum plates connected to the angles, provide a better support for the LVDTs.

Some of the earlier columns in the first set were tested using three LVDTs rather than four.

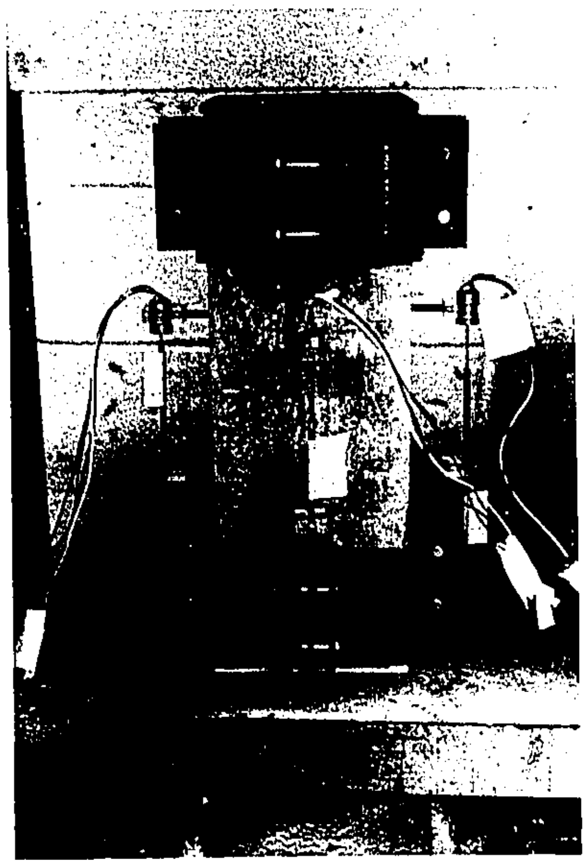

Figure 2.14: Test setup used for columns 1(a) and 2(a)

2.6 Test procedure

The same steel brackets were used for testing all the specimens. Upon fixing these brackets, each column was placed in the center of the testing machine. LVDTs were connected to the column carefully, to ensure that the pin for each LVDT could move freely. An initial load of 90 to 180 kN was applied. Column strain was recorded by all four LVDTs. If the readings were far from each other, the test was then stopped to adjust the head of the machine after unloading the column. This procedure of trial and error was repeated to minimize the effect of eccentricity.

The load was recorded manually at the same time when the strains were recorded by the computer. In the high strain range, the test was stopped to adjust the 10 mm LVDT, to allow for a higher range of measurements.

Specimens were loaded until one of the following conditions occurred:

- Excessive spalling of concrete cover which could damage the LVDTs.
- The load was dropping fast.
- The bottom plate of the testing machine was rotating, due to excessive deformations which disturbed the LVDT readings.

Figure 2.15 shows column 3(a) in the testing machine before and after the test.

Figure 2.15: Column 3(a) before and after testing

Chapter 3

Observed Behavior and Test Results

This chapter provides the rationale behind the design of columns in each set. Test results, in terms of axial load–axial strain relationship, and the observations made during testing are presented in detail. Specimen properties can be found in table 2.1 to 2.3. The analysis of test results is discussed in Chapter 4.

The specimens were cast in three sets, which represented the staging of testing. The observed behavior and test results in a given set was a constructive step towards the design of the next set. The specimen design, test results and observed behavior, discussed in this chapter, follow the same sequence as the test program.

3.1 General Observed Behavior

The columns showed similar response under increasing concentric compression. The peak strain and the behavior after the peak load varied somewhat depending on the confinement characteristics of the specimens. First set of cracks appeared on column faces at a strain of approximately 0.2%. These cracks propagated vertically and increased in width before ultimate strength was reached. At ultimate load, concrete cover was spalled off in most of the specimens. It was noted however that columns with closely spaced ties and those reinforced with WWF continued resisting load increase even after the cover concrete has totally spalled off. This observation shows that the drop in strength due to the reduction of effective concrete area was balanced by the enhancement of strength due to confinement. The load started dropping, in most of the columns, when buckling of one or more of the longitudinal bars took place. At this time LVDT readings started deviating substantially from each other. This indicated load redistribution, which resulted in eccentric loading. This behavior could be attributed to uneven spalling of the concrete cover and buckling of longitudinal bars at different times. Once all the longitudinal bars have buckled, it was observed that the loading was nearly concentric. The reduction in load resistance continued at different rates until the end of testing, depending on the test variables.

3.2 Set one

3.2.1 General

This set was designed for pilot tests to investigate the possibility of using WWF as confinement reinforcement in columns. Column pairs 1 and 2 were designed to have lateral ties spaced at d/2 center to center. In addition, they were provided with WWF placed between the longitudinal steel and the lateral ties. WWF was overlapped with a 90 degree bend and extended a distance of d/2. The 90 degree tie hooks, were extended ten times the tie diameter. It was not possible to provide 135 degree tie hooks due to the presence of welded wire fabric. It was anticipated that the presence of welded wire fabric would reduce the pressure on the ties and hence become effective even with the 90 degree hooks. The orientation of the hooks in plan was such that the overlap corner was diagonally opposite to the WWF overlap corner. This arrangement would insure that both corners would not open simultaneously.

Column pairs 1 and 2 differ only in the WWF size in order to examine its effect on concrete confinement. Column pairs 3 was designed according to the code requirements for structures located at seismically active regions, forming part of a ductile moment resisting frame[18]. Accordingly lateral ties were spaced at d/4 center to center with 135 degree hooks, without the WWF. These columns were used as a reference for comparison purposes.

Column pair 4 was designed to have the same reinforcement as that for column pair 3, except that the lateral ties were provided at d/2 center to center. Column pair 5 was designed to have the same reinforcement as column pair 1 and 2, but it did not contain WWF.

Comparison between the behaviors of column pairs 4 and 5 provides information on the effect of hook angle. Comparison of column pairs 5 and 2 or 5 and 1 shows the effect of WWF on concrete confinement.

3.2.2 Observed Behavior

Columns 1(a) and 1(b)

Columns 1(a) and 1(b) were prepared with 4 No.15 longitudinal bars. Ties with 90 degree hooks were placed at d/2 spacing. WWF (12.7 mm x 12.7 mm x 10 gage) was placed between the longitudinal and transverse reinforcement.

Figure 3.1 illustrates the axial load versus axial strain relationship obtained during the test. Columns behaved in a ductile manner till ties started opening. WWF started tearing off only after the ties have opened, and generally within the same corner of tie overlap. Once ties have opened, the load started dropping at a steep rate with respect to the longitudinal strain. Results of strain gages showed that most ties did not yield neither.

before nor after the peak load. However few strain gages indicated yielding after the peak load. This indicates that full capacity of ties was not utilized and WWF was participating in sustaining the lateral pressure. Buckling of longitudinal bars took place gradually while the ties were opening.

Although columns 1(a) and 1(b) were identical in design, their test setups were different. Column 1(a) was the first column tested under the old setup where pins were used to connect the LVDTs. Moreover, in this setup small range LVDTs with 10 mm stroke, were used, compared to the 150 mm stroke LVDTs used in column 1(b). Hence it is anticipated that the results of column 1(b) are more reliable than those of column 1(a).

Columns 2(a) and 2(b)

Columns 2(a) and 2(b) were provided with 4 No.15 longitudinal bars. Ties with 90 degree hooks were placed at d/2 spacing. WWF (25.4 mm x 25.4 mm x 14 gage) was placed between the longitudinal and transverse reinforcement.

Figure 3.2 shows the results for columns 2(a) and 2(b). The observed behavior was similar to column pair 1. Before opening of ties the columns behaved in a ductile manner, showing a well developed yield plateau. However, while ties were opening, longitudinal bars were bending gradually tearing the WWF and causing the load to drop at a fast rate. Results of strain gages showed that the ties were not yielding at peak load. This indi-

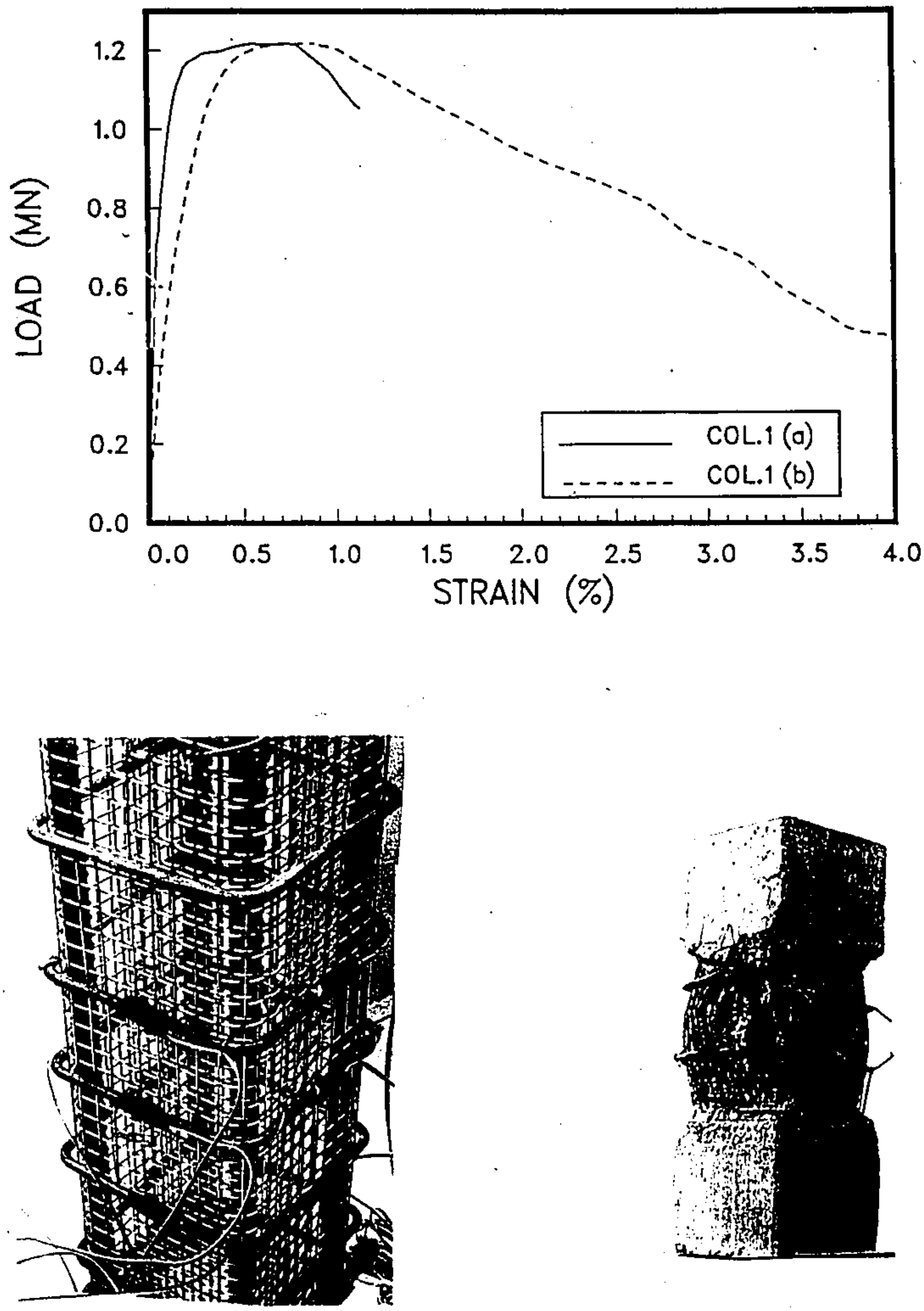

Figure 3.1: Load vs. average strain for columns 1(a) and 1(b)

cates that full capacity of ties was not utilized and WWF was participating in sustaining the lateral pressure. Buckling of longitudinal bars took place gradually while the ties were opening.

It is to be noted that three 10 mm stroke LVDTs were used for column 2(a), whereas three 150 mm stroke and one 10 mm stroke LVDTs were used for column 2(b).

Columns 3(a) and 3(b)

Columns 3(a) and 3(b) were designed to have 4 No.15 longitudinal bars. Ties with 135 degree hooks were placed at d/4 spacing. WWF was not used in these specimens.

Figure 3.3 illustrates the axial load–axial strain relationship recorded during the test. The columns behaved in a ductile manner. The slope of the falling branch of the load - strain relationship was small, approaching horizontal. Ties were observed to open at a very late stage of loading. All strain gages indicated yielding of tie bars at or shortly before the ultimate load. This indicated that the lateral reinforcement was fully utilized.

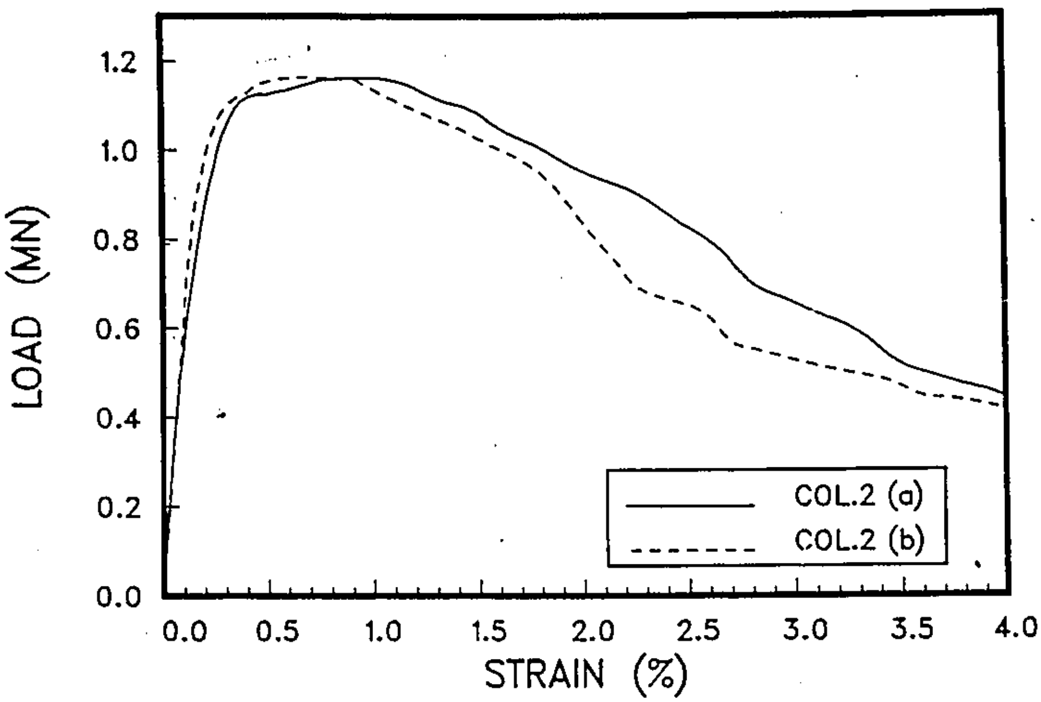

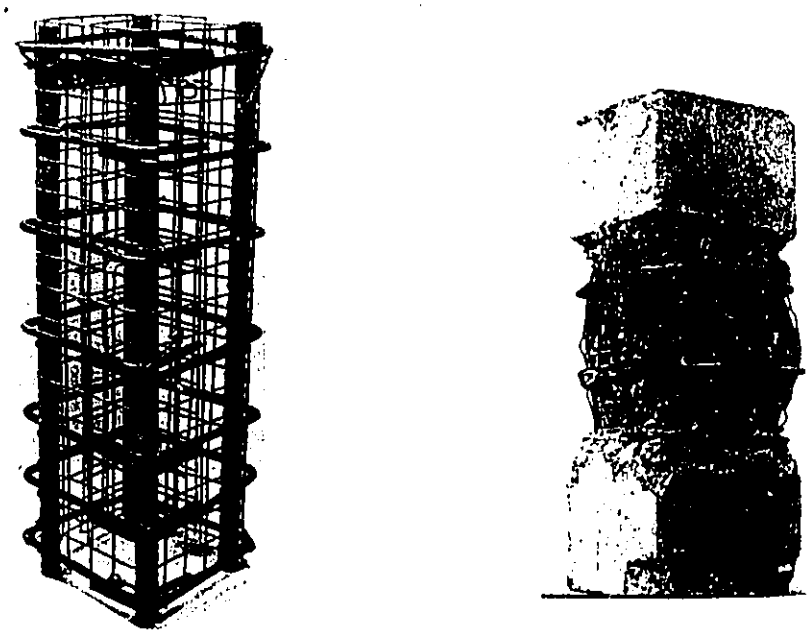

Figure 3.2: Load vs. average strain for columns 2(a) and 2(b)

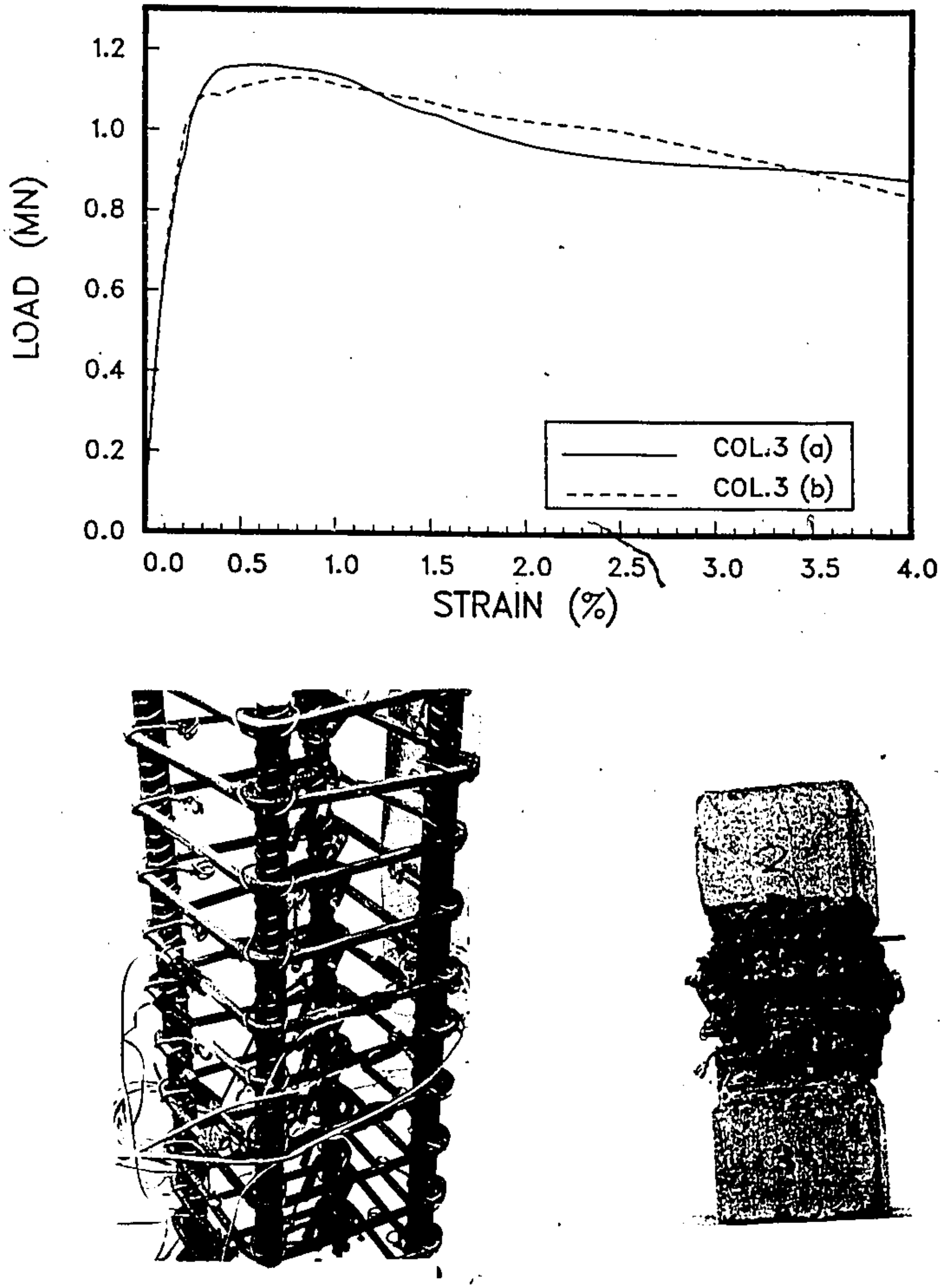

Figure 3.3: Load vs. average strain for columns 3(a) and 3(b)

Columns 4(a) and 4(b)

Columns 4(a) and 4(b) were provided with 4 No.15 longitudinal bars. Ties with 135 degree hooks were placed at d/2 spacing. WWF was not used in these specimens.

Figure 3.4 shows the test results for these columns. The load started dropping at a fast rate immediately past the peak load. All the strain gages showed yielding of tie steel when the peak load was reached. At a high strain level the lateral ties were observed to open.

In an effort to improve the loading mechanism, a different technique was utilized for testing column 4(b). A small piece of plywood, covering most of the core area, was placed on the column and the load was applied through the plywood. This procedure was not successful. Significant eccentricity was observed accompanied by a substantial drop in strength. Therefore the results for column 4(b) are not used in the analysis.

Columns 5(a) and 5(b)

Columns 5(a) and 5(b) were provided with 4 No.15 longitudinal bars. Ties with 90 degree hooks were placed at d/2 spacing. WWF was not used in these specimens.

Figure 3.5 illustrates the recorded test results for columns 5(a) and 5(b).

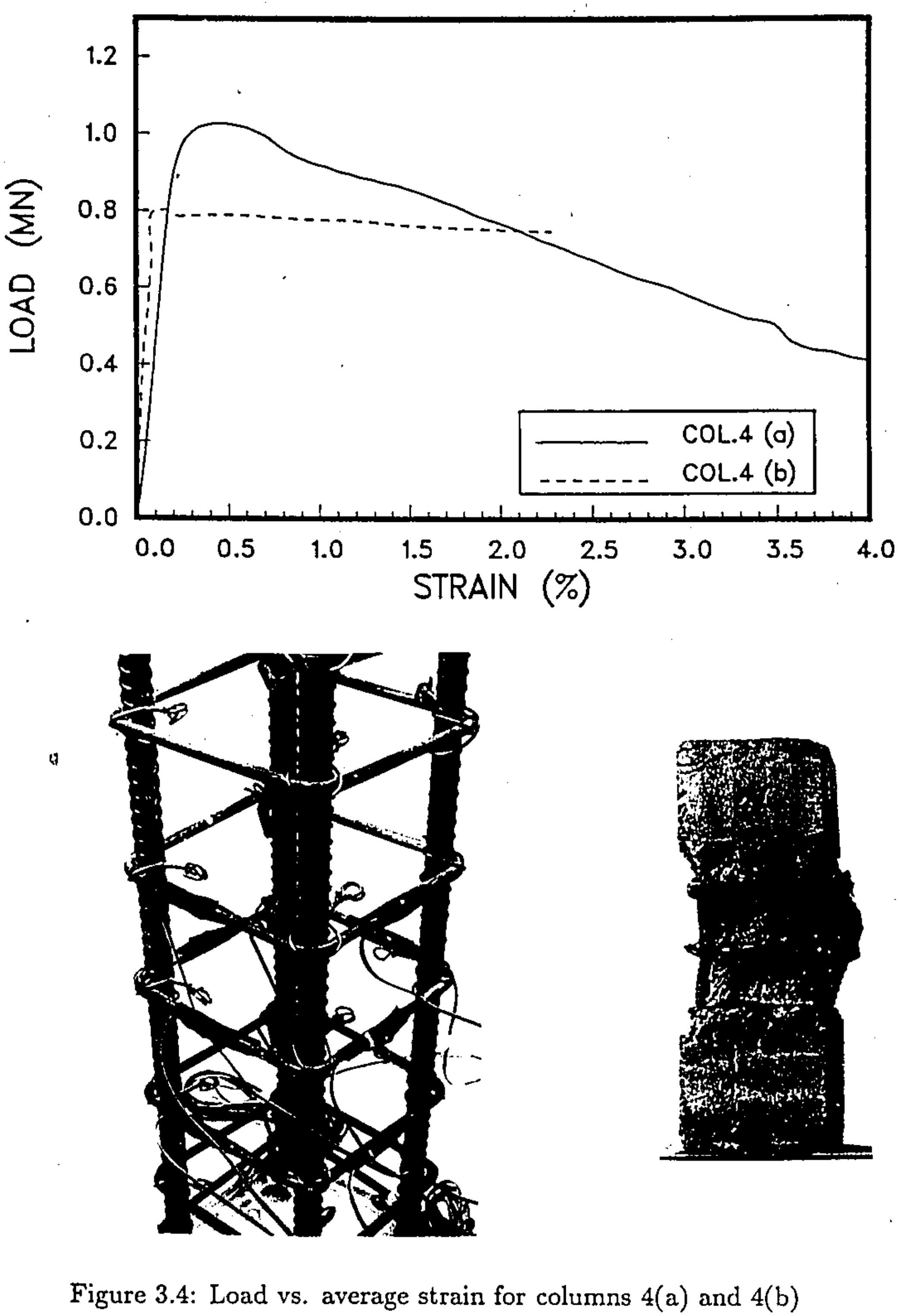

Figure 3.4: Load vs. average strain for columns 4(a) and 4(b)

Beyond the peak load, the load started dropping at a fast rate as the ties were opening. Yielding of tie steel was observed in the tie legs opposite to the hooks. Gradual buckling of longitudinal bars was observed, as the ties ceased to provide the necessary support. It is to be noted that only three 10 mm stroke LVDTs were used for Column 5(a).

3.3 Set Two

3.3.1 General

Specimens in this set were designed based on the conclusions drawn from the test results in set one, which had indicated that WWF improved the behavior of columns at high strain range. The rationale in testing columns of set two was to investigate and quantify the influence of WWF on concrete confinement.

Column pair 6 was designed according to the code requirements (i.e., lateral ties were spaced d/4 center to center with 135 degree hooks). Column pair 7 was similar to column pair 6, but the spacing between the lateral ties was d/2.

Column pairs 8, 9 and 10 were prepared with WWF but without the ties. All WWF was bent 90 degrees at the corners, enclosing longitudinal corner bars. The overlap of WWF extended along the full column face. The only

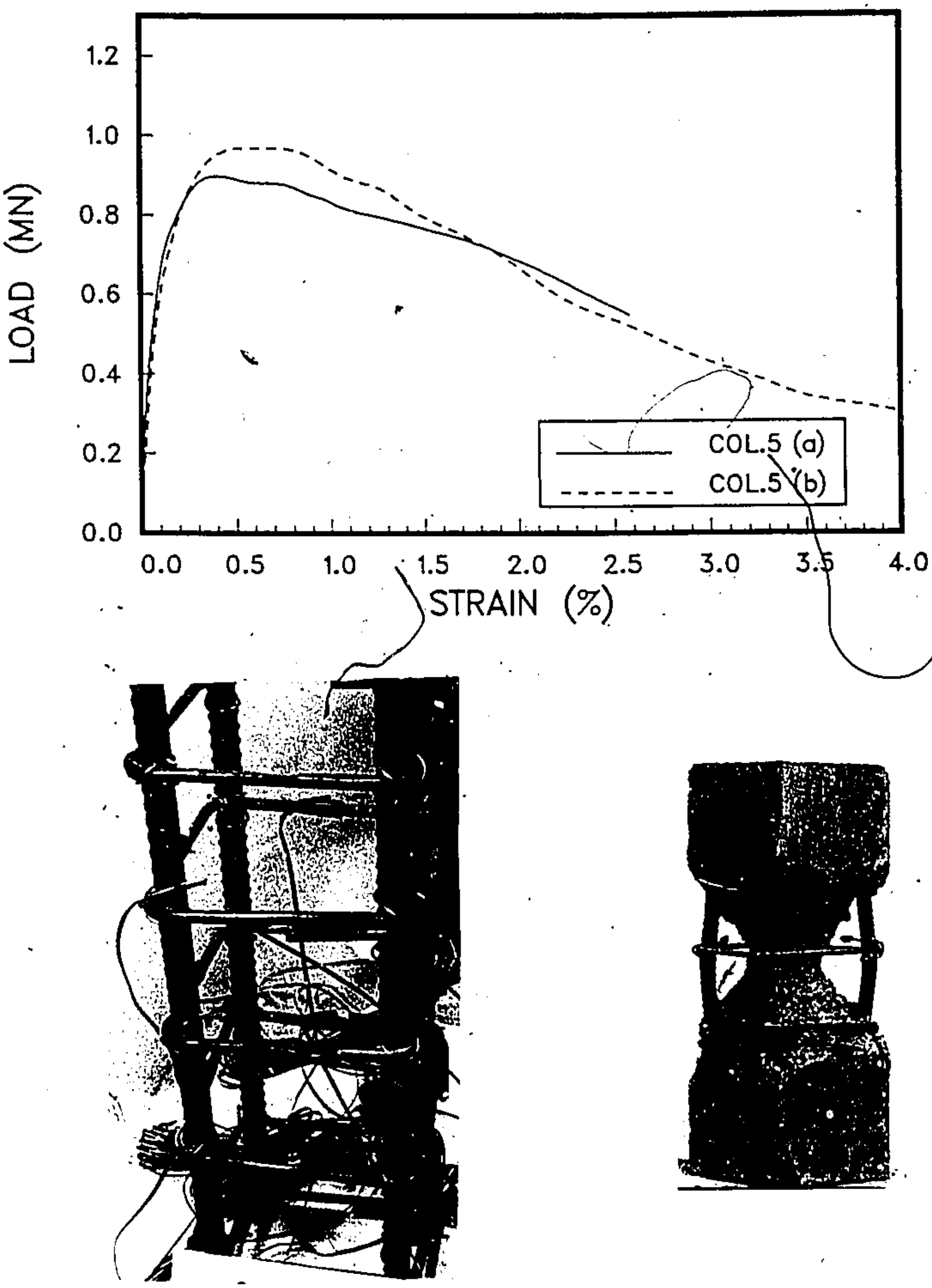

Figure 3.5: Load vs. average strain for columns 5(a)and 5(b)

difference between these three columns was the manner in which the WWF overlaps were tied. In column pair 8, WWF was welded to the overlap layer. In column pair 9, mechanical connectors were used to ensure that WWF would not open at the overlaps. In column pair 10 the overlaps were tied together by means of 1.5 mm diameter wires.

Column pair 11 was similar to column pair 10 except for the WWF size.

It is to be noted that the building code requires the diameter of lateral ties to be at least 30% of the longitudinal bar diameter. In order to comply with this requirement, bar No. 10 was used as longitudinal reinforcement in this set instead of No. 15 which was used in the previous set.

3.3.2 Observed Behavior

Columns 6(a) and 6(b)

Columns 6(a) and 6(b) were prepared with 4 No.10 longitudinal bars. Ties with 135 degree hooks were placed at d/4 spacing. WWF was not used in these specimens.

Figure 3.6 illustrates the axial load–axial strain relationships recorded during the tests. The columns behaved in a ductile manner, showing relatively high deformations with a little drop in the axial load. Most of the strain gages indicated yielding of the tie steel before the column reached its ultimate capacity. Concrete was properly confined even after yielding of the ties. Ties were observed to open towards the end of testing. Severe buckling of longitudinal bars between the ties was observed at the end of testing.

Columns 7 (a) and 7 (b)

Columns 7(a) and 7(b) were prepared with 4 No.10 longitudinal bars. Ties with 135 degree hooks were placed at d/2 spacing. WWF was not used in these specimens.

Figure 3.7 illustrates the axial load–axial strain relationships recorded during the tests. A gradual reduction in load resistance can be seen immediately after the peak load. This indicates ineffectiveness of ties as confinement reinforcement when the spacing was too large. At the end of the test, opening of ties was observed, accompanied by buckling of longitudinal bars between the ties.

Columns 8 (a) and 8 (b)

Columns 8(a) and 8(b) were prepared with 4 No.10 longitudinal bars. WWF (25.5 mm x 50.8 mm x 10 gage) was provided as transverse reinforcement without ties.

Figure 3.8 illustrates the axial load–axial strain relationships recorded dur-

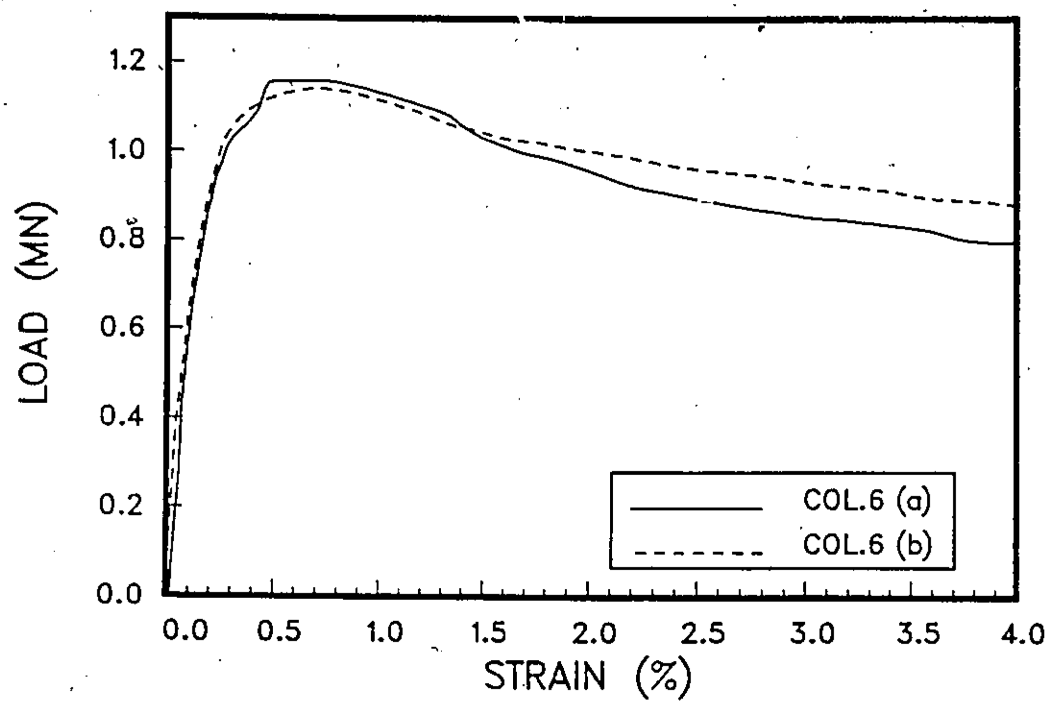

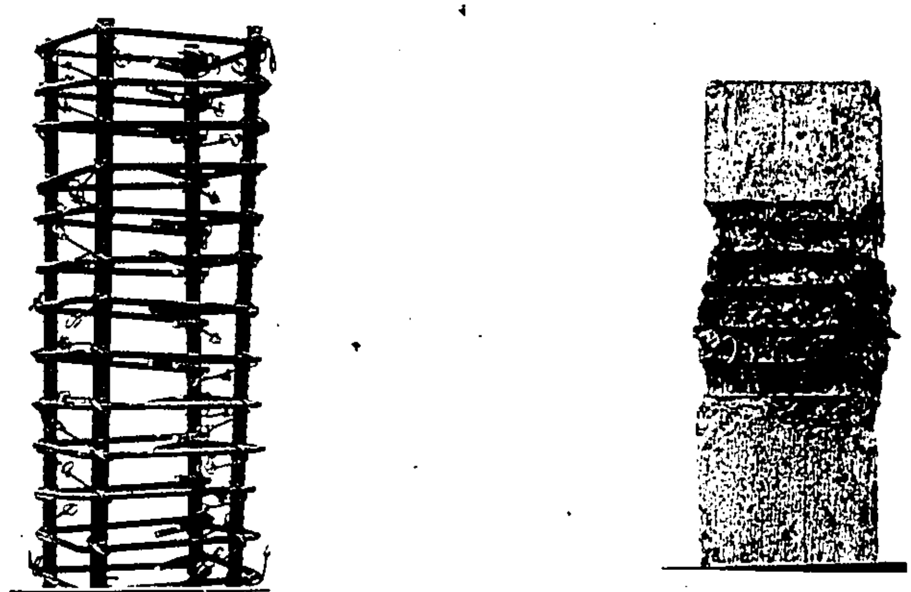

Figure 3.6: Load vs. average strain for columns 6(a) and 6(b)

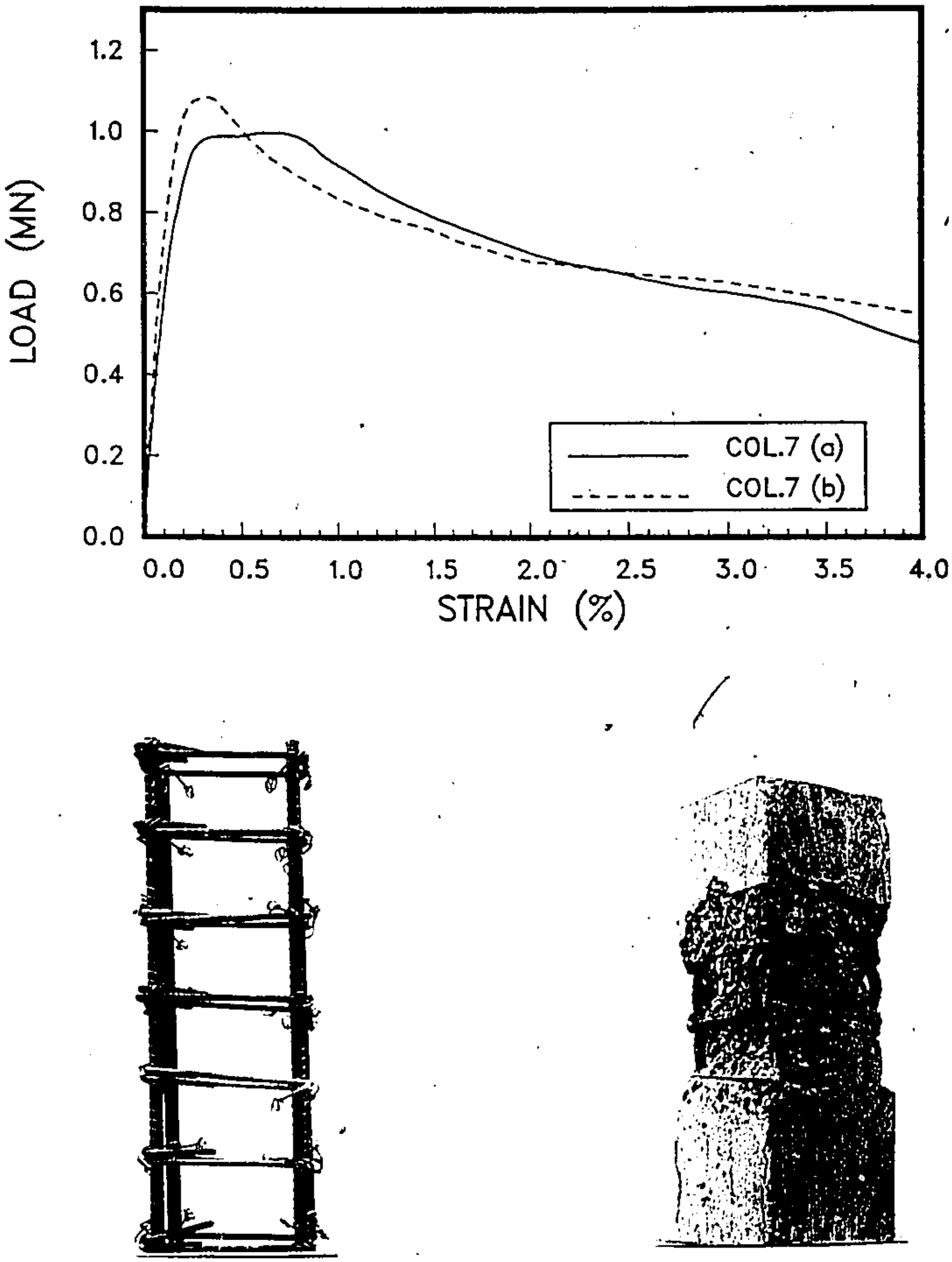

Figure 3.7: Load vs. average strain for columns 7 (a) and 7 (b)

ing the tests. Columns behaved in a brittle manner. Sudden drop of load was observed immediately after reaching the peak load. The drop in load was attributed to premature bending of longitudinal bars and rapture of the WWF. It was observed that WWF did not open at overlap locations. Instead, it tore along one of the vertical corner bars due to the pressure applied by these bars. A particular behavior of column pairs 8 and 9, observed during the test was stepwise drop in load after the peak. This can be explained by a gradual rupture of the WWF. Slight buckling of longitudinal bars was observed at the end of the test.

Columns 9 (a) and 9 (b)

Columns 9(a) and 9(b) were prepared with 4 No.10 longitudinal bars. Mechanically connected WWF (25.5 mm x 50.8 mm x 10 gage) was provided without ties.

Figure 3.9 illustrates the axial load–axial strain relationships recorded during the tests. The behavior of these columns was similar to that of column pair 8. The columns behaved in a brittle manner showing a sudden drop in load immediately after reaching the peak load. The stepwise drop in load was observed after the peak. The mechanical connection used in these columns was effective in preventing WWF from opening at overlap locations. Due to the pressure applied by longitudinal bars, WWF was observed to tear along one of the longitudinal bars. Slight buckling of longitudinal

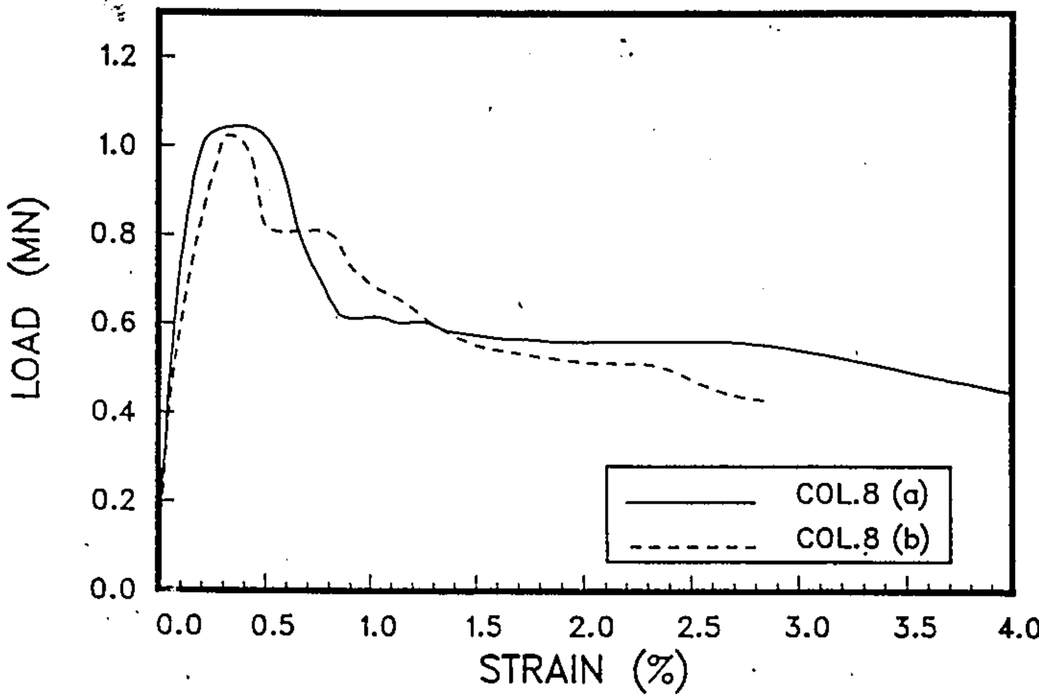

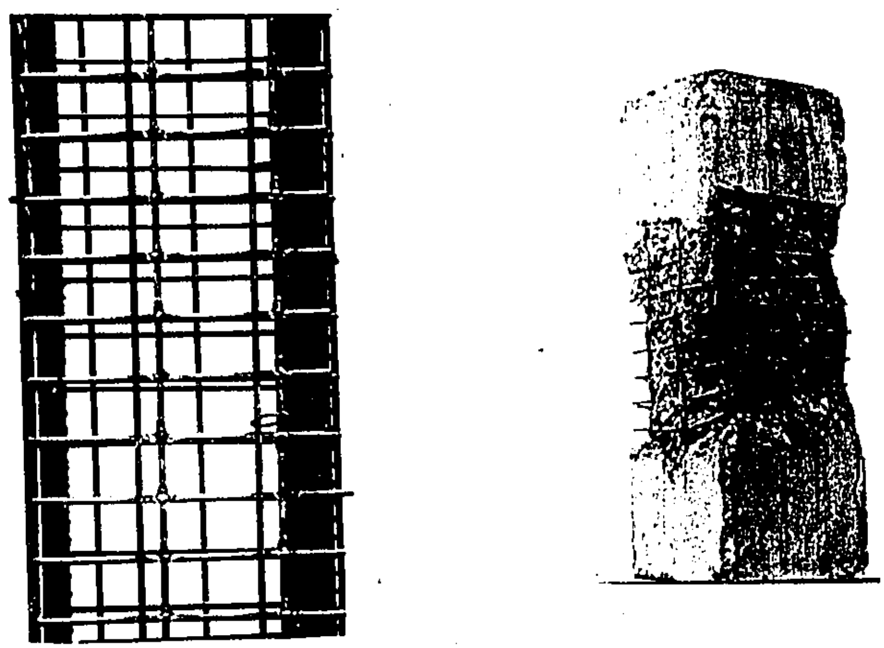

Figure 3.8: Load vs. average strain for columns 8(a) and 8 (b)

bars was observed at the end of the test.

Columns 10 (a) and 10 (b)

Columns 10(a) and 10(b) were prepared with 4 No.10 longitudinal bars. WWF (25.5 mm x 50.8 mm x 10 gage), was connected with wires at the overlap location.

Figure 3.10 illustrates the axial load–axial strain relationships recorded during the tests. The columns behaved in a brittle manner. WWF was observed to tear at one of the corners. Slight buckling of longitudinal bars was observed at the end of the test.

Columns 11 (a) and 11 (b)

Columns 11(a) and 11(b) were prepared with 4 No.10 longitudinal bars. WWF (12.7 mm x 12.7 mm x 16 gage) was connected with wires at the overlap location.

Figure 3.11 illustrates the axial load–axial strain relationships recorded during the tests. The behavior of these columns showed the same trend observed in the previous three pairs of columns without tie reinforcement. A sudden drop was observed in load resistance immediately after the peak load. The drop in load was attributed to gradual buckling of longitudinal

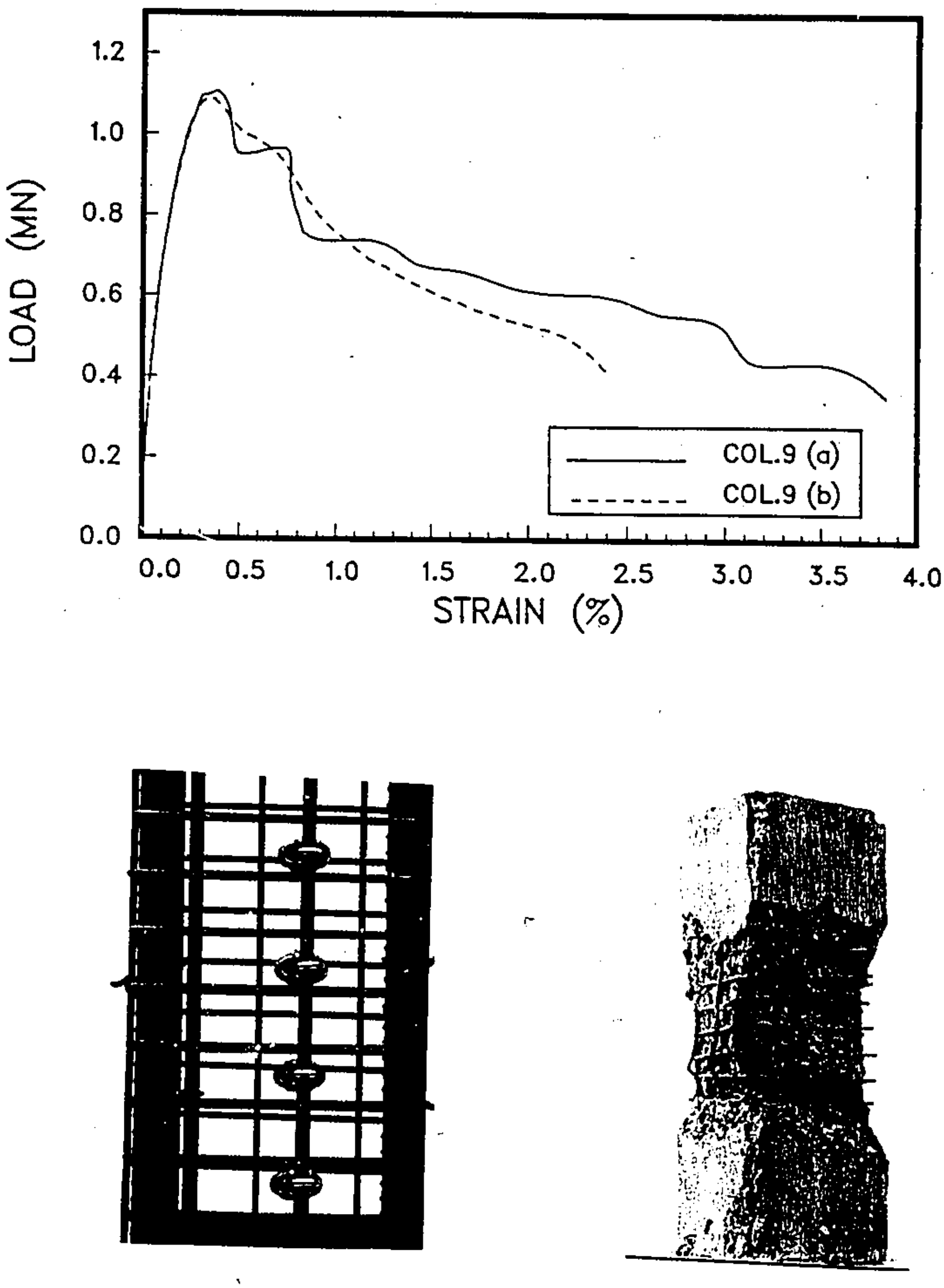

Figure 3.9: Load vs. average strain for columns 9 (a) and 9 (b)

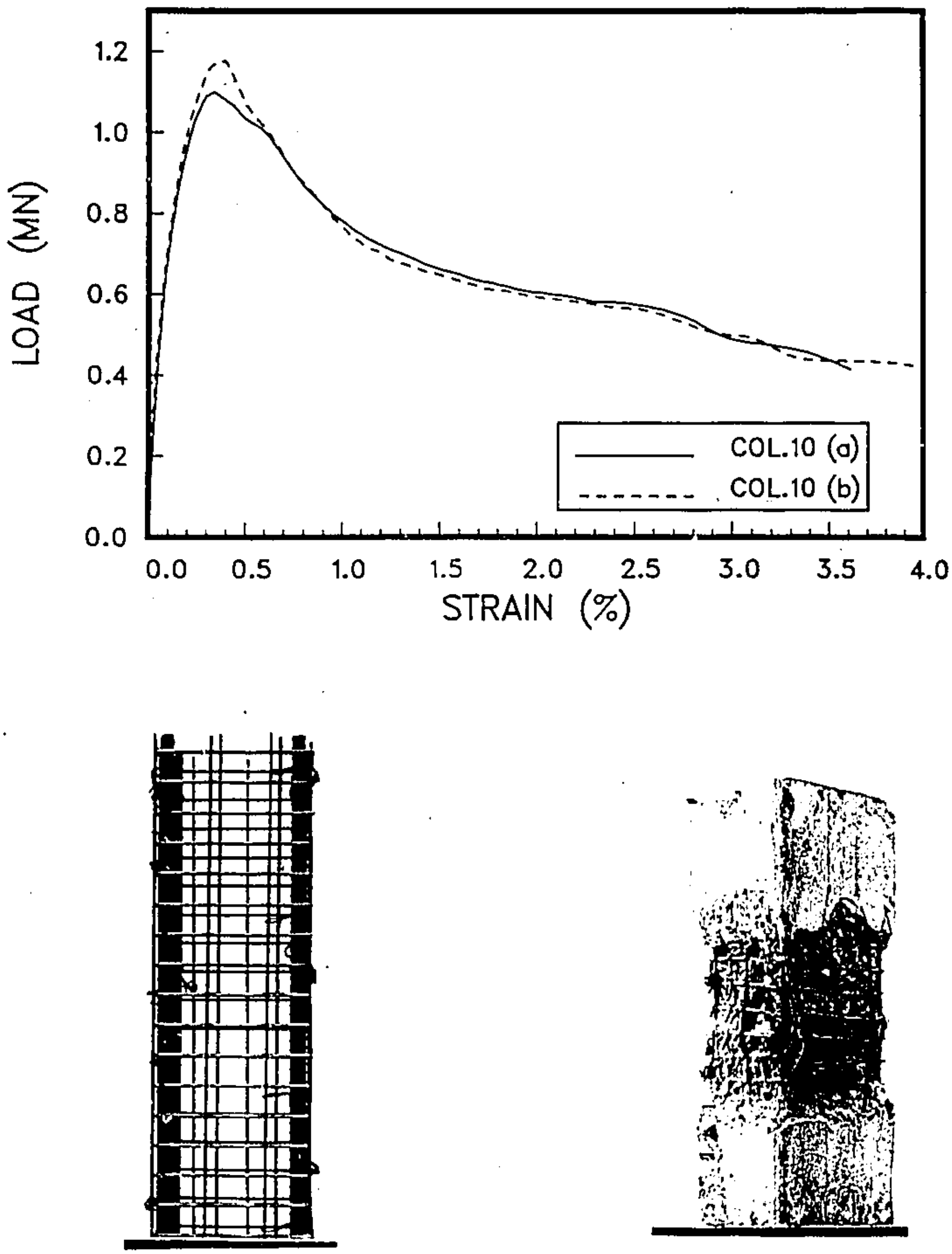

Figure 3.10: Load vs. average strain for columns 10 (a) and 10 (b)

reinforcement and accompanied rapture of the WWF.

3.4 Set three

3.4.1 General

It was observed in set one, that the WWF was effective in confining the concrete till the lateral ties started opening. Observations from set two indicated the brittle behavior of columns without any lateral ties even if the WWF was used. Hence most of the columns in set three were designed to have both WWF and lateral ties. Ties were prevented from opening either by welding them or by providing 135 degree hooks.

Column pairs 12 and 13 were designed to have lateral ties spaced at d/2 with 90 degree hooks welded at the ends. WWF was placed inside the reinforcement cage, located in the concrete core, inside both the tie and longitudinal reinforcement. The only difference between column pairs 12 and 13 was WWF size.

Column pair 14 was the same as column pair 13, but WWF was placed between the longitudinal steel and lateral ties with welded 90 degree hooks. Column pair 16 was designed based on the code requirements, as a reference for all columns in this set. Column pair 15 was the same as column pair 16 but having twice the lateral tie spacing. Columns 17(a) and 18(a) had

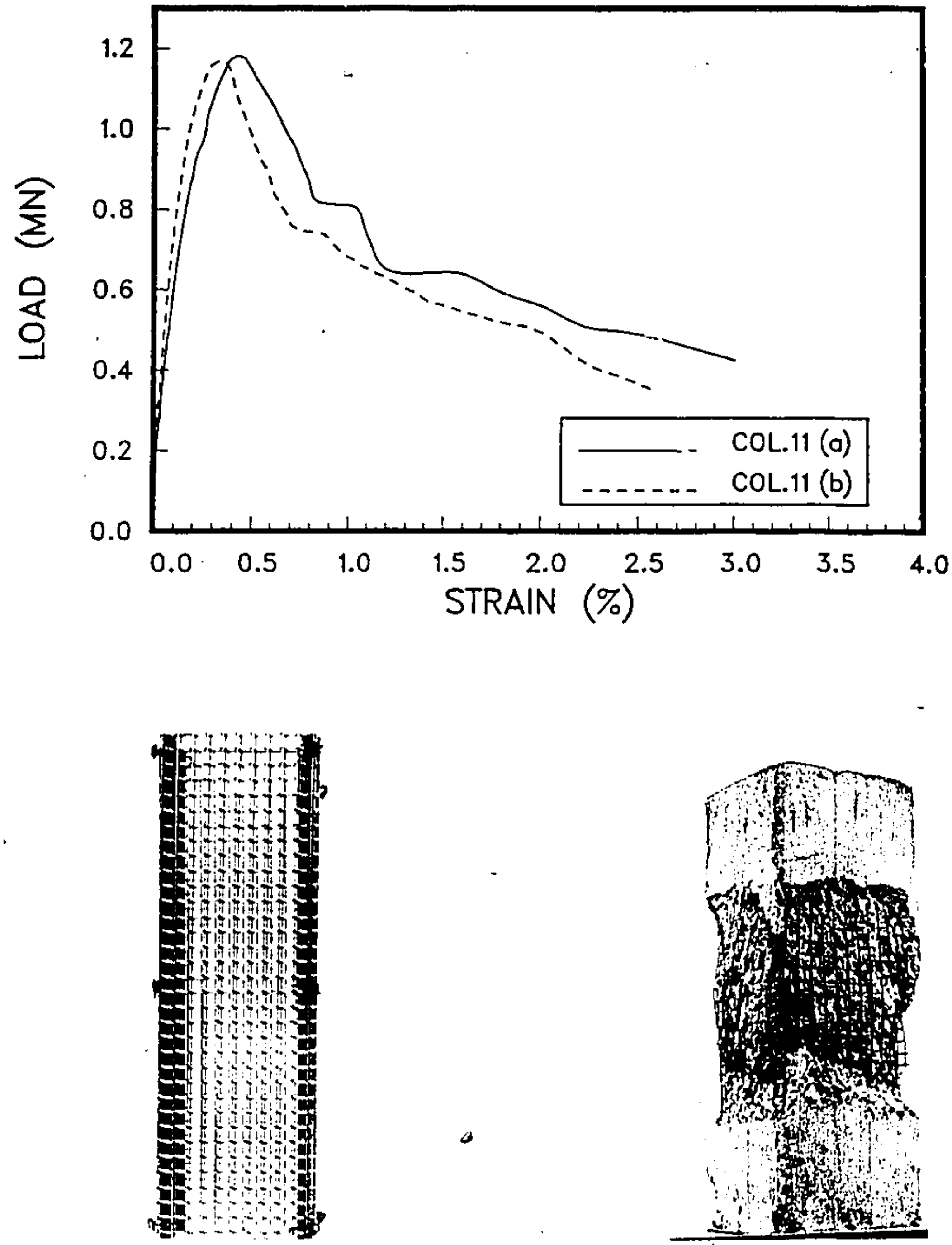

Figure 3.11: Load vs. average strain for columns 11(a) and 11(b)

lateral ties at d/2 with 135 degree hooks and WWF placed in the same fashion as in column pairs 12 and 13. Furthermore WWF in these two columns were different in size.

3.4.2 Observed Behavior

Columns 12(a) and 12 (b)

Columns 12(a) and 12(b) were prepared with 4 No.15 longitudinal bars. Ties with 90 degree hooks, welded at the ends, were placed at d/2 spacing. WWF (25.4 mm x 25.4 mm x14 gage) was placed between the longitudinal bars and the welded ties.

Figure 3.12 illustrates the axial load–axial strain relationships recorded during the tests. The columns behaved in a ductile manner showing high axial deformations with a small drop in the axial load. After the peak load, it was observed that WWF started tearing off at a load corresponding to approximately 75% of the peak load. Tests continued till the middle tie was ruptured at a load of about 55% of the peak load. Ties were observed to rupture at the weld locations. Sudden drop in the load was observed immediately after the rupture of the middle tie accompanied by buckling of longitudinal bars. All strain gages showed that ties were yielding at or shortly before the peak load.

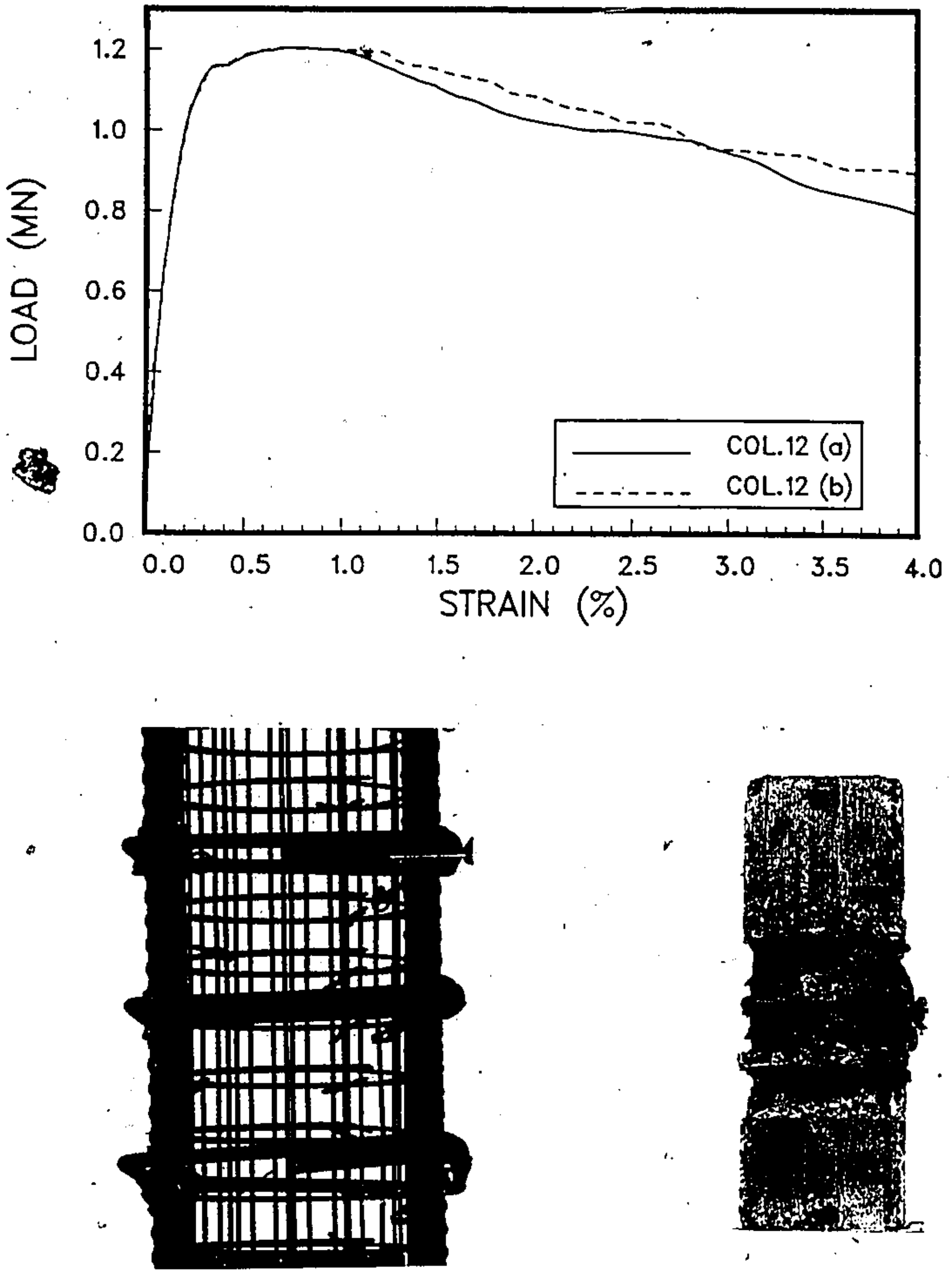

Figure 3.12: Load vs. average strain for columns 12(a) and 12(b)

Columns 13(a) and 13 (b)

Columns 13(a) and 13(b) were prepared with 4 No.15 longitudinal bars. Ties with 90 degree hooks, welded at the ends, were placed at d/2 spacing. WWF (12.7 mm x 12.7 mm x 16 gage) was placed inside the longitudinal bars and the welded ties.

Figure 3.13 illustrates the axial load–axial strain relationships recorded during the tests. The columns behaved in a ductile manner showing high axial deformations with a small drop in the axial load. The falling branch of the load deformation curve was almost a horizontal line. After the peak load, it was observed that WWF started tearing off at a load corresponding to approximately 70% of the peak load. Test continued till the middle tie was ruptured at a load of about 55% of the peak load. Ties were observed to rupture at the weld locations. Sudden drop in the load was observed immediately after the rupture of the middle tie, accompanied by buckling of longitudinal bars. All strain gages showed that the ties were yielding at or shortly before the peak load.

Columns 14(a) and 14 (b)

Columns 14(a) and 14(b) were prepared with 4 No.15 longitudinal bars. Ties with 90 degree hooks, welded at the ends, were placed at d/2 spacing. WWF (12.7 mm x 12.7 mm x 16 gage) was placed between the longitudinal

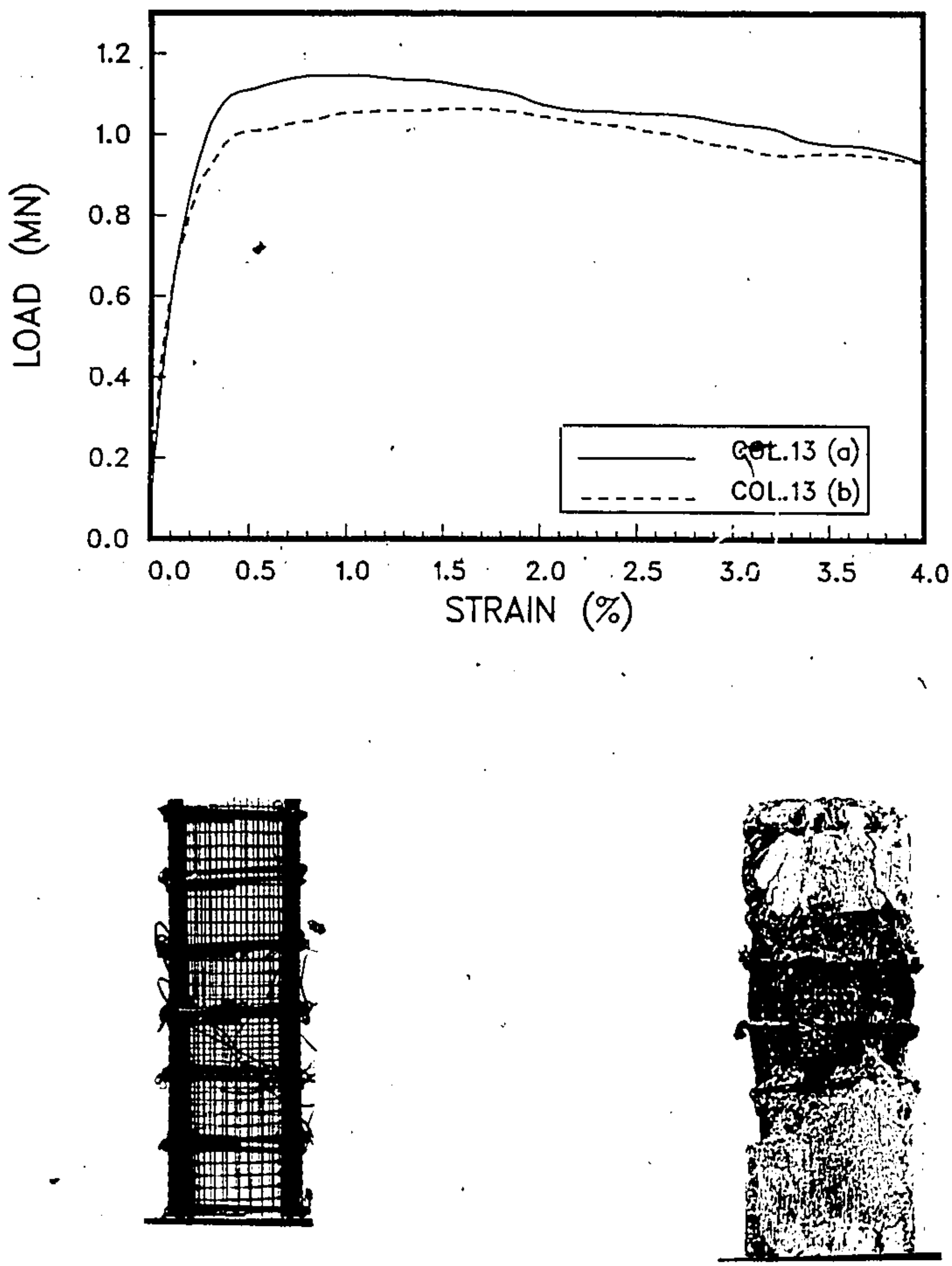

Figure 3.13: Load vs. average strain for columns 13(a) and 13(b)

bars and the welded ties.

Figure 3.14 illustrates the axial load–axial strain relationships recorded during the tests. The columns behaved in a ductile manner. WWF started tearing off at the corners of the column at a load corresponding to 85% of the maximum load carried by the column. Middle ties were observed to rupture at 60% of the peak load, near the corner.The WWF tore off at the same location. Sudden drop in load was observed after the rupture of the middle tie.

Columns 15(a), and 15(b)

Columns 15(a) and 15(b) were prepared with 4 No.15 longitudinal bars. Ties with 135 degree hooks were placed at d/2 spacing. WWF was not used in these specimens.

Figure 3.15 illustrates the axial load–axial strain relationships recorded during the tests. Gradual decrease in load resistance was observed immediately after the peak. At high strain levels the lateral ties were not capable of preventing longitudinal bars from buckling. Opening of ties was observed at the end of the test.

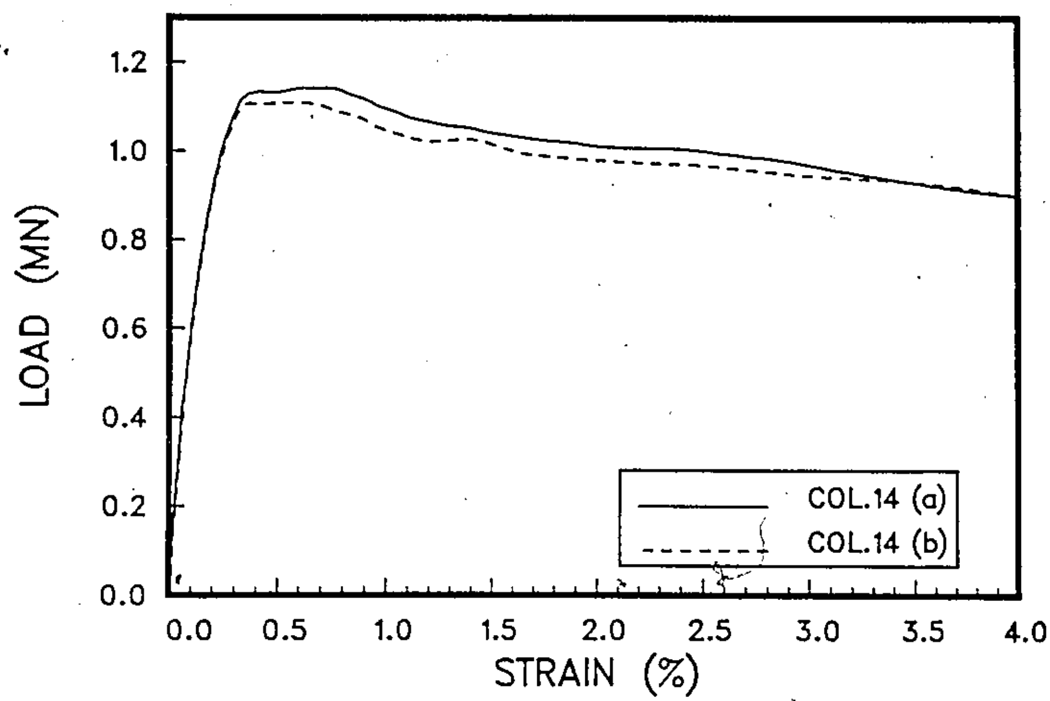

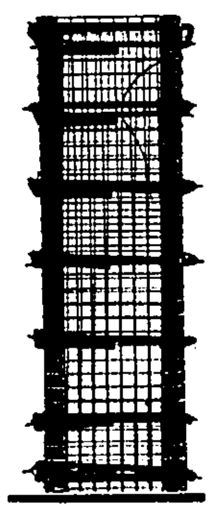

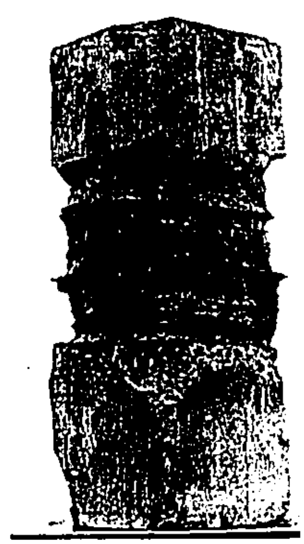

Figure 3.14: Load vs. average strain for columns 14(a) and 14(b)

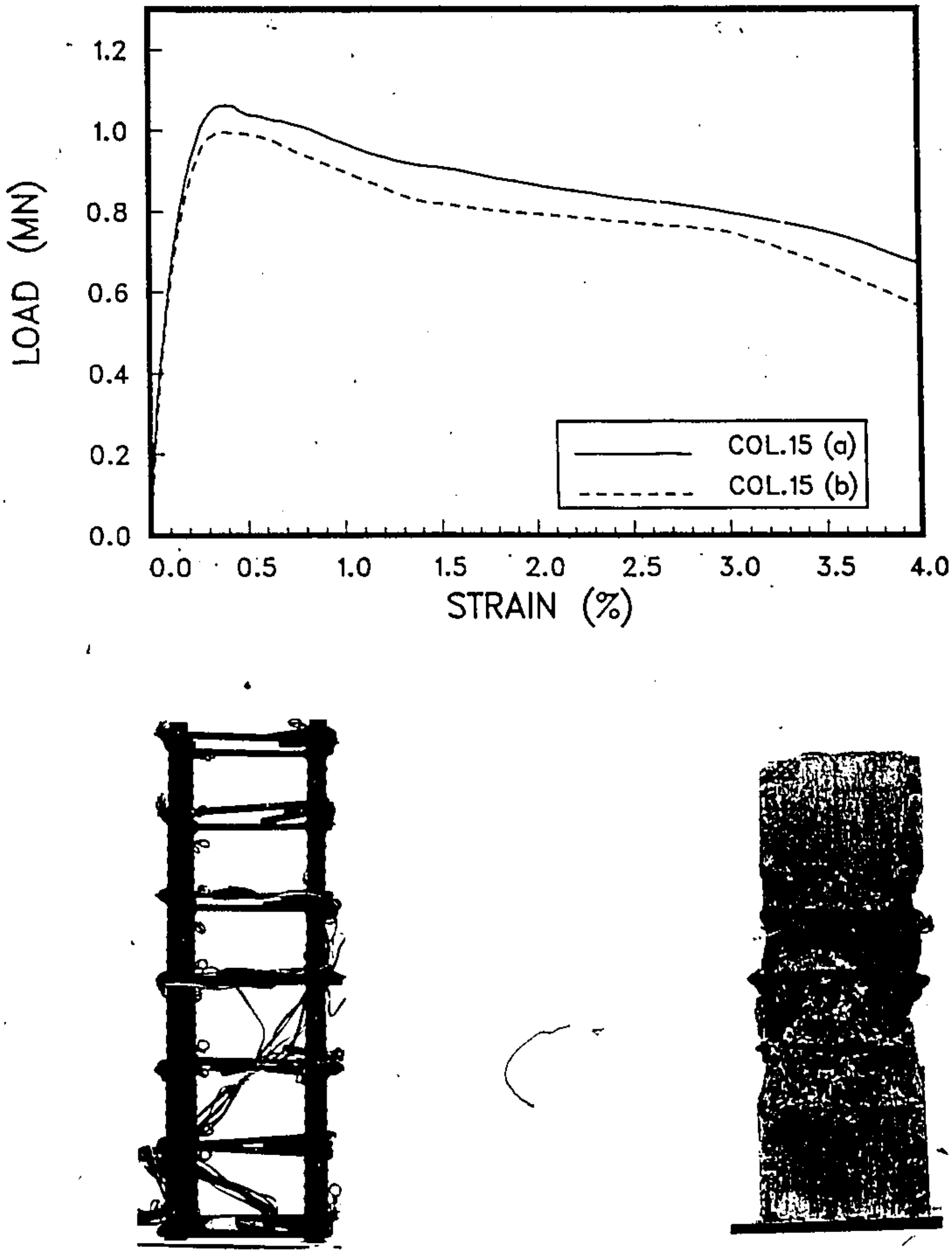

Figure 3.15: Load vs. average strain for columns 15(a) and 15(b)

Columns 16(a), and 16(b)

Columns 16(a) and 16(b) were prepared with 4 No.15 longitudinal bars. Ties with 135 degree hooks were placed at d/4 spacing. WWF was not used in these specimens.

Figure 3.16 illustrates the axial load–axial strain relationships recorded during the tests. The columns behaved in a ductile manner due to the high confinement efficiency of closely spaced ties. Ties were yielding at the ultimate load, and they were observed to open at load corresponding to 50% of the maximum load resisted by the columns. Buckling of longitudinal bars was observed at the end of the test.

It is to be noted that due to excessive deformation of column 16(a) the bottom plate of the testing machine was twisted, and affected the LVDT readings.

Column 17 (a)

Column 17(a) was prepared with 4 No.15 longitudinal bars. Ties with 135 degree hooks were placed at d/2 spacing. WWF (12.7 mm x 12.7 mm x 16 gage) was placed inside the longitudinal and transverse reinforcement.

Figure 3.17 illustrates the axial load–axial strain relationship recorded during the test. In spite of the reduction of the area confined by WWF, the

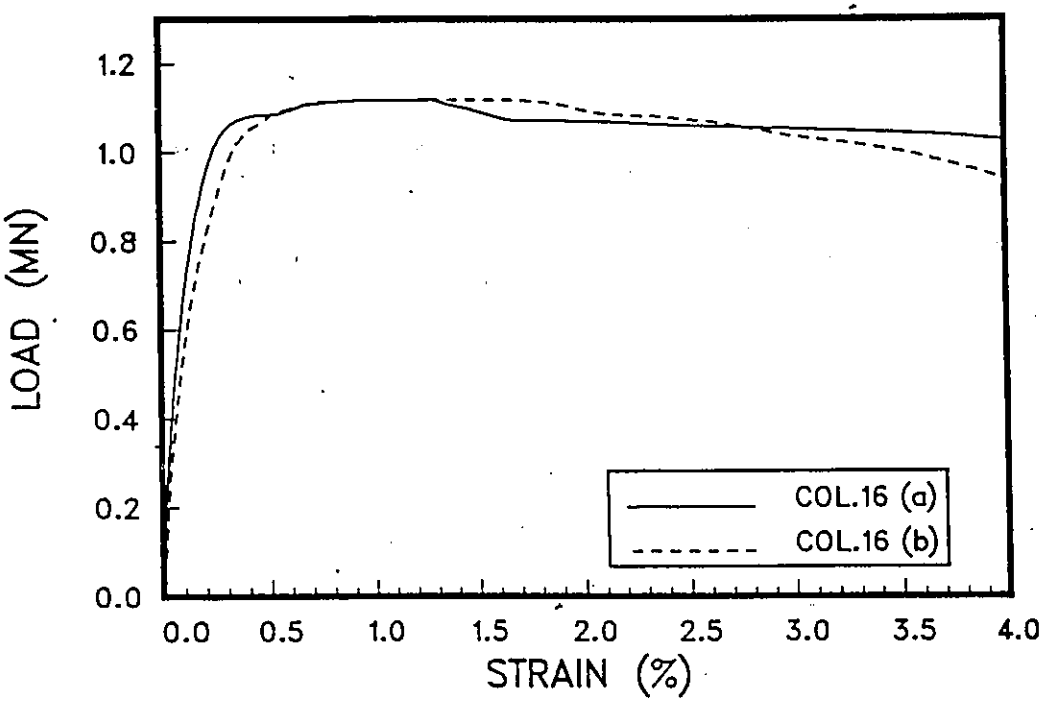

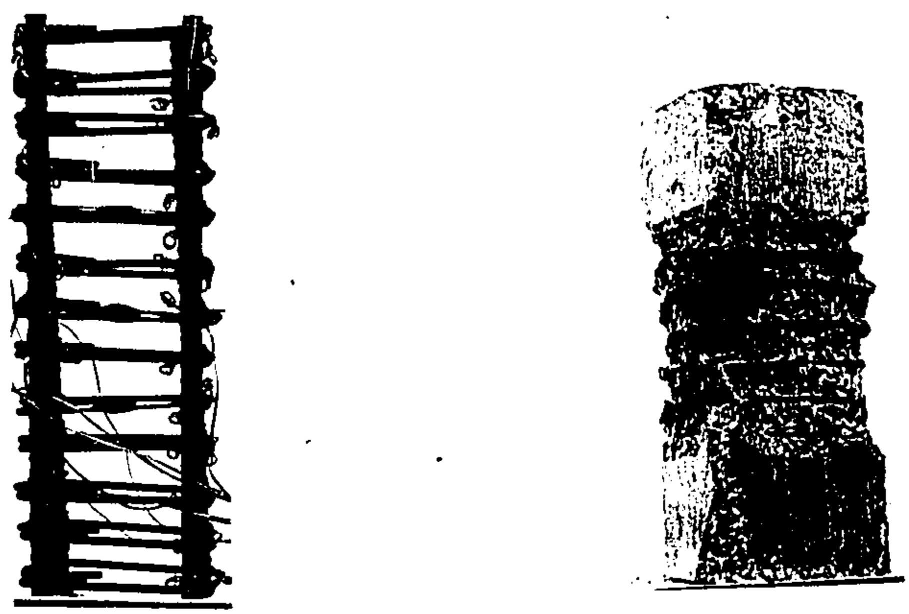

Figure 3.16: Load vs. average strain for columns 16 (a) and 16 (b)

column behaved in a fairly ductile manner. WWF was observed to fracture after the peak at a load corresponding to 75% of the maximum load. Ties were yielding when maximum load was reached and started opening at 45% of the maximum load following the peak load.

Column 18 (a)

Column 18(a) was prepared with 4 No.15 longitudinal bars. Ties with 135 degree hooks were placed at d/2 spacing. WWF (25.4 mm x 25.4 mm x 14 gage) was placed inside the longitudinal and transverse reinforcement.

Figure 3.18 illustrates the axial load–axial strain relationship recorded during the test. The column behaved in a ductile manner, showing the same trend observed in column 17. WWF was observed to fracture after the peak at a load corresponding to 80% of the maximum load. Ties were yielding when maximum load was reached and started opening at 45% of the maximum load following the peak load.

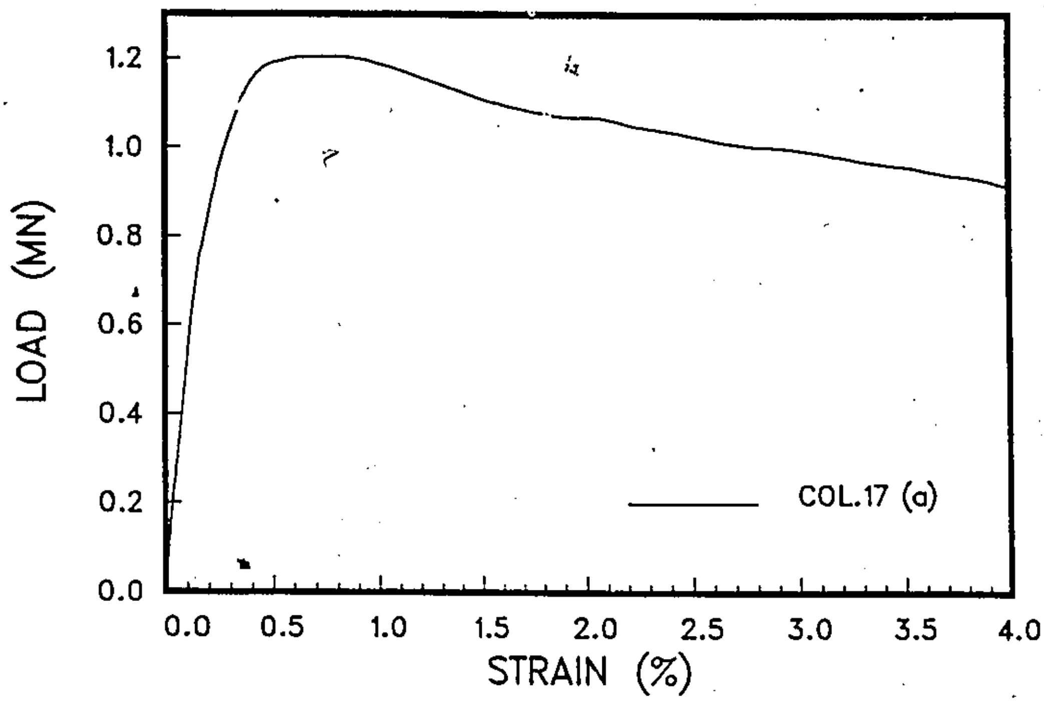

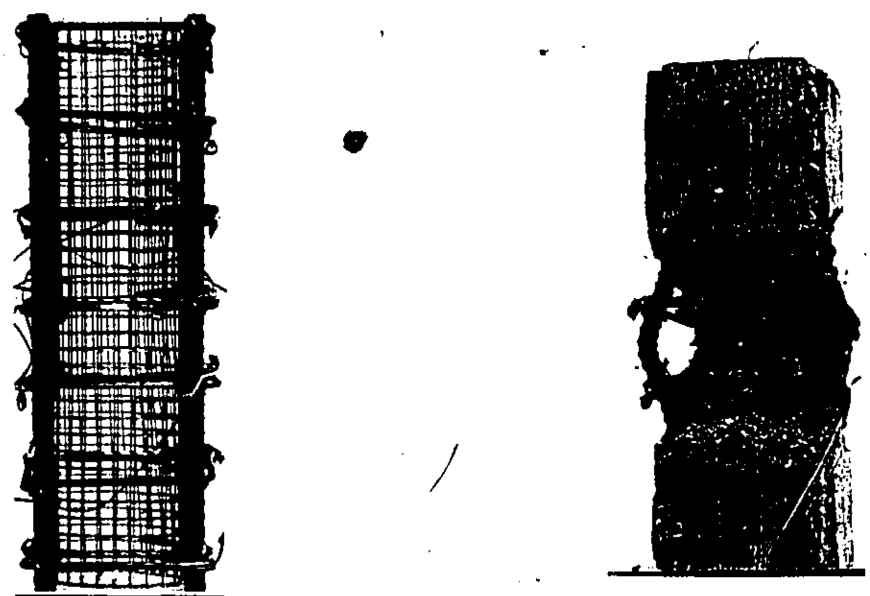

Figure 3.17: Load vs. average strain for column 17 (a)

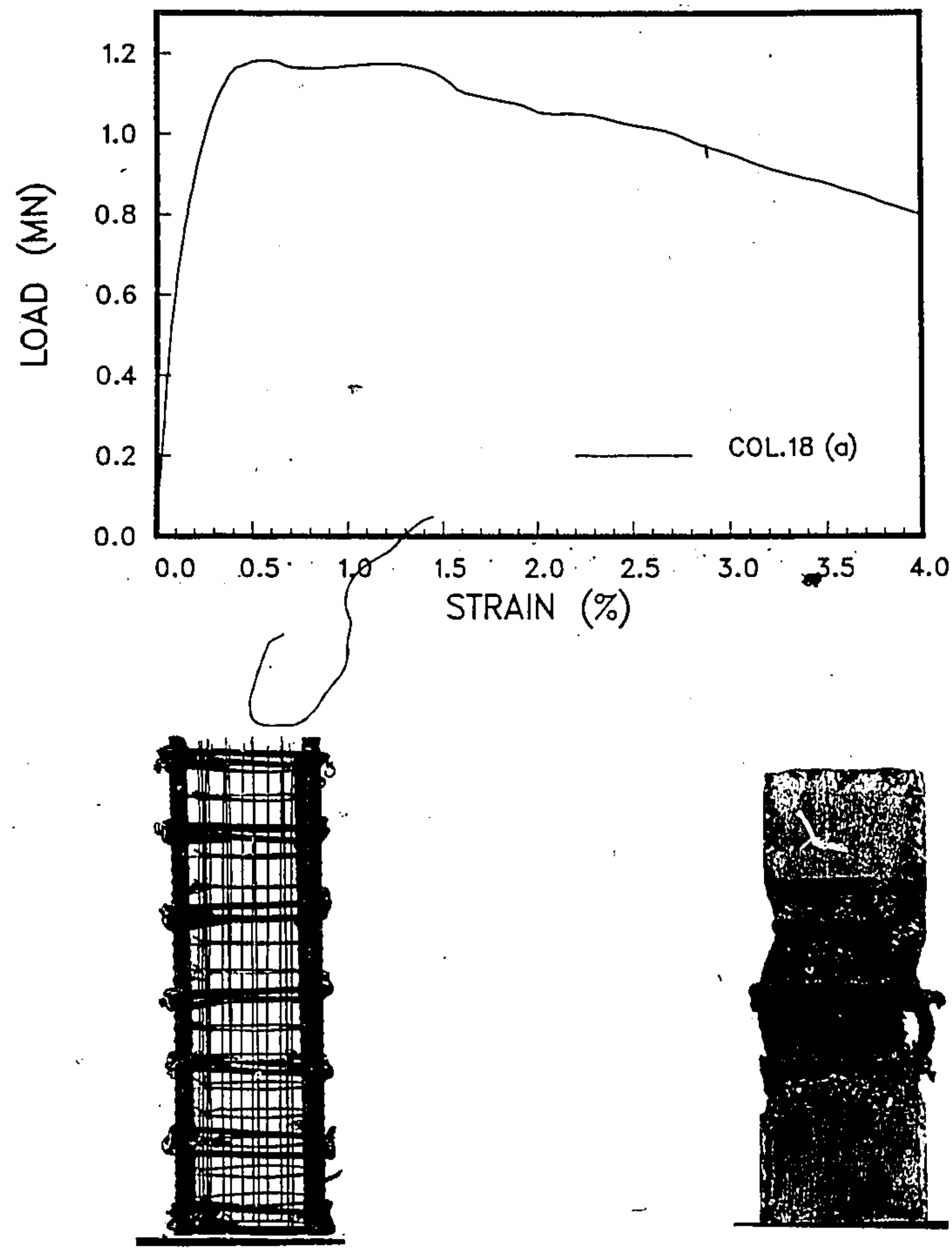

Figure 3.18: Load vs. average strain for column 18

Chapter 4

Analysis of Test Results

This chapter outlines the techniques used to evaluate test results. It provides comparison of test results and discussions of the effects of different test variables considered in the program. Analytical predictions of columns are presented in chapter 5.

4.1 Evaluation of Test Data

The test data was evaluated to show two fundamental mechanical properties of confined concrete namely, the strength and ductility. In order to study the characteristics of confined concrete, it was necessary to separate the contribution of steel to the behavior of test specimens. This would provide information on strength and ductility increase due to confinement. The following procedure was followed to obtain concrete axial load versus axial strain relationship from the recorded test data:

1. Experimental load carried by concrete was calculated as follows :

$$P_{conc} = P_{col} - P_{st} \tag{4.1}$$

2. It was assumed that the longitudinal strain in steel is equal to that of the surrounding concrete. Experiments showed that this assumption is quite accurate before yielding of steel. However, after yielding of steel this equality may not be valid [1].

$$\epsilon_c = \epsilon_s \tag{4.2}$$

3. Three separate models for stress–strain relationship of longitudinal steel were used. These models are shown in Figure 4.1. The strain hardening of steel was not considered in model 2. A gradual reduction of stress, carried by longitudinal column steel, was assumed in model 3. This was felt essential in the light of experimental observations. Longitudinal bars were observed to start bending shortly after the ultimate load was exceeded. Bending of bars was not always in the form of buckling between the ties. Columns with closely spaced ties, with or without WWF, showed gradual bending with bending spanning a distance longer than the tie spacing. This is shown in Figures 3.1 through 3.18. Similar figures were shown by other researchers [1] indicating bending of bars starting shortly after peak load.

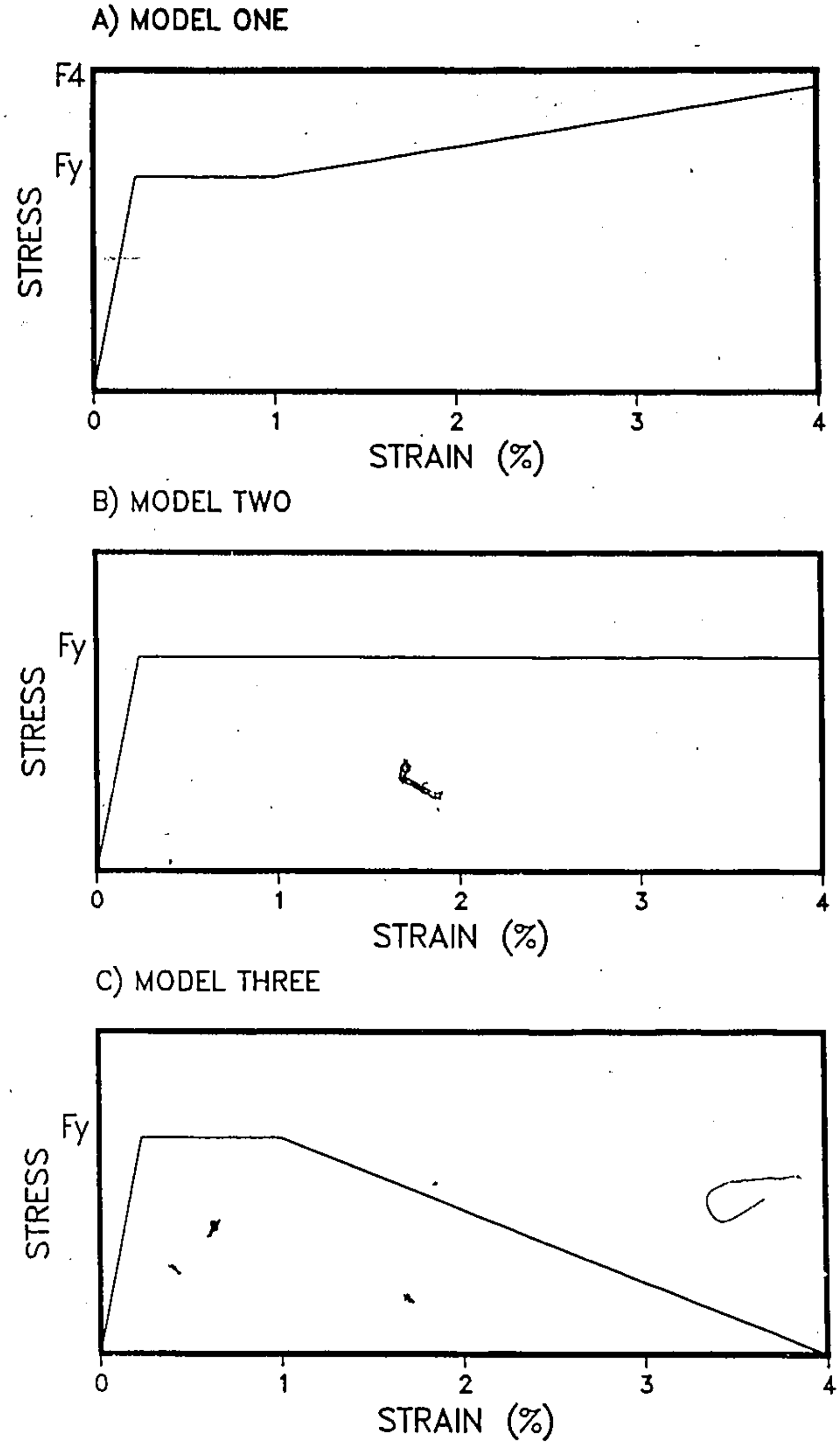

Figure 4.1: Stress vs. strain for longitudinal steel

During the tests as bending of bars took place, unloading of steel followed. When one or more longitudinal bars started bending, severe eccentricity was indicated by the substantial deviation in the LVDT readings. As bending of all four bars was underway, the LVDT readings approached approximately the same value. While the eccentric behavior of columns can be attributed to nonuniform column properties and uneven spalling of concrete, the behavior at high strain levels is influenced significantly by the behavior of reinforcement. Appendix A contains the individual LVDT readings for columns.

Analyses of columns in set one, based on the three steel models discussed above shows that:

- Steel models 1 and 2 overestimate the load carried by steel at high strain range. This can be seen by examining the load deformation relationship of column 5(b) which is the least confined column in set one. Figure 4.2 shows the load carried by concrete alone, and was obtained by separating the steel contribution based on the previously discussed steel models. If models 1 and 2 represented the true behavior of steel, the concrete in the column would have carried negative axial load beyond 3% and 3.5% axial strain levels respectively. Because this is not realistic, models 1 and 2 do not represent the actual behavior of steel in the column.
- Model 3, on the other hand, underestimates the load carried by steel. Column 3, which has the best confinement among the

columns in set one, was analyzed using this model. It showed that concrete resistance to axial compression continued to increase even at a strain of 4%. This was not realistic. Figure 4.3 illustrates the analysis results.

In the absence of sufficient test data to establish the behavior of steel stress-strain relationship in a column, it was not possible to establish the concrete stress-strain relationship accurately. However, in predicting member response, concrete and steel contributions are superimposed. Consequently, even if the behavior of steel in concrete is not known accurately, provided the same material properties are used in seperating the concrete response from the member response, and superimposing the two material responses to find the member response, no error is introduced in the procedure. Previos researchers adopted model 1 as the correct representation of steel stress- strain characteristics in a column. To be consistent with the previos research, and to be able to compare the results of this investigation with those of the others, Model 1 was also adopted here to evaluate the test data.

4. Based on the previous research [1,8], which confirms the observed behavior in the present test program, it was assumed that:

   - Cracks started appearing on concrete cover at longitudinal strain of 0.2%. Therefore total concrete area, including the cover, was assumed effective in resisting the load up to 0.2% of axial strain.

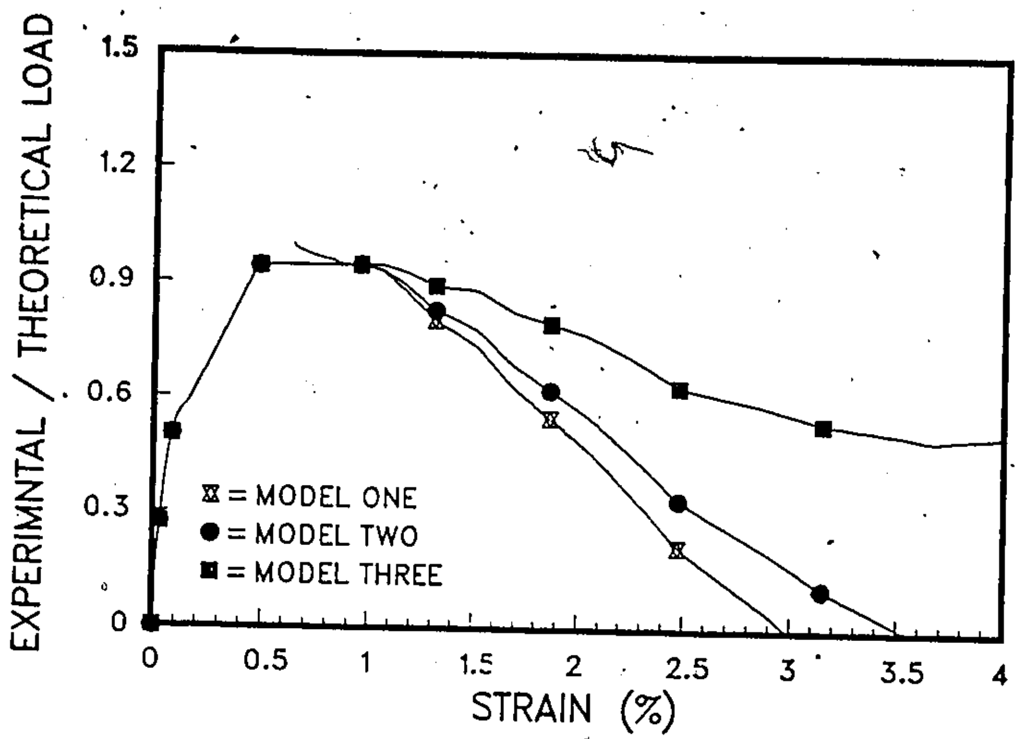

Figure 4.2: Axial load carried by concrete vs. strain for column 5(b) based on three models for steel

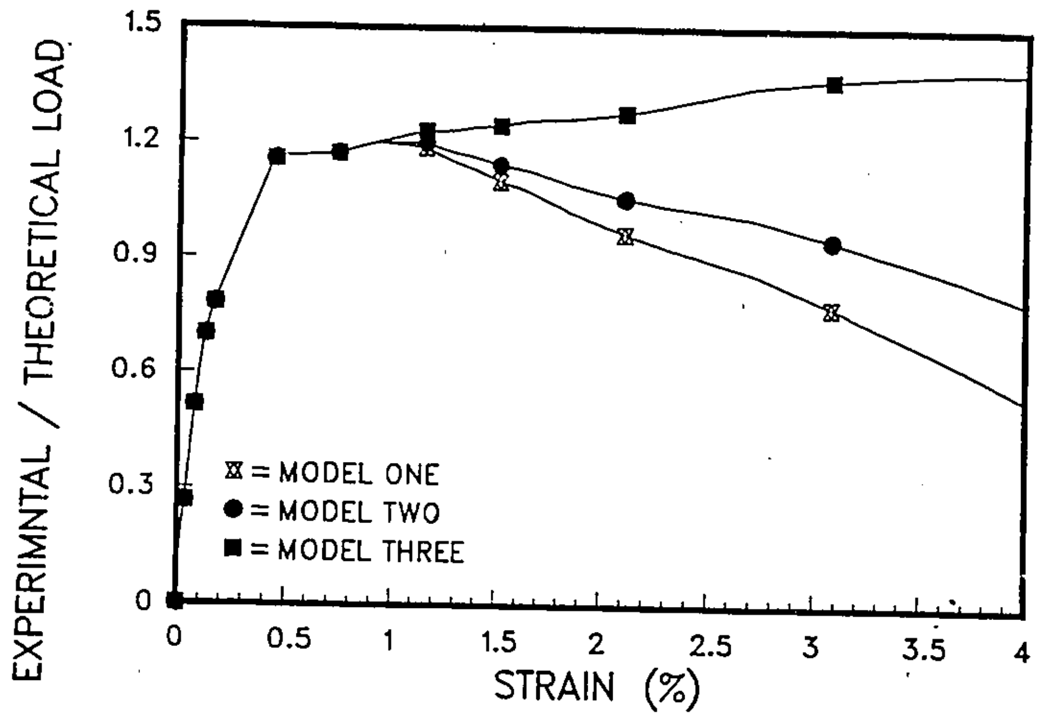

Figure 4.3: Axial load carried by concrete vs. strain for column 3(b) based on three models for steel

- Concrete cover was assumed to be spalled completely at a strain of 0.4%, although the actual value varies between 0.4 and 0.5%. Consequently, only the core concrete was taken as effective concrete resisting the load beyond 0.4% of axial strain.
- For the strain range between 0.2 and 0.4%, a gradual transition was assumed between the gross concrete area and the core area.

The above procedure was followed to establish the load resistance by concrete under increasing axial strain. These relationships for columns in set three are given in Appendix B.

The peak loads carried by concrete in different columns are tabulated and compared with analytical predictions based on unconfined concrete. Table 4.1, 4.2 and 4.3 present the results for set one, two and three respectively. It is to be noted however that the values presented in these tables are the average values for each pair of columns with identical test parameters. In some cases, if one of the columns in a pair did not show reliable results, this set of results was not included and the other companion column results were used. In such cases the actual column specimens, whose results were used, are indicated in the tables as (a) or (b). The load parameters presented in these tables are defined as follows:

$$P_o = f'_c(A_g - A_s) + A_s f_y \quad (4.3)$$

$$P_{oc} = f'_c(A_g - A_s) \quad (4.4)$$

$$P_{occ} = f'_c(A_{co} - A_s) \quad (4.5)$$

Column No.	1(b)	2	3	4(a)	5(b)
$P_o(kN)$	1191	1193	1170	1170	1170
$P_{oc}(kN)$	791	791	794	794	794
$P_{occ}(kN)$	622	622	625	625	625
$P_{test}(kN)$	1217	1161	1141	1023	968
$P_{cmax}(kN)$	817	760	765	647	592
P_{test}/P_o	1.022	0.973	0.975	0.870	0.827
P_{cmax}/P_{occ}	1.313	1.222	1.224	1.036	0.948
$\varepsilon_{c0}\%$	0.718	0.730	0.550	0.380	0.540
$\varepsilon_{c85}\%$	1.670	1.730	2.420	1.400	1.370
$\delta P(kN)$	416	503	147	315	425

Table 4.1: Results for columns in set one

Column No.	6	7(b)	8	9	10	11(b)
$P_o(kN)$	1175	1175	1225	1225	1225	1195
$P_{oc}(kN)$	983	983	978	978	978	980
$P_{occ}(kN)$	722	722	721	721	721	681
$P_{test}(kN)$	1148	1084	1032	1099	1138	1170
$P_{cmax}(kN)$	956	892	785	852	891	954
P_{test}/P_o	0.977	0.922	0.842	0.895	0.928	0.978
P_{cmax}/P_{occ}	1.324	1.235	1.089	1.182	1.235	1.400
$\varepsilon_{c0}\%$	0.521	0.325	0.308	0.337	0.347	0.325
$\varepsilon_{c85}\%$	1.94	0.715	0.640	0.655	0.670	0.490
$\delta P(kN)$	230	429	495	600	560	770

Table 4.2: Results for columns in set two

Column No.	12	13	14	15	16(b)	17	18
$P_o(kN)$	1119	1117	1117	1095	1095	1117	1119
$P_{oc}(kN)$	717	717	717	719	719	717	717
$P_{occ}(kN)$	564	564	564	566	566	564	564
$P_{test}(kN)$	1201	1104	1124	1028	1117	1203	1181
$P_{cmax}(kN)$	799	704	724	652	741	803	780
P_{test}/P_o	1.073	0.988	1.007	0.940	1.020	1.076	1.056
P_{cmax}/P_{occ}	1.416	1.248	1.282	1.150	1.310	1.420	1.380
$\varepsilon_{c0}\%$	0.700	1.227	0.548	0.404	0.908	0.788	0.521
$\varepsilon_{c85}\%$	2.44	4.02	2.94	1.46	3.96	2.67	2.72
$\delta P(kN)$	196	123	154	217	84	175	167

Table 4.3: Results for columns in set three

In columns where WWF was used, loads are defined as follows :

$$P_o = f_c'(A_g - A_s - A_s') + A_s f_y + A_s' f_{ywwf}' \qquad (4.6)$$

$$P_{oc} = f_c'(A_g - A_s - A_s') \qquad (4.7)$$

$$P_{occ} = f_c'(A_{co} - A_s - A_s') \qquad (4.8)$$

It is important to note that, in the above expressions, the cylinder strength of concrete is assumed to be the same as the concrete strength in the specimen. This assumption was made because of the similarities in specimen size and a standard cylinder.

Strength enhancement in core concrete due to confinement is indicated in Tables 4.1 through 4.3 by the ratio P_{cmax}/P_{occ}. However, if the concrete cover was not spalled completely at peak load, this ratio overestimates the strength enhancement.

The second important characteristic of confined concrete is the increase in ductility. Ductility in a general sense, is defined as the ability to deform without a significant loss of strength. This is indicated by the slope of the load strain relationship of the concrete. To quantify ductility of concrete the following techniques were used:

- Strain at 85% of Peak

  In this procedure the strain corresponding to 85% of the maximum load, within the falling branch of the load strain curve, was found. An increase at this strain level would indicate an increase in ductility. These values are also tabulated in Tables 4.1 through 4.3 for each column. These tables also include strains at peak load. The ratio of the strains at 85% of peak and peak loads gives the ductility ratio.

- Slope of Unloading Branch of Load–Strain Diagram

  The rate at which the falling branch in the load strain diagram is dropping may be used as another measure of column ductility. Tables 4.1 through 4.3 include the drop in load between the peak and the strain corresponding to peak plus 2% strain. These values are indicated as δP in the tables.

- Energy Absorption

  Energy absorbed by the specimen during deformation can also be used as a measure of ductility. Here one has to integrate the area under the load strain curve at different strain levels. The absorbed energy versus strain diagram provides a general idea about the column ductility for comparison purposes. The absorbed energy versus strain is shown in Figures 4.4, 4.5 and 4.6.

It is important to note that although the above three techniques provide some measure of ductility, these measures do not quantify the overall column ductility in an absolute term. Hence, one should exercise some engineering judgment in describing the overall column ductility.

4.2 Effects of Test Variables

Variables affecting concrete confinement, which were considered in this experimental study, are discussed in this section. The following main variables were studied in the test program:

1. Tie spacing and amount of lateral reinforcement.
2. Tie hooks.
3. WWF as confinement steel when placed between the longitudinal and transverse reinforcement.
4. WWF as confinement steel when placed in the concrete core.

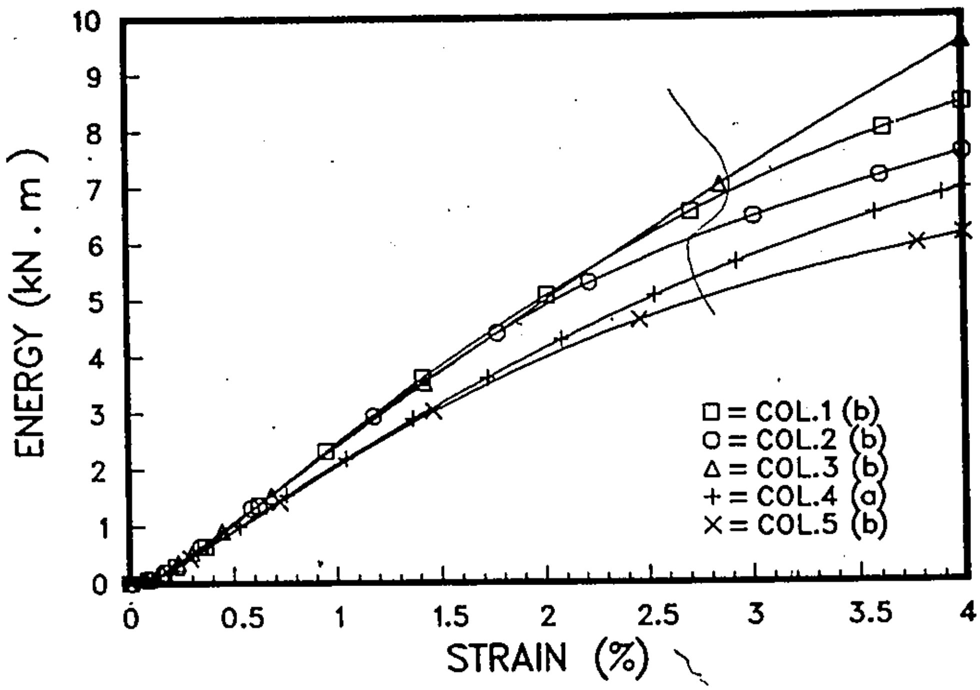

Figure 4.4: Absorbed Energy vs Strain for set one

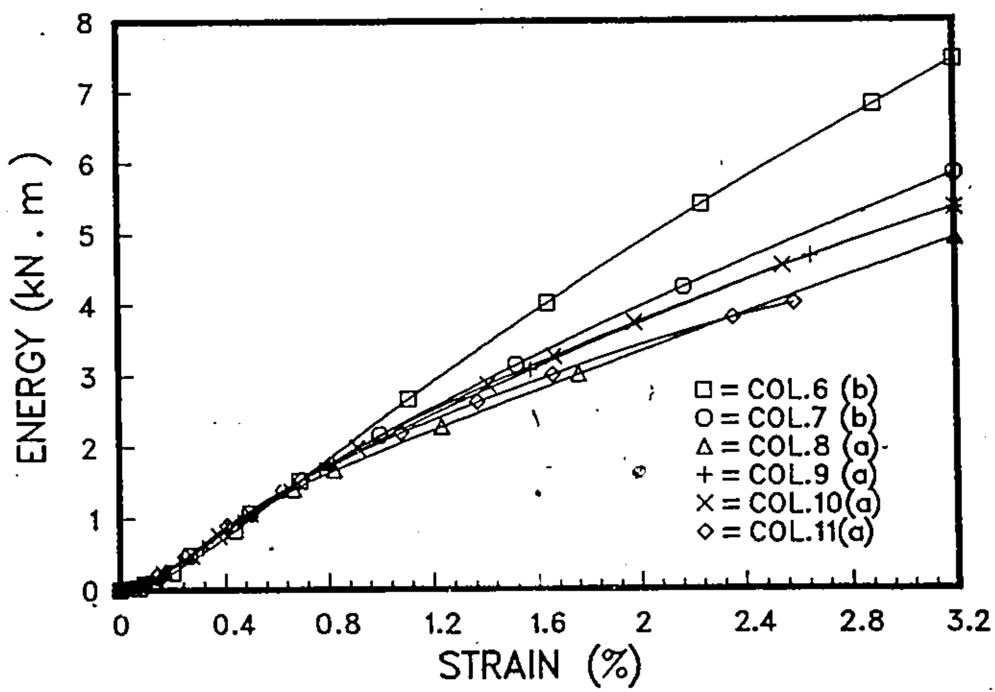

Figure 4.5: Absorbed Energy vs Strain for set two

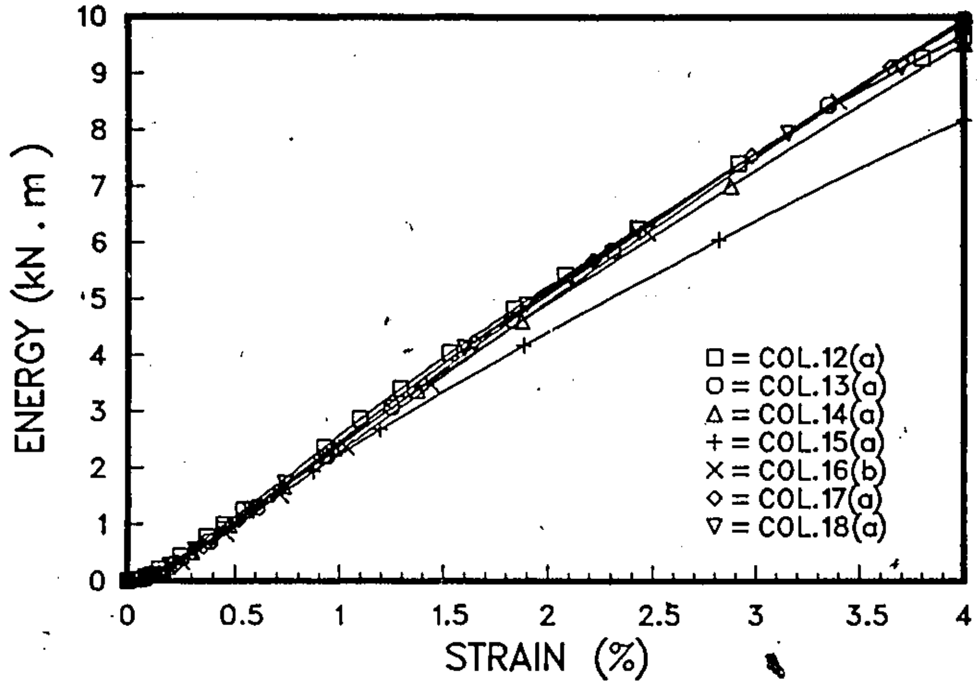

Figure 4.6: Absorbed Energy vs Strain for set three

5. WWF as lateral reinforcement without the ties.

In addition the following variables were considered within some of the main variables:

- WWF size.
- WWF hook details.
- Welding of tie steel.

4.2.1 Tie Spacing and Amount of Lateral Reinforcement

The combined effect of tie spacing and amount of lateral reinforcement was studied in each of the three sets of test specimens. A total of 12 columns were tested for this purpose with ties having 135 degree hooks. Six columns had d/2 tie spacing while the companian six had d/4 spacing. Comparisons of representative pairs are shown in Figures 4.7 through 4.9. The results confirm the findings of previous investigators. Reducing tie spacing increases the area of the effectively confined core concrete and hence increases both strength an ductility. The increase in the amount of lateral reinforcement increases the lateral pressure on concrete provided by tie steel and hence improves concrete strength and ductility.

4.2.2 Tie Hooks

Previous investigators have reported that 90 degree hooks perform poorly under lateral pressure and tend to open up early in response. Hook angle was an important consideration in the test program since it affected the detailing of the WWF to be used as confinement reinforcement. Four columns with d/2 tie spacing were tested for this purpose. Two of the columns had 90 degree hooks, while the other two companion columns had 135 degree hooks. The results are compared in Figure 4.10 for two columns. As can be observed from this figure, columns with 135 degree hooks, well anchored into the core concrete behaved superior to those with 90 degree hooks.

The effect of tie hook was further studied in conjunction with the other variables. Generally, it was observed that, at closer tie spacing, the effect of hook angle becomes more pronounced. This is illustrated when columns

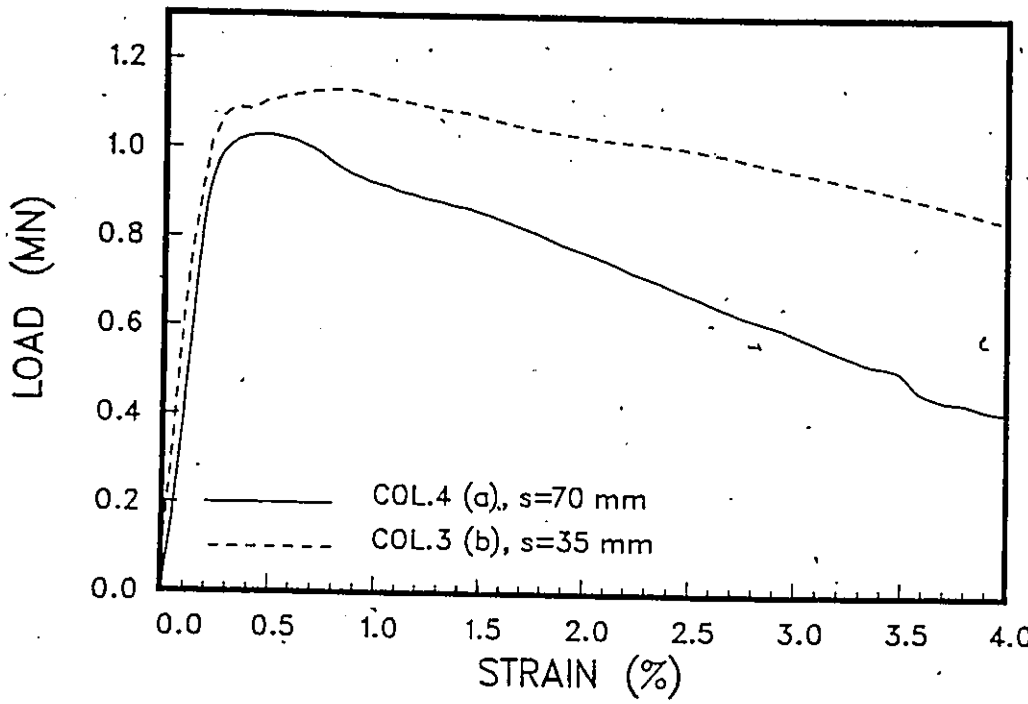

Figure 4.7: Axial load vs. strain for columns 3(b), and 4(a)

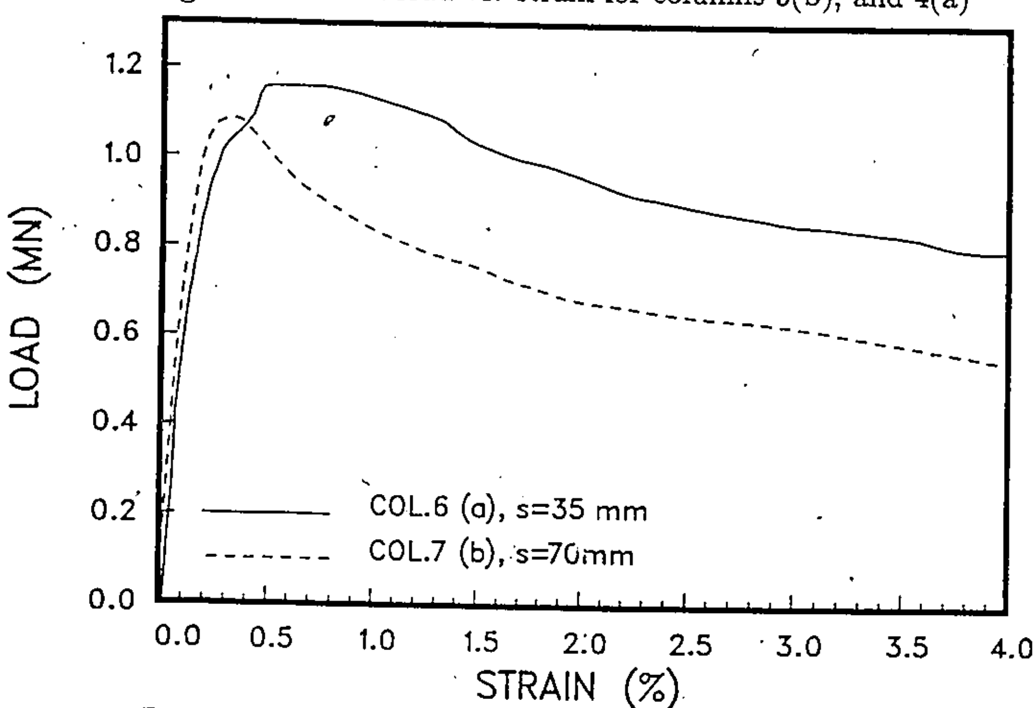

Figure 4.8: Axial load vs. strain for columns 6(a), and 7(b)

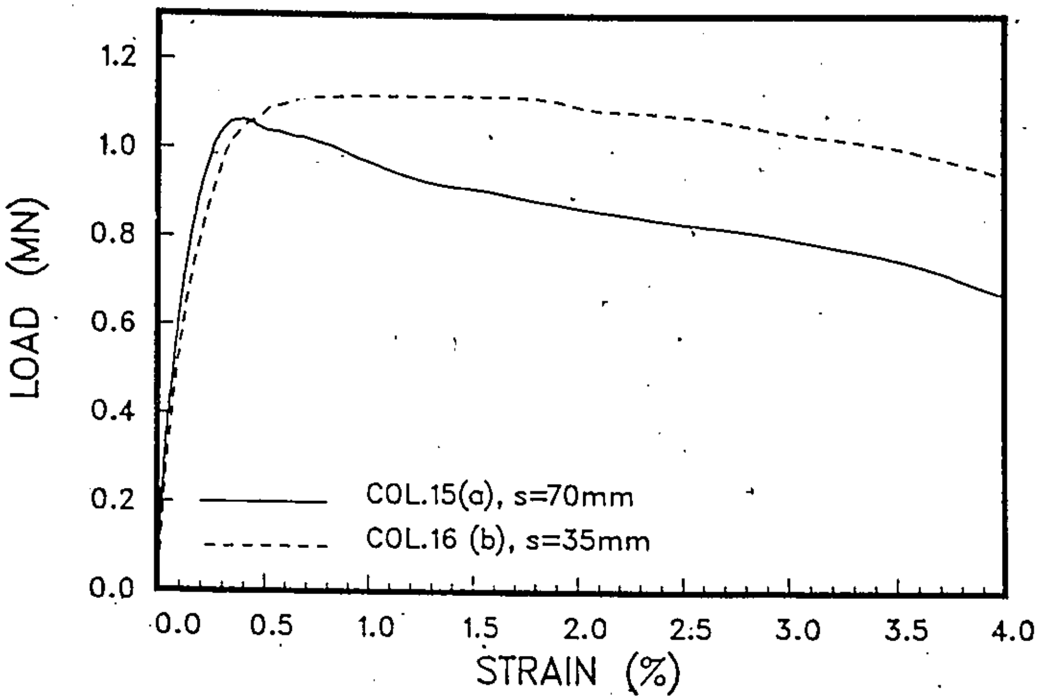

Figure 4.9: Axial load vs. strain for columns 15(a), and 16(b)

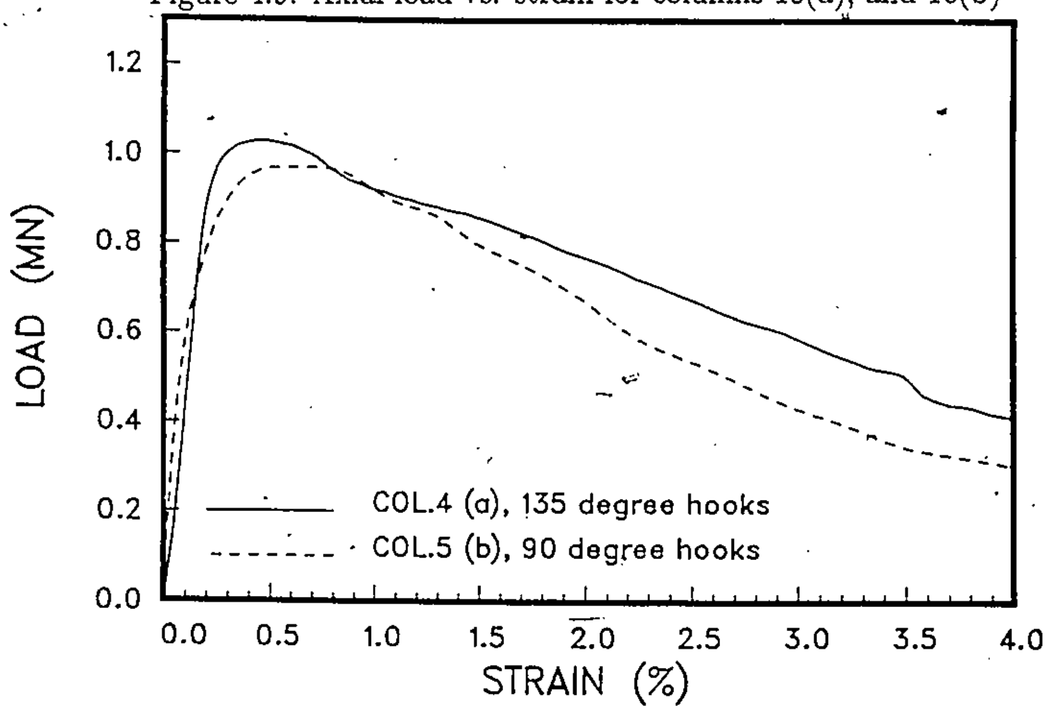

Figure 4.10: Axial load vs. strain for columns 4(a) and 5(b)

with WWF and ties are discussed.

4.2.3 WWF as Confinement Steel When Placed Between Longitudinal and Tie Reinforcement

The effect of WWF as confinement reinforcement was investigated extensively. Two pairs of columns were prepared in set one with WWF placed between the longitudinal and tie reinforcement. Each pair had a different size of WWF. Tie spacing was d/2. The ties had 90 degree hooks and the WWF had a 90 degree overlap at the opposite corner of the columns. One column from each pair is compared with a column without the WWF, Colum 5(b), in Figure 4.11. The ultimate strength for columns with WWF (1(b) and 2(b)) was increased significantly as compared to column 5 (b) with ties alone. In addition, higher strain was achieved at peak loads. This behavior was due to the effect of WWF which confined the core concrete and reduced the pressure on the ties. Once the ties opened, WWF lost the support and started tearing off, due to the concrete and longitudinal steel pressures. Hence confinement became inefficient. The slope of the unloading branch of load – strain diagram for columns 1(b) and 2(b) is about the same for column 5(b). This indicates the inefficiency of WWF once the ties were opened. Although the column behavior was improved using WWF, Figure 4.12 shows that this improvement did not produce a column as good as a column with 135 degree hooks at d/4 spacing, which is required by the current design practice.

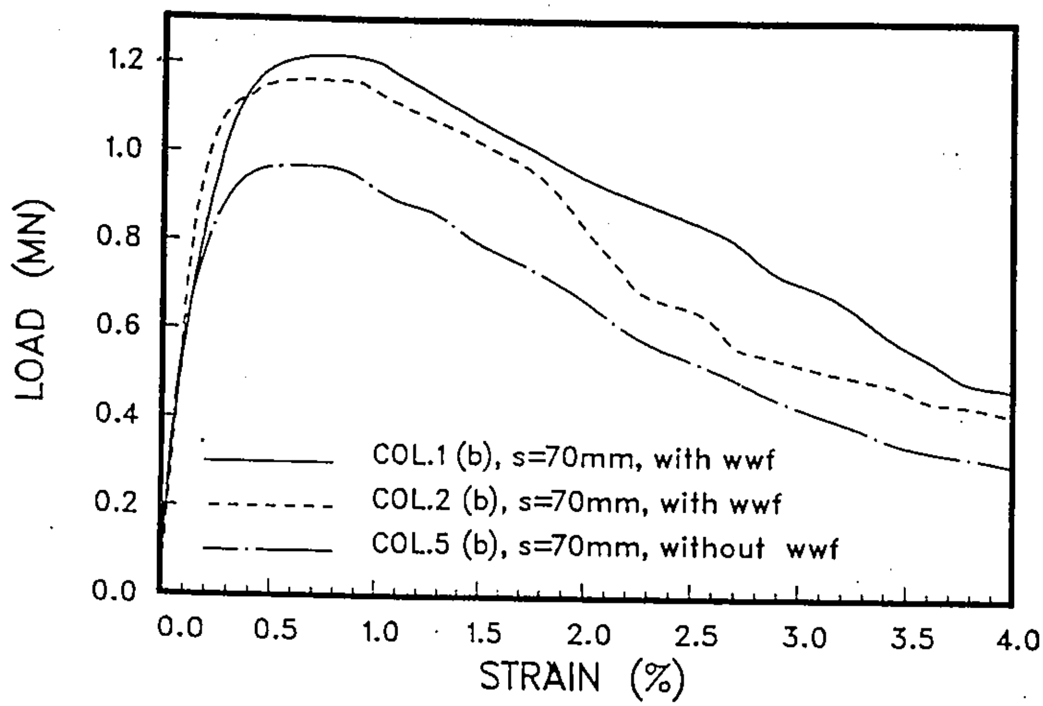

Figure 4.11: Axial load vs. strain for columns 1(b), 2(b) and 5(b)

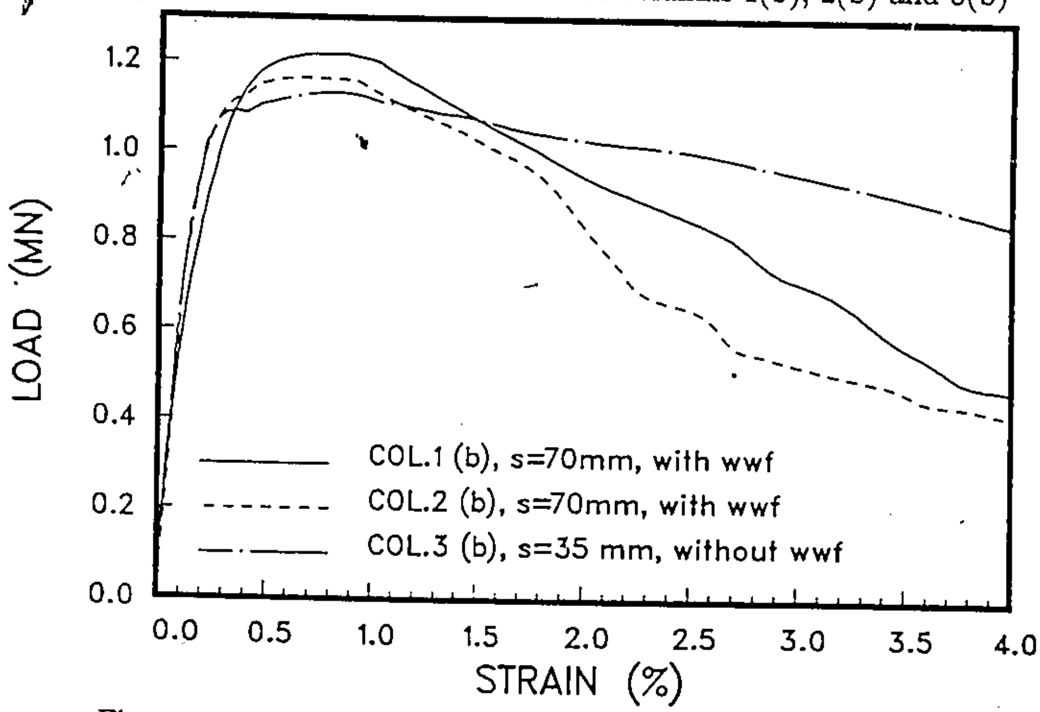

Figure 4.12: Axial load vs. strain for columns 1(b), 2(b) and 3(b)

Two sizes of WWF were used as confinement steel in set one. Column pair 2, although had approximately the same percentage of transverse steel, had coarser mesh size compared with column pair 1. The responses shown in Figures 4.11 and 4.12 illustrate that the coarser size mesh produces a slightly higher loss of strength at high strain region.

An additional pair of columns were prepared in set three with WWF and ties at d/2 spacing, where ties had 90 degree hooks welded at the overlaps to prevent opening under lateral pressure. These hooks were used to substitute for the 135 degree hooks which could not be used due to the presence of WWF.

One of the columns in the pair, column 14 (a), is compared in Figure 4.13 with column 15 (a) which had ties with 135 degree hooks spaced at d/2. The results indicate an improvement in strength and ductility with the use of WWF as confinement steel. Furthermore the improved response due to WWF is comparable to the response of column 16 (b) without the WWF but with twice as many ties spaced at d/4. This is shown in Figure 4.14. Since column 16 (b) represents the current design practice, the achievement of similar strength and ductility response with half as many ties at twice the tie spacing, attributed to WWF, is regarded as a favorable indication of possible use of WWF as confinement steel.

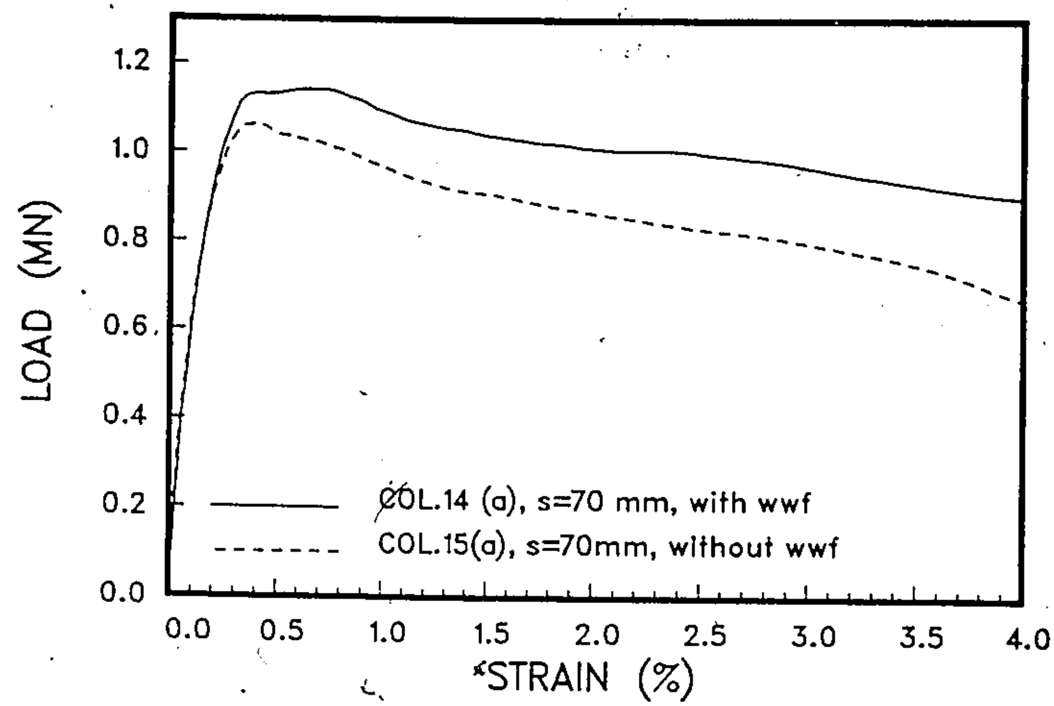

Figure 4.13: Axial load vs. strain for columns 14(a) and 15(a)

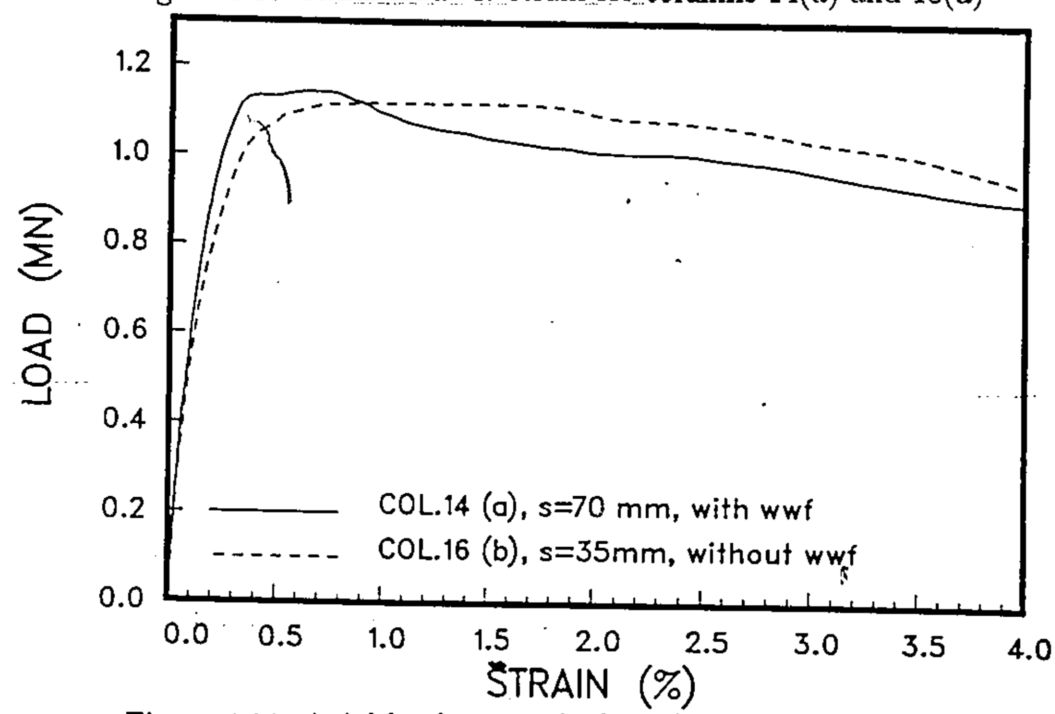

Figure 4.14: Axial load vs. strain for columns 14(a) and 16(b)

4.2.4 WWF as Confinement Steel When Placed in the Concrete Core

The failure mechanism of the columns with WWF placed between the longitudinal and transverse reinforcement indicated that the longitudinal bars would exert pressure on WWF, causing tearing along the corners. This would limit the usefulness of WWF as confinement steel. Therefore another reinforcement arrangement was tried where WWF was placed inside the longitudinal reinforcement to confine the core concrete while the ties were providing lateral support to the vertical bars.

Column pairs 12 and 13 were prepared with ties at d/2 spacing, having 90 degree hooks, welded at the overlaps. The responses of one column from each pair are compared with that of column 15(a) with the same tie spacing but without the WWF. This is shown in Figure 4.15. The results indicate a significant improvement in strength and ductility with WWF. The comparison of the same two columns with column 16(b), with twice as many ties at d/4 spacing, indicates a similar response. This is shown in Figure 4.16.

The same WWF arrangement was repeated in set three with ties having 135 degree hooks, instead of the welded 90 degree hooks used in column pairs 12 and 13. The responses of these columns are compared with columns 15(a) and 16(b) in Figures 4.17 and 4.18 respectively. The same improvements noted in column pairs 12 and 13 are also noted in column pair 17 and 18.

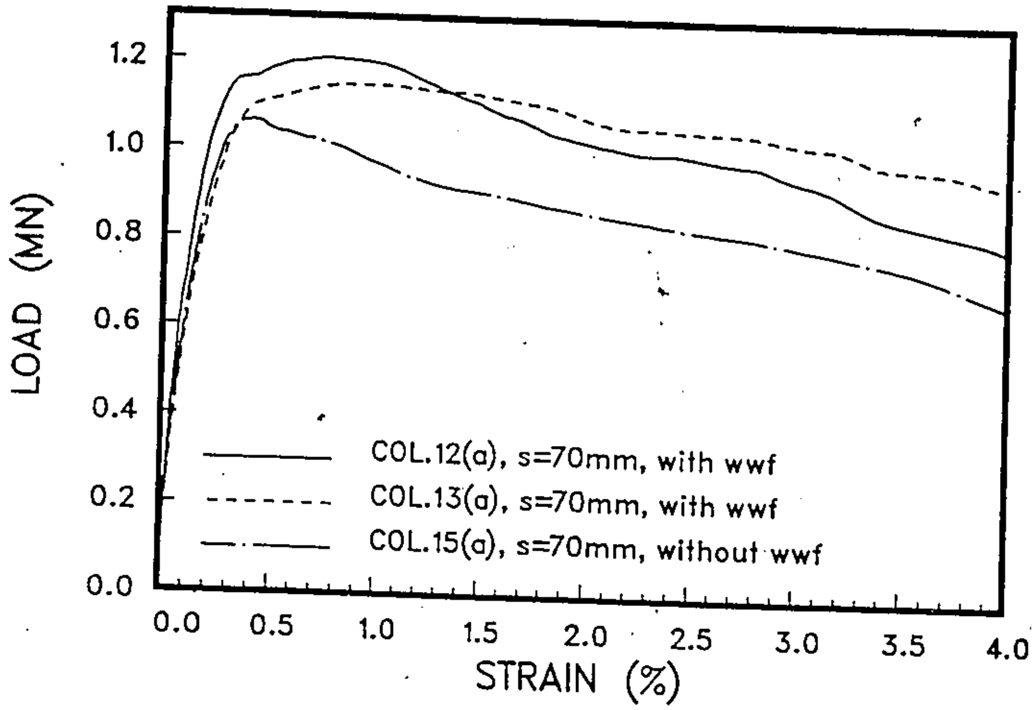

Figure 4.15: Axial load vs. strain for columns 12(a), 13(a) and 15(a)

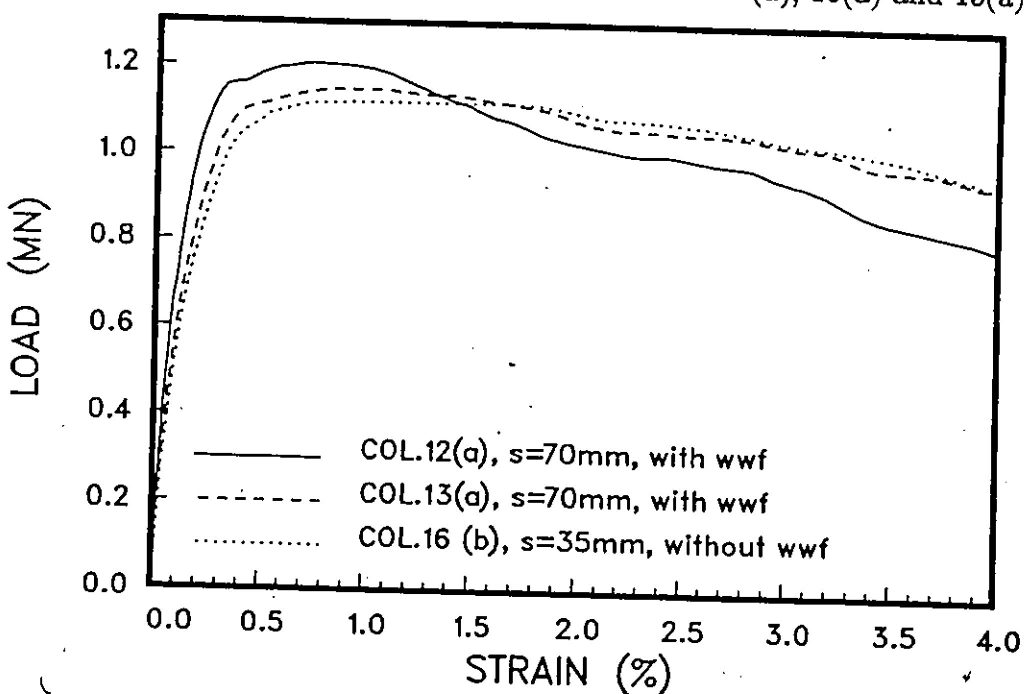

Figure 4.16: Axial load vs. strain for columns 12(a), 13(a) and 16(b)

This further substantiates the idea of confining concrete using WWF while preventing lateral ties from opening.

Two sizes of WWF were used in the four pairs of columns discussed above. In general the behavior of WWF of 12.7mm x 12.7mm x 16 gage was better than that of 25.4mm x 25.4mm x 14 gage. This may be attributed to the reduced spacing of wires. However the behavior of these two sizes in columns 17(a) and 18(a) were almost similar. The effect of WWF size can be seen by examining Figures 4.15 and 4.17.

4.2.5 WWF as Lateral Reinforcement Without Ties

The possibility of using WWF as lateral reinforcement without ties was considered in set two. Four sets of columns were tested for this purpose. The first three pairs had the same WWF. The results are compared to that of column 7(b) which had ties at d/2 as lateral reinforcement. Figure 4.19 shows the comparison. From the test results it can be concluded that WWF can not replace the use of ties as lateral reinforcement. Figure 4.19 indicates a brittle response immediately after reaching the peak load. It was observed that WWF could not provide sufficient lateral support for longitudinal bars to prevent them from buckling. The concentrated pressure applied by longitudinal bars caused them to rupture suddenly.

Three types of connections were used at the overlap locations to connect the WWF. Column pair 8 was welded at the overlap to prevent opening

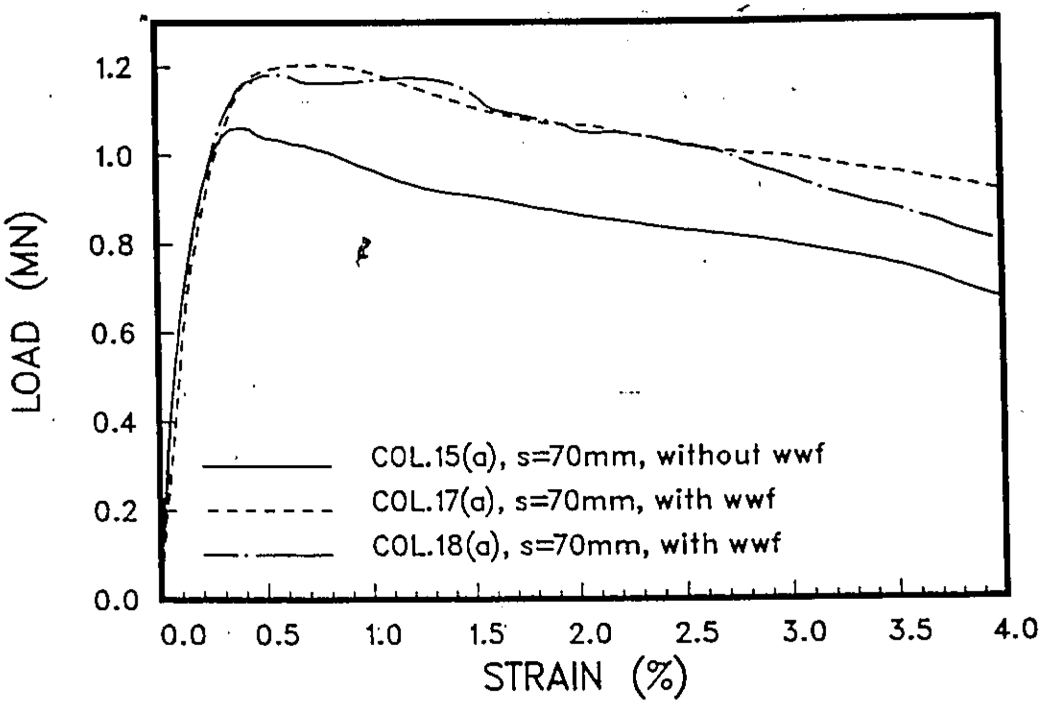

Figure 4.17: Axial load vs. strain for columns 15(a), 17(a) and 18(a)

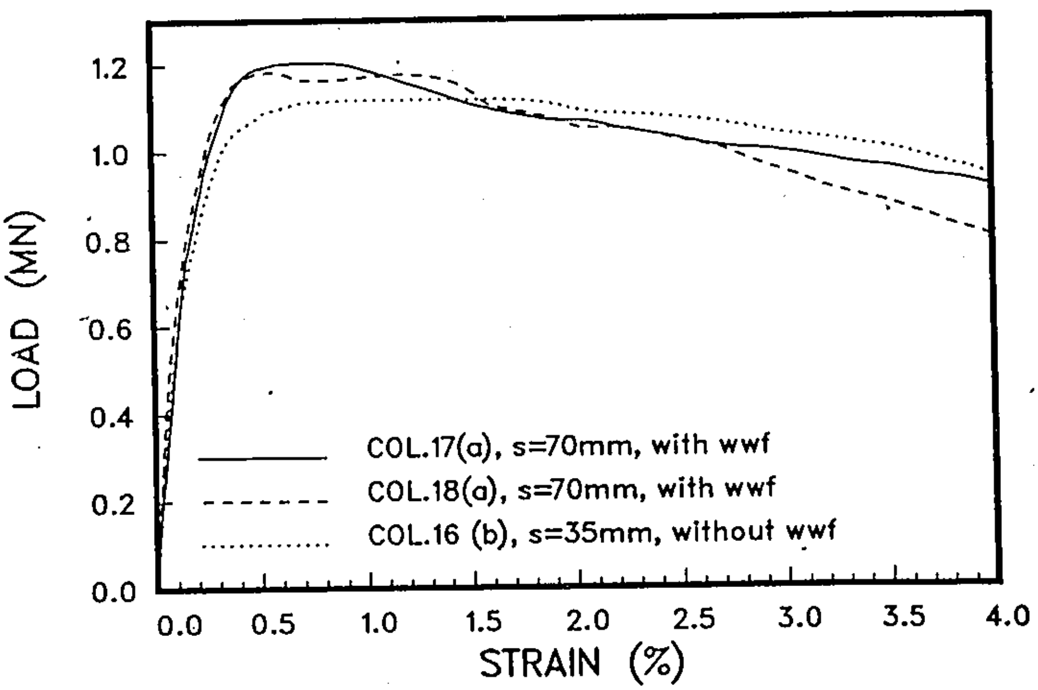

Figure 4.18: Axial load vs. strain for columns 16(b),17(a) and 18(a)

of the mesh. This pair of columns developed the least strength among the group. The exposure to heat during welding may explain the slight reduction in strength. Column pair 9 had WWF mechanically connected at the overlaps. This column developed approximately the same strength as that of the column with ties at d/2 spacing having 135 degree hooks. Column pair 10 had WWF simply lapped in the corner with 1.5 mm wire. This pair of columns developed the highest strength in the group. The behaviors of the three types of columns are almost similar in terms of ductility. This was expected since the WWF fracture preceded opening at the overlaps. Another size WWF with finer mesh size but 60% less total steel area was used in column pair 11. The response of column 11(b) is compared in figure 4.20 with that of a column from the previous group with different WWF size. The results indicate that while both show brittle response, the one with less percentage of lateral steel shows a higher rate of strength drop after the peak load.

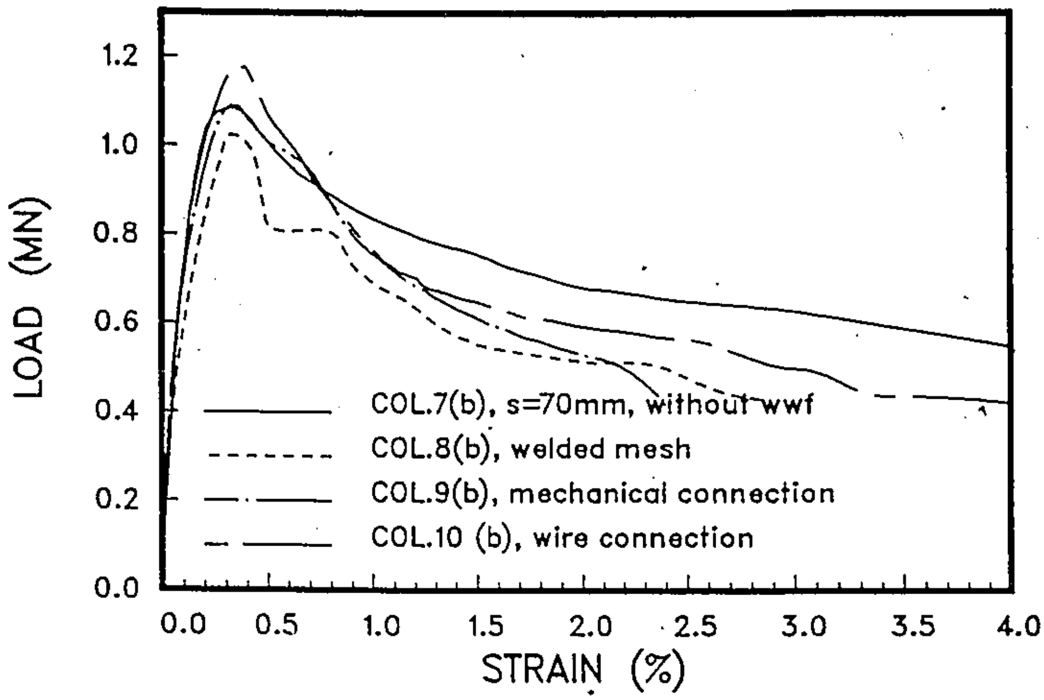

Figure 4.19: Axial load vs. strain for columns 8(b), 9(b) ,10(b) and 7(b)

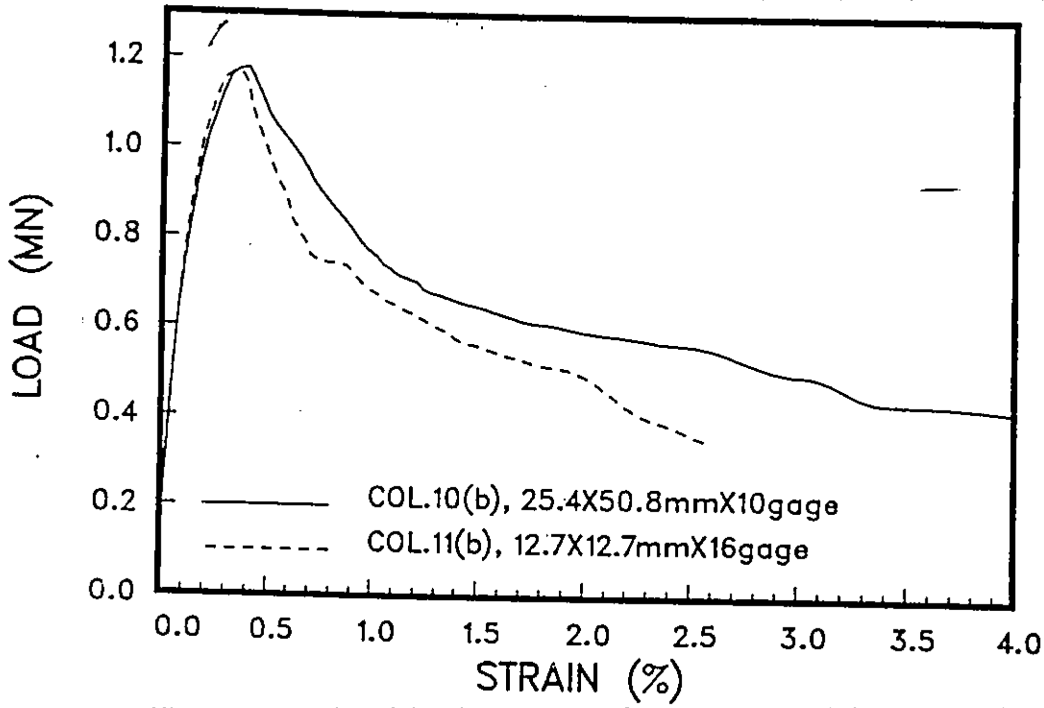

Figure 4.20: Axial load vs. strain for columns 10(b) and 11(b)

Chapter 5

Analytical Predictions

In addition to the experimental research reported in the previous chapters, column confinement was also studied analytically. Available models for concrete confined by rectilinear ties were reviewed. A comparison between the experimental behavior of tied columns tested in this program and the predicted behavior by two analytical models was made. An analytical procedure is recommended for modeling the stress - strain relationship of concrete confined by welded wire fabric and/or rectilinear ties.

5.1 Available Models

5.1.1 Chan (1955)

Chan's model consists of a trilinear curve as shown in Figure 5.1 (a). In the figure, OA and BC represent the elastic plastic ranges respectively. The slope of BC is controlled by the volumetric ratio of lateral steel and the modulus of elasticity of concrete (i.e. $slope = \lambda_2 E_c$, where λ_2 is a function of lateral steel content). For plain concrete the slope of BC is negative, while for confined concrete the positive slope reflects the additional strength and ductility due to confinement. The model considers the volumetric ratio of lateral steel to be the only factor affecting the strength and ductility of confined concrete. The proposed relationship between the ultimate strength, ultimate deformation and lateral steel content can be found elsewhere [13].

5.1.2 Roy and Sozen (1964)

The bilinear stress-strain relationship proposed by Roy and Sozen , which is shown in Figure 5.1(b), assumes no enhancement of concrete strength due to confinement. The concrete is assumed to reach its peak stress at a strain of 0.002. The descending branch of the bilinear curve is defined by the strain corresponding to 50% of the maximum stress(ϵ_{50}). According to this model the ductility of concrete is affected only by the volumetric ratio of lateral steel and tie spacing.

5.1.3 Soliman and Yu (1967)

The stress-strain relationship proposed by Soliman and Yu consists of a parabola and two straight lines, as shown in Figure 5.1(c). The model considers the following variables to be effective in strength and ductility of confined concrete [14]:

- Spacing of ties.
- Ratio of confined area to total area.
- Size of ties.

Stresses and strains required to define the complete stress-strain relationship are:

$$q'' = (1.4\frac{A_b}{A_c} - 0.45)\frac{A_s''(s_0 - s)}{A_s''s + 0.0028Bs^2} \tag{5.1}$$

$$f_{cc} = 0.9f_c'(1 + 0.05q'') \tag{5.2}$$

$$\epsilon_{cc} = 0.55f_c' \times 10^{-6} \tag{5.3}$$

$$\epsilon_{cs} = 0.0025(1 + q'') \tag{5.4}$$

$$\epsilon_{cf} = 0.0045(1 + 0.85q'') \tag{5.5}$$

It is to be noted that this model ignores the effect of tie strength. It does not distinguish maximum stresses in gross and core concrete areas.

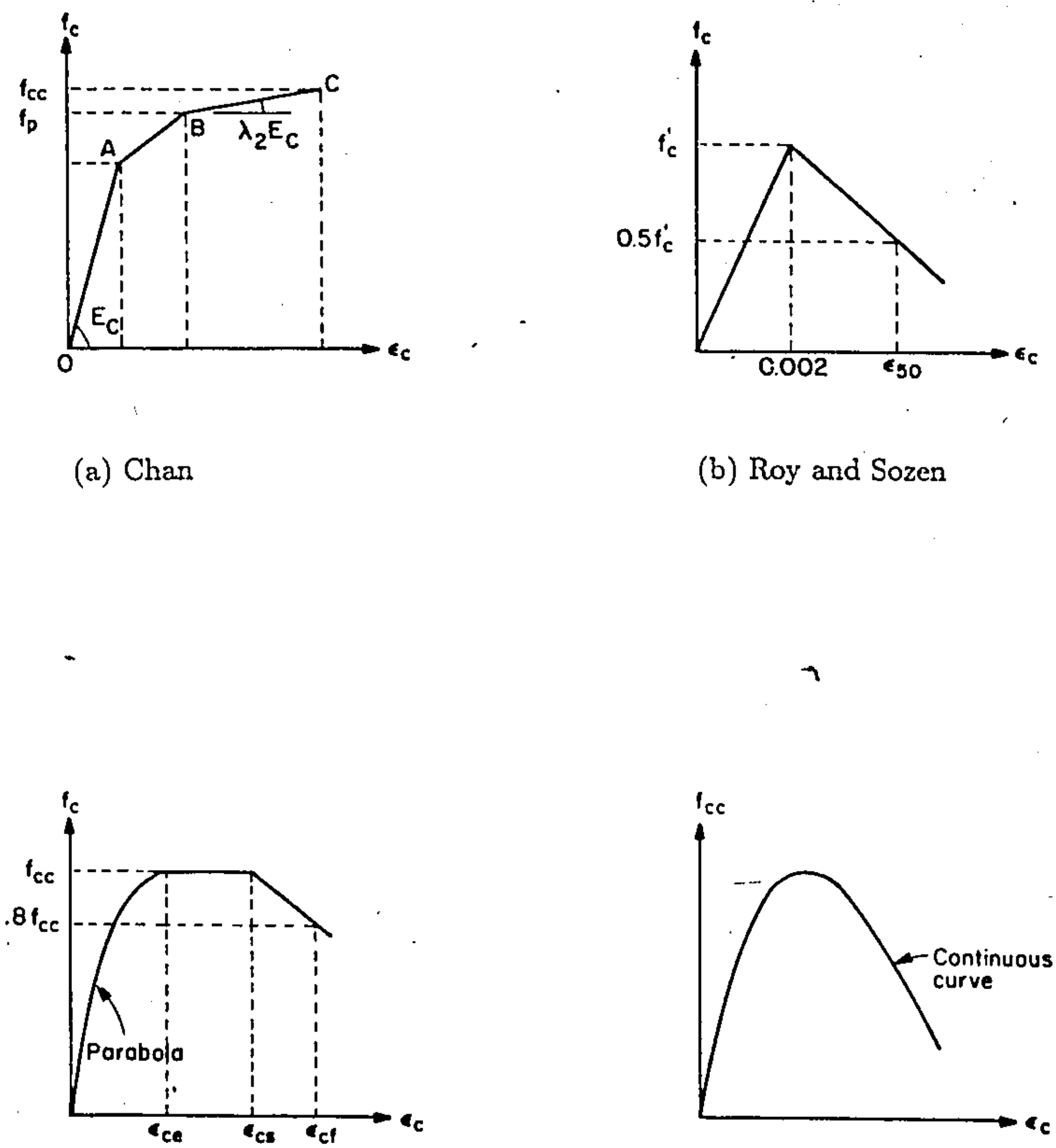

(a) Chan

(b) Roy and Sozen

(c) Soliman and Yu

(d) Sargin et. al.

Figure 5.1: Confined concrete models

5.1.4 Sargin, et al. (1971)

Sargin et al. proposed a continuous stress-strain ourve to predict the behavior of confined concrete as shown in Figure 5.1(d). Strength and ductility enhancement are assumed to be related to the following variables:

- Lateral steel content, spacing and yield strength .
- Concrete strength.
- Strain gradient.

Based on a regression analysis of test results, Sargin et al. proposed the following equation to estimate the ratio of maximum stress in confined concrete core to cylinder strength:

$$K_{3c} = K_{3o}\left\{1 + \left[0.007\sqrt{\frac{(kd)_o}{kd}} + 0.015\left(1 - 0.25\frac{s}{B}\right)\right]\frac{12.05\rho_s f'_y}{\sqrt{f'_c}}\right\} \quad (5.6)$$

Two other equations were suggested for estimation of K_{3c}, based on theoretical studies and previous research. These equations can be found elsewhere [15]. The strain corresponding to the maximum stress was given by the following equation:

$$\epsilon_{oc} = \epsilon_{oo}\left\{1 + \left[0.25\sqrt{\frac{(kd)_o}{kd}} + 0.154\left(1 - 0.7\frac{s}{B}\right)\right]\frac{12.05\rho_s f'_y}{\sqrt{f'_c}}\right\} \quad (5.7)$$

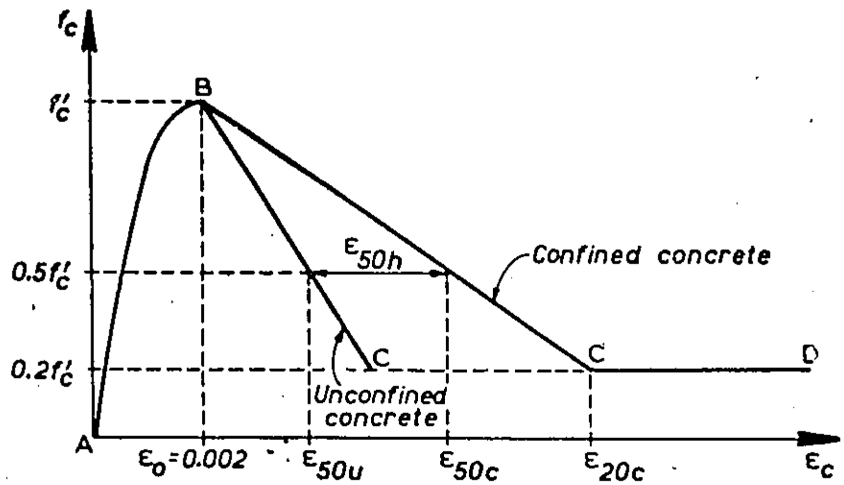

Figure 5.2: Kent and Park's Model

5.1.5 .Kent and Park (1971)

Based on experimental evidence, Kent and Park proposed a model which combined many of the features of previously proposed curves. The ascending portion of the stress-strain curve, which is shown in Figure 5.2, was assumed to be a parabola, and was not affected by confinement. No strength enhancement due to confinement was considered. Furthermore, the strain corresponding to the peak stress was assumed to be 0.2%. Region AB of the curve, shown in Figure 5.2 was defined by the following equation:

$$f_c = f'_c\left\{\frac{2\epsilon_c}{\epsilon_o} - \left(\frac{\epsilon_c}{\epsilon_o}\right)^2\right\} \tag{5.8}$$

Where

$$\epsilon_o = 0.002 \tag{5.9}$$

The falling branch of the curve (region BC) was assumed to be linear and its slope was specified as follows:

- For unconfined concrete, the strain when concrete stress has fallen to 50% of maximum stress (i.e. ϵ_{50u}) was used to determine the slope.

$$\epsilon_{50u} = \frac{3 + 0.002 f'_c}{f'_c - 1000} \tag{5.10}$$

- For confined concrete region BC was defined by the following equation:

$$\begin{aligned} f_c &= f'_c \{1 - z(\epsilon_c - \epsilon_o)\} && (5.11) \\ z &= \frac{0.5}{\epsilon_{50h} + \epsilon_{50u} - \epsilon_o} && (5.12) \\ \epsilon_{50h} &= \frac{3}{4} p'' \sqrt{b''/s} && (5.13) \end{aligned}$$

Region CD was defined by a horizontal line starting from a stress corresponding to $0.2 f'_c$ to infinity.

5.1.6 Sheikh and Uzumeri (1978)

An analytical model was developed by Sheikh and Uzumeri based on extensive test data[7]. The proposed relationship representing the behavior of confined concrete is shown in Figure 5.3. The curve consists of three parts:

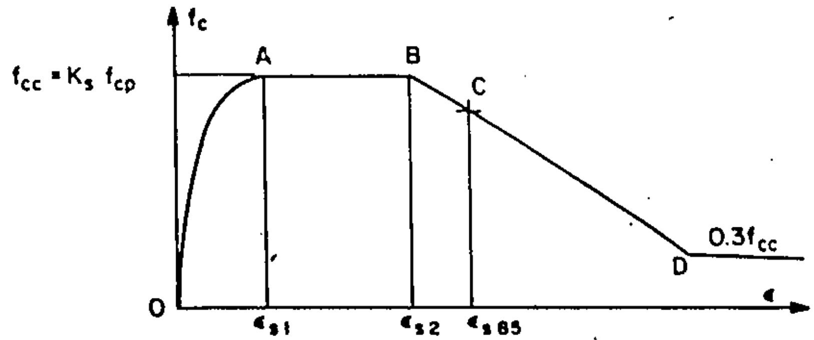

Figure 5.3: Sheikh and Uzumeri's Model

- Part OA is a second degree parabola, in which point A is defined by f_{cc} and ϵ_{s1}.
- Part AB is a straight line, in which point B is defined by f_{cc} and ϵ_{s2}.
- Part BC is a straight line, in which point C is defined by $.85f_c'$ and ϵ_{s85}. Beyond point C the curve continues with the same slope till point D where the stress is dropped to 30% of f_{cc}.
- Beyond point D the curve continues as a horizontal line.

The model uses the concept of effectively confined core to predict strength enhancement due to confinement. The variables considered in this model are:

- Tie configuration.
- Tie spacing.
- Confining pressure as governed by the volumetric ratio and yield strength of transverse steel.

The use of the model requires the following steps:

1. The ratio of the area of effectively confined concrete to the core area at tie level, can be calculated from the following equation:
$$\lambda = 1 - \frac{\sum_{i=1}^{n} C_i^2}{\alpha A_{co}} \tag{5.14}$$
2. The ratio of the area of effectively confined concrete to the core area at the critical section between ties can be found from the following equation:
$$\lambda^* = \lambda \left(1 - \frac{0.5s\ tan\theta}{B}\right)\left(1 - \frac{0.5s\ tan\theta}{H}\right) \tag{5.15}$$
3. The extra load carrying capacity of the concrete due to confinement (P_{add}) is calculated as follows:
$$P_{add} = \lambda^* A_{co} \beta \left(\rho_s f_s'\right)^{\gamma} \tag{5.16}$$
4. K_s and f_{cc} can be found as:
$$K_s = 1 + \frac{P_{add}}{P_{occ}} \tag{5.17}$$
$$f_{cc} = K_s f_{cp} \tag{5.18}$$

5. Strains $\epsilon_{s1}, \epsilon_{s2}$ and ϵ_{s85} are defined below:

$$\begin{aligned}
\epsilon_{s1} &= 80K_s f'_c \times 10^{-6} && (5.19)\\
\frac{\epsilon_{s2}}{\epsilon_{oo}} &= 1 + \frac{248}{C}\left\{1 - 5\,(s/B)^2\right\}\frac{\rho_s f'_s}{\sqrt{f'_c}} && (5.20)\\
\epsilon_{s85} &= 0.225\rho_s\sqrt{\frac{B}{s}} + \epsilon_{s2} && (5.21)
\end{aligned}$$

From regression analyses the following coefficients were obtained:
$\alpha = 5.5, \theta = 45°$ $, \gamma = 0.5$, $\beta = 0.0071$.

5.1.7 Modified Kent and Park (1982)

To account for the strength enhancement in confined concrete, the Kent and Park model was modified to introduce factor K . Factor K is given by:

$$K = 1 + \frac{p'' f_{yh}}{f'_c} \tag{5.22}$$

The modified model is shown in figure 5.4 and defined as follows:
Region AB ($\epsilon c < 0.002K$)

$$f_c = Kf'_c\left\{\frac{2\epsilon_c}{0.002K} - \left(\frac{\epsilon_c}{0.002K}\right)^2\right\} \tag{5.23}$$

Region BC ($\epsilon_c > 0.002$)

$$f_c = Kf'_c\left\{1 - z_m\left(\epsilon_c - 0.002K\right)\right\} \geq 0.2Kf'_c \tag{5.24}$$

But not less than $0.2Kf'_c$, where;

$$z_m = \frac{0.5}{\frac{3+0.29f'_c}{145f'_c-1000} + .75\rho_s\sqrt{\frac{h''}{s}} - 0.002K} \tag{5.25}$$

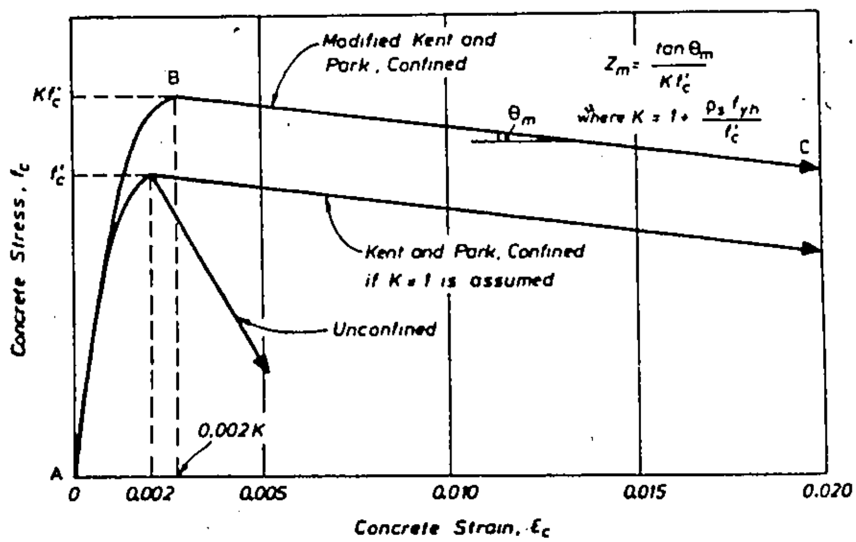

Figure 5.4: Modified Kent and Park Model

5.1.8 Fafitis and Shah (1985)

Fafitis and Shah developed a model for confined and unconfined concrete in spirally reinforced columns[5]. Their model is shown in Figure 5.5. The following expressions define the model: For the ascending part

$$f = f_o \left[1 - \left(1 - \frac{\epsilon}{\epsilon_p}\right)^A\right] \tag{5.26}$$

For the descending part

$$f = f_o \exp\left[-k\left(\epsilon - \epsilon_p\right)^{1.15}\right] \tag{5.27}$$

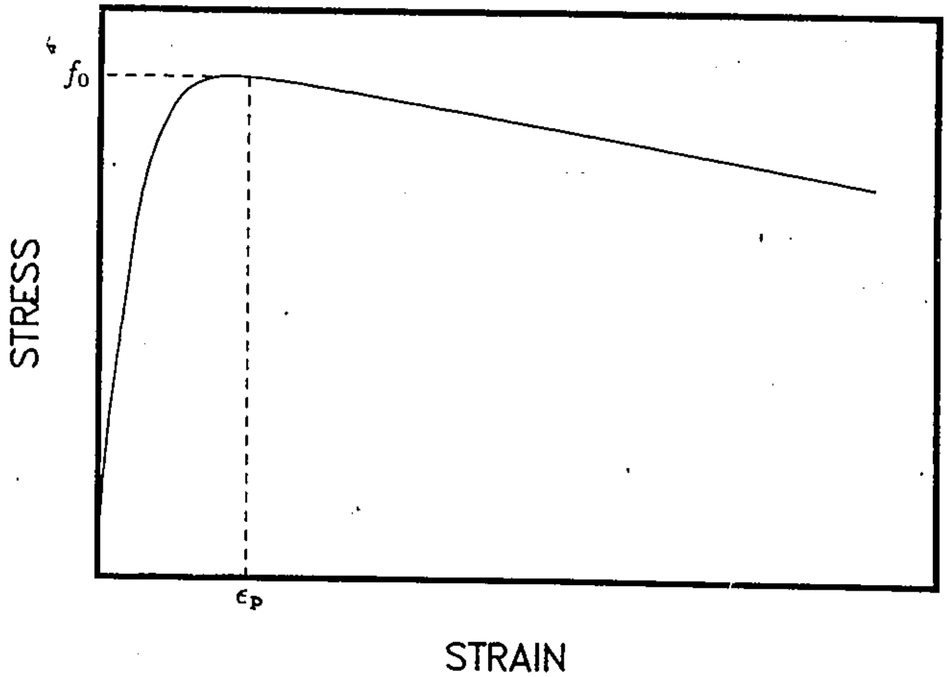

Figure 5.5: Fafitis and Shah Model

The values of A and k are given below

$$A = \frac{E_c \epsilon_p}{f_o} \tag{5.28}$$

$$k = 0.17 f_c' \exp\left(-0.01 f_r\right) \tag{5.29}$$

Where

$$f_r = \frac{2 a_s f_y'}{s d} \tag{5.30}$$

$$f_o = f_c' + \left(1.15 + \frac{3048}{f_c'}\right) f_r \tag{5.31}$$

$$\epsilon_p = 1.027 \times 10^{-7} f_c' + 0.0296 \frac{f_r}{f_c'} + 0.00195 \tag{5.32}$$

The stress-strain curve for the cover concrete is predicted by substituting $f_r = 0$ in the above equations. The model was simplified to be applicable to square columns. It was assumed that the square column is equivalent to a circular column with an equivalent diameter equal to the core dimension. The modified f_r for a square column is calculated as follows:

$$f_r = \frac{A_{sh} f'_y}{d_c s} \tag{5.33}$$

where A_{sh} is the total cross sectional area of the ties.

It is to be noted that the model treats cross ties in the same way as perimeter ties. In doing so the model overestimates ρ_s. Furthermore it ignores the effect of tie spacing (for a constant ρ_s), effect of longitudinal reinforcement distribution and the resulting tie configuration.

5.2 Application of Previous Models to Ottawa Tests

In this section the behavior of tied columns, without WWF, is compared with the predicted behavior by two models. The models considered are the Sheikh and Uzumeri and Modified Kent and Park Models for confined concrete. These models were studied in detail prior to their use to predict the observed response.

Both models were developed for column concrete were the longitudinal column reinforcement was assumed to be capable of developing stresses in the strain hardening region. However, the column tests performed in this investigation indicated that the longitudinal column reinforcements bend under concentric axial loading. The actual behavior of steel is such that the reinforcement starts unloading beyond certain level of inelastic axial strain. This puts burden on the concrete to resist the applied axial load. However, because the previous models are based on the assumption that the steel stress-strain relationship observed in tension tests, can be developed in the column, this relationship for steel is used in predicting the concrete response.

The standard error involved in determining the additional load due to confinement, in the Sheikh and Uzumeri model, appears to be too high for the accuracy implied in the computational procedure. Based on the results of 24 columns tested by Sheikh and Uzumeri, the standard error in estimating $(K_s - 1)$ was found to be 0.0629, using the following equation:

$$\sigma_e = \sqrt{\frac{\sum_{i=1}^{n}\left\{\frac{(P_{add})_{pred}-(P_{add})_{exp}}{P_{occ}}\right\}^2}{N - m}} \tag{5.34}$$

For 99.9% confidence

$$\frac{P_{add}}{P_{occ}} = \left(\frac{P_{add}}{P_{occ}}\right)_{pred} \mp 3\sigma_e \tag{5.35}$$

Hence for a value of $\frac{P_{add}}{P_{occ}} = 0.3$

$$\frac{P_{add}}{P_{occ}} = \left(\frac{P_{add}}{P_{occ}}\right)_{pred} \mp \frac{0.1887}{0.3} \tag{5.36}$$

$$= \left(\frac{P_{add}}{P_{occ}}\right)_{pred} \mp 63\% \tag{5.37}$$

Similarly for $\frac{P_{add}}{P_{occ}} = 0.6$

$$\frac{P_{add}}{P_{occ}} = \left(\frac{P_{add}}{P_{occ}}\right)_{pred} \mp 31.5\% \tag{5.38}$$

The Sheikh and Uzumeri model predicts the behavior of well confined concrete reasonably well. However, if the spacing of ties is equal to 45% of the column core dimension (B) or more, the model assumes $\epsilon_{s2} < \epsilon_{s1}$ which is not realistic. On the other hand it is assumed that the concrete carrying capacity increases even if the spacing is equal to B, which appears to be contradictory. Furthermore, researchers showed that the enhancement of the compressive strength due to confinement depends on the compressive strength of unconfined concrete, which was not considered in the Sheikh and Uzumeri model.

In the modified Kent and Park model the proposed equation to calculate strength enhancement is simple. However it does not include the effect of tie spacing and distribution of longitudinal reinforcement. The model assumes that the descending branch starts immediately at the peak, while experiments showed that there is almost always a yield plateau.

The comparisons of the experimental results with those predicted by the two models discussed above are shown in Figures 5.6 through 5.11. Generally the agreement between the predicted and the observed responses is good for well confined columns. However for those columns where the tie spacing was d/2, the analytical predictions are poor.

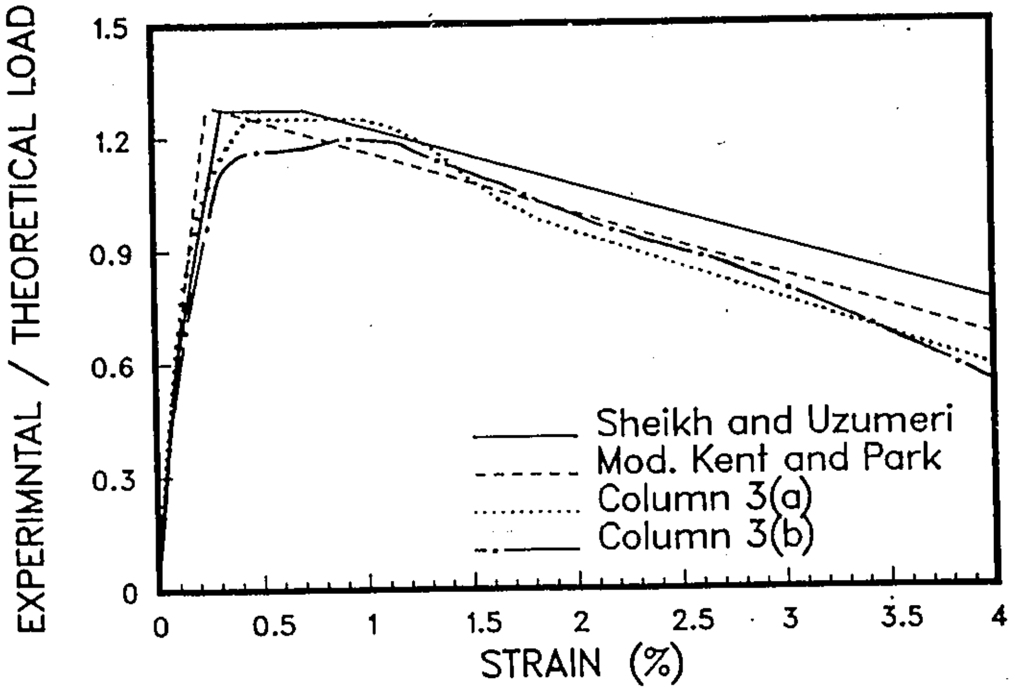

Figure 5.6: Comparison between the predicted and experimental behavior for columns 3(a) and 3(b)

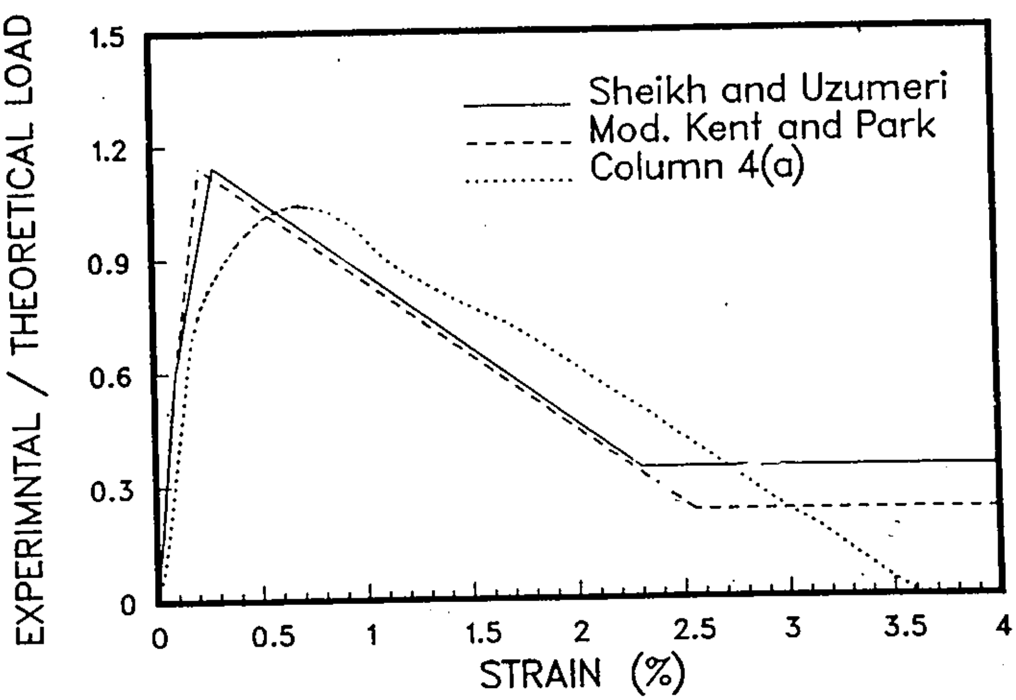

Figure 5.7: Comparison between the predicted and experimental behavior for column4 (a)

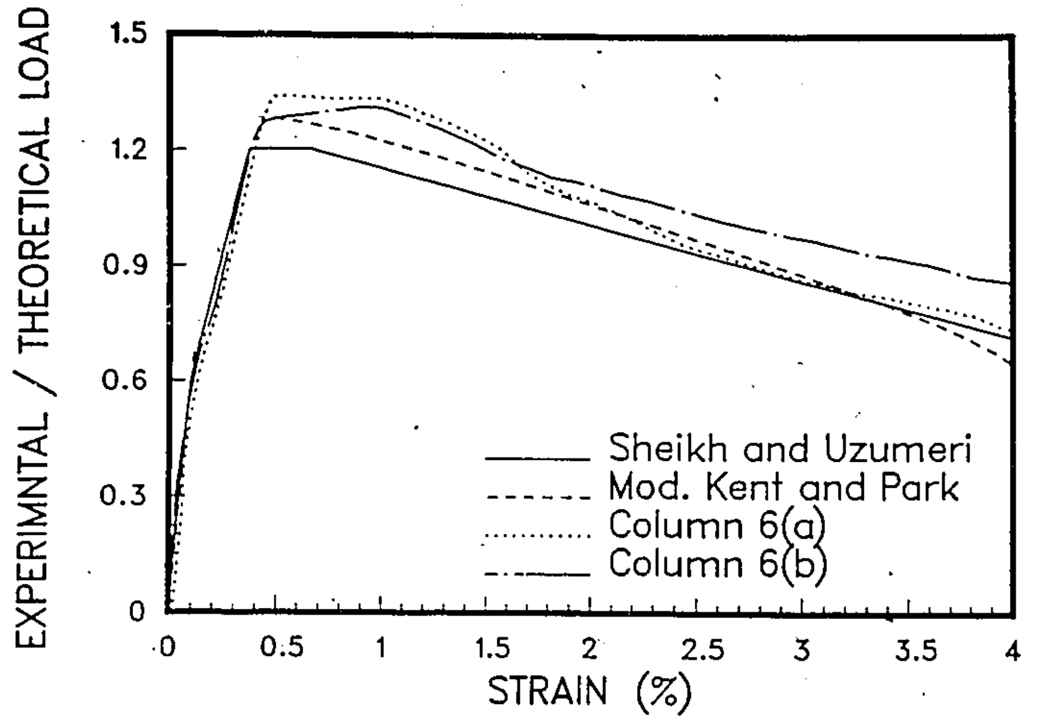

Figure 5.8: Comparison between the predicted and experimental behavior for columns 6(a) and 6(b)

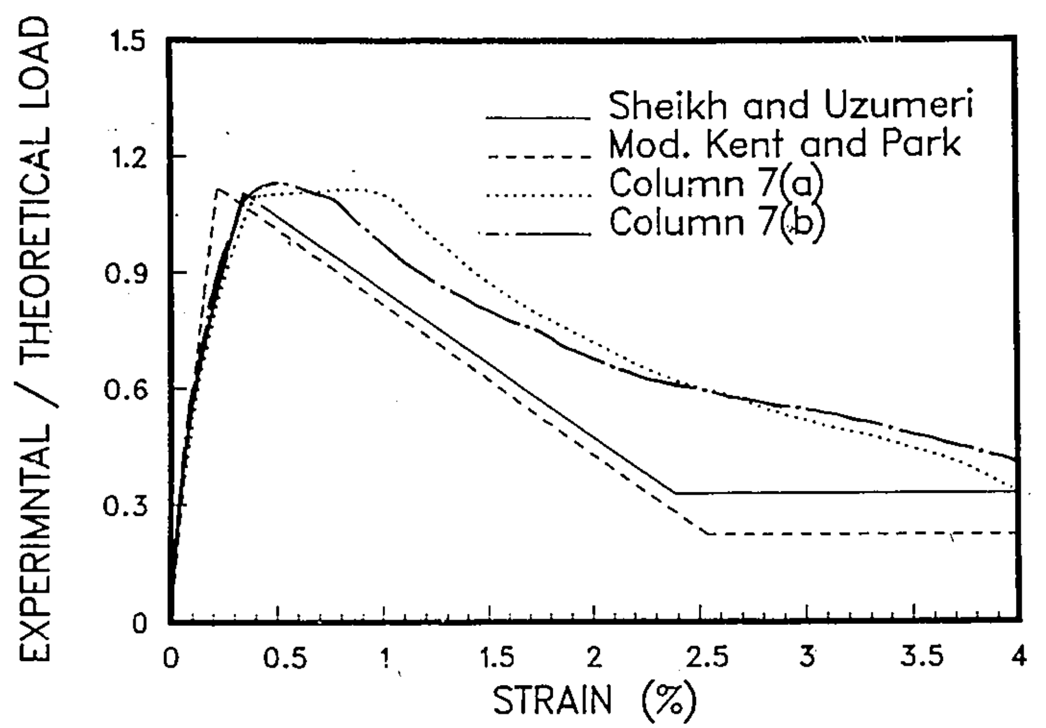

Figure 5.9: Comparison between the predicted and experimental behavior for column7(a) and 7(b)

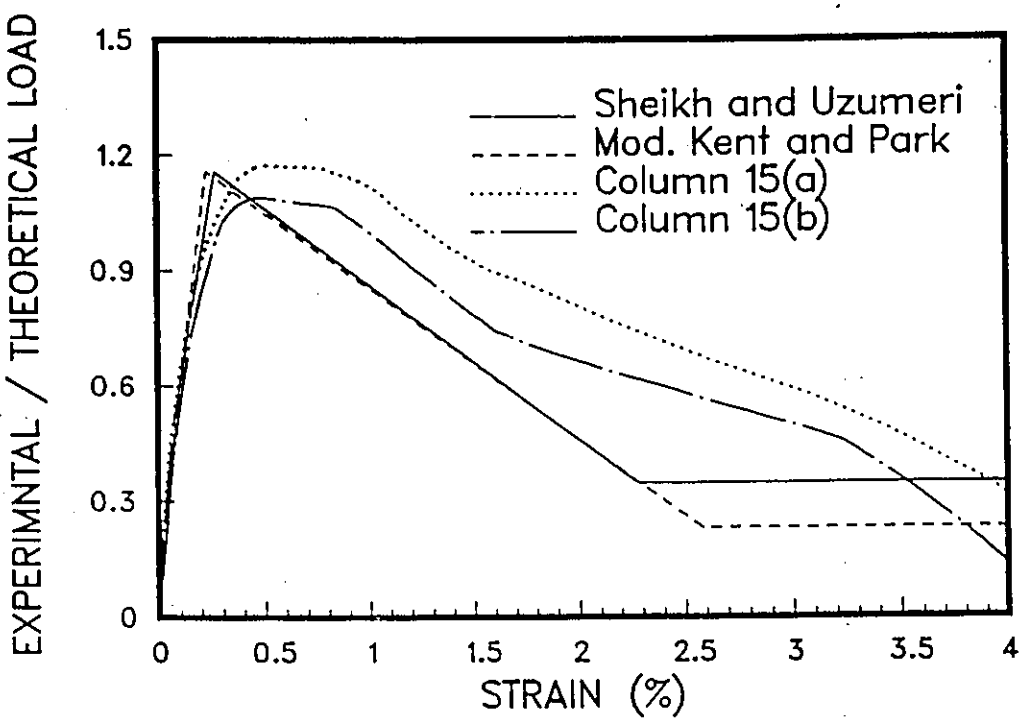

Figure 5.10: Comparison between the predicted and experimental behavior for columns 15(a) and 15(b)

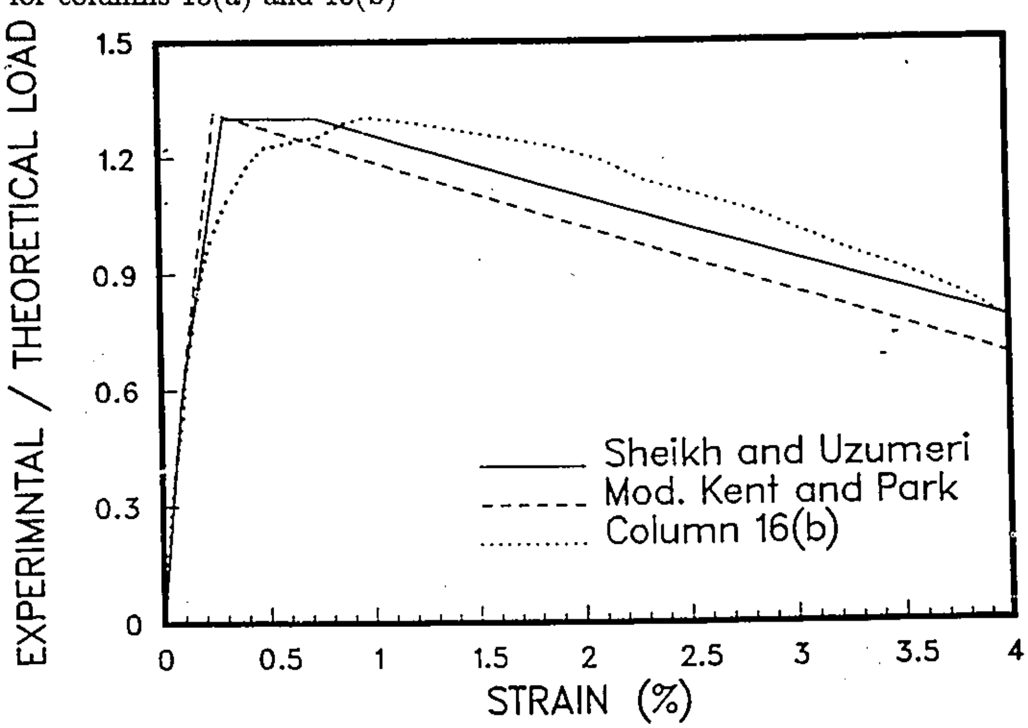

Figure 5.11: Comparison between the predicted and experimental behavior for column16(b)

5.3 Proposed Analytical Model

In this section a model is proposed to predict the stress-strain relationship for confined concrete. The model is based on experimental data and the equations previously proposed by different researchers.

Variables considered in this model are:

1. Lateral pressure provided by ties and WWF.
2. Spacing of ties.
3. Spacing of longitudinal column reinforcement.
4. Grid size of WWF. (Horizontal and Vertical)
5. Concrete strength.

Unlike the previous models, which dealt with one type of lateral reinforcement, in this model the concept of equivalent lateral steel was used to account for the two types of lateral reinforcement, namely ties and WWF. These equivalent parameters are defined as follows:

$$\rho_{equiv.} = \rho_s + \rho'_s \tag{5.39}$$

$$d^2_{equiv.} = \frac{\rho_s d^2_{tie} + \rho'_s d^2_{wwf}}{\rho_{equiv.}} \tag{5.40}$$

$$s_{equiv.} = \frac{As_{equiv.}L}{A_{co}\rho_{equiv.}} \tag{5.41}$$

$$f_{yequiv.} = \frac{\rho_s f'_y + \rho'_s f_{ywwf}}{\rho_{equiv.}} \tag{5.42}$$

Where

$\rho_{equiv.}$ = equivalent volumetric lateral steel ratio

ρ_{tie} = volumetric ratio of lateral tie steel

ρ'_{tie} = volumetric ratio of lateral wires in wwf

$d_{equiv.}$ = equivalent lateral steel diameter

d_{tie} = diameter of tie steel

d_{wwf} = diameter of wire in WWF

$s_{equiv.}$ = equivalent spacing of lateral steel

$As_{equiv.}$ = equivalent cross sectional area of lateral steel

$f_{yequiv.}$ = equivalent yield strength of lateral steel

Among the different shapes of stress-strain curves reported in the literature, the one proposed by Soliman and Yu in 1967 and later used by Sheikh and Uzumeri in 1978 was found to be the most representative of the observed response in column tests. Therefore this shape was adopted for the proposed model. Figure 5.12 illustrates the general features of the stress-strain curve adopted in the model. It is evident that only three independent points are required to completely define the relationship for the confined concrete. These are the beginning points of the flat and ascending portions of the curve and the strain on the ascending portion corresponding to 85% of the peak stress.

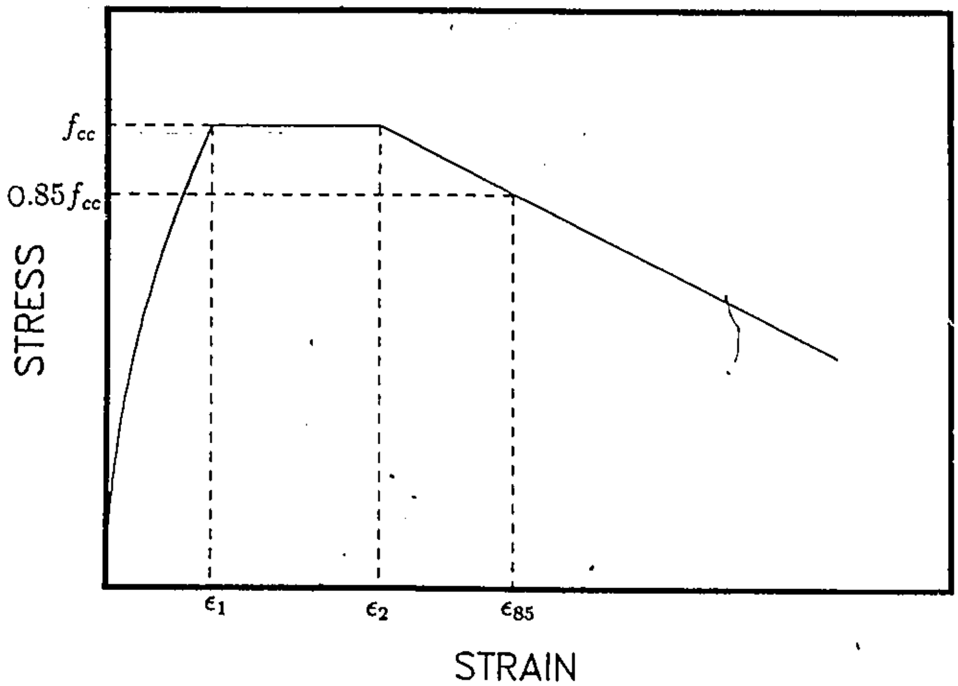

Figure 5.12: Proposed stress-strain curve for confined concrete

Strength Enhancement Coefficient (K)

Most of the previously proposed expressions for predicting strength enhancement ignore the effect of tie spacing and/or distribution of longitudinal reinforcement. In the Sheikh and Uzumeri model, these variables are included in determining the strength enhancement coefficient. However, the expression suggested is quite involved and implied accuracy may not be warranted. In fact if this equation is to be modified to include the combined effect of WWF and lateral ties, then it would become even more complicated and consequently impractical for use.

A regression analysis was performed using the results of 26 column tests conducted by two different groups of researchers[1,3] along with the results of 10 columns tested in this program. A relationship was established between the additional load carried by confined concrete and the following parameters

- Lateral steel content, strength and spacing.
- Spacing of longitudinal reinforcement.
- Concrete strength.

The following test data were used in the regression analysis:

1. Ottawa tests (five pairs of columns).
2. Scott and Kent (two columns).
3. Sheikh and Uzumeri (twenty four columns).

The resulting equation may be written as follows:

$$K = 1.0246 + 0.9 \left\{ \frac{\left(\rho_s f_y'\right)^{0.5}}{(f_c')^{1.15}} \ln \frac{B^2}{sC} \right\} \tag{5.43}$$

In which f_c' and f_y are in ksi. Or

$$K = 1.0246 + 3.154 \left\{ \frac{\left(\rho_s f_y'\right)^{0.5}}{(f_c')^{1.15}} \ln \frac{B^2}{sC} \right\} \tag{5.44}$$

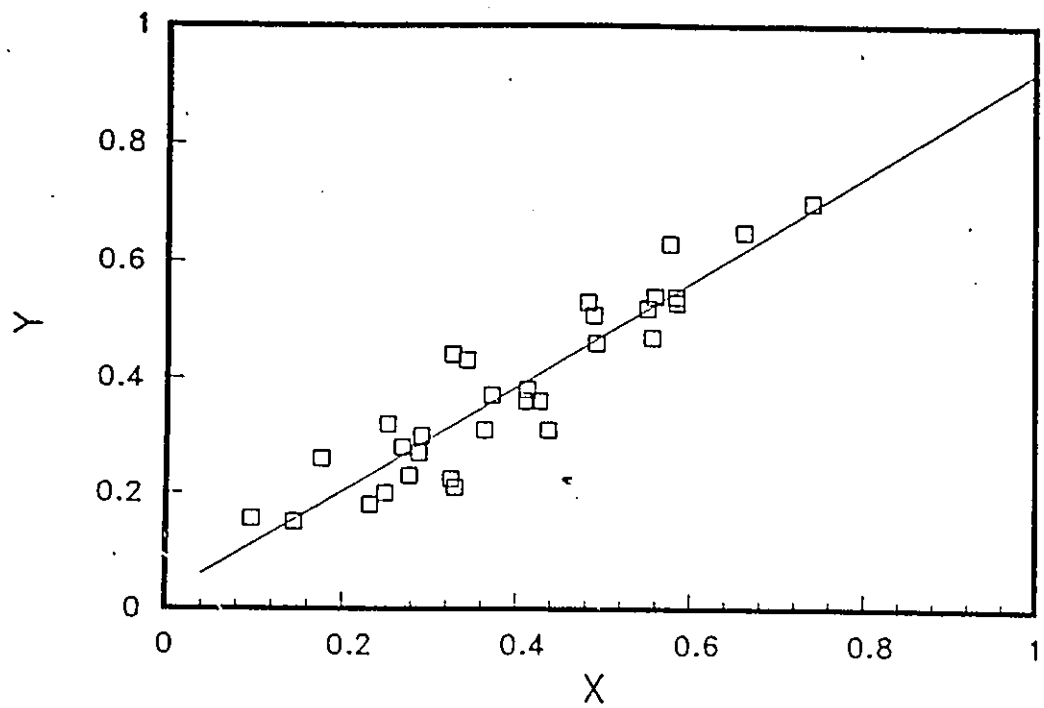

$$x = \frac{(\rho_s f_y)^{0.5}}{(f_c')^{1.15}} \ln \frac{B^2}{sC}$$

$$y = K\text{-}1$$

Figure 5.13: Best fit curve for the test data

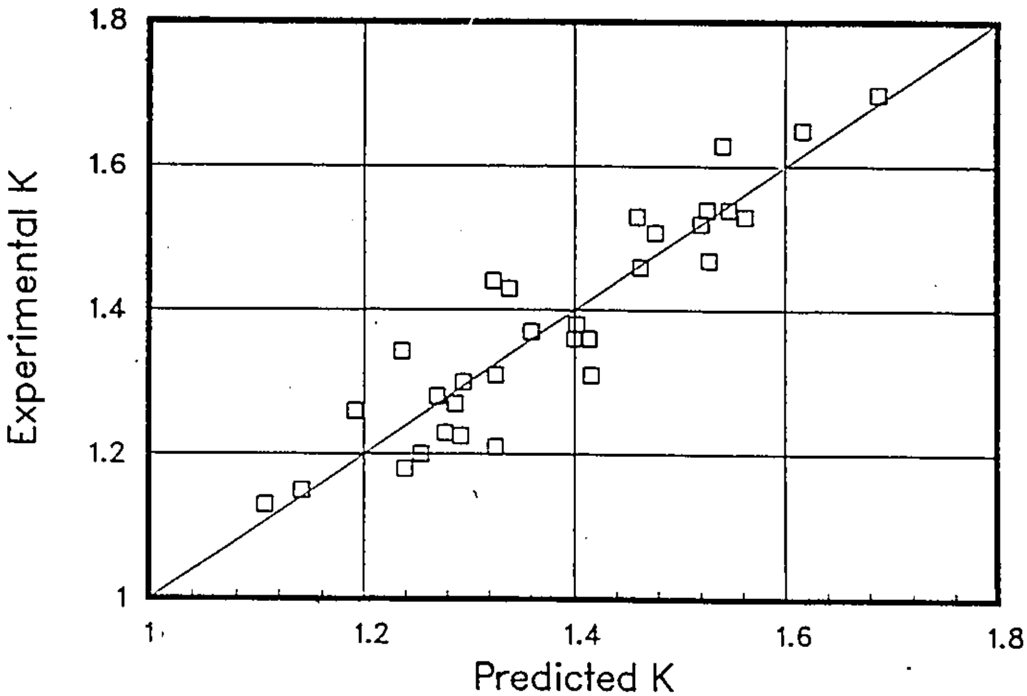

Figure 5.14: Experimental K vs. predicted K by proposed eqn.

In which f_c' and f_y are in MPa.

The coefficient of correlation was found to be equal to 85.4%. Figure 5.13 shows the proposed equation and the test data. The value of K predicted using the proposed model versus the experimental value is depicted in Figure 5.14. Figure 5.15 shows the same relationship using K as predicted by the Sheikh and Uzumeri model. It is evident that both equations are suitable in estimating strength enhancement. However the proposed equation has the advantage of being simpler while maintaining approximately the same accuracy. The data used in the above mentioned figures are tabulated for reference purposes in Tables 5.1 through 5.3. The proposed equation may be limited to confined columns with maximum tie spacing of $B/2$, since none of the tested columns had a larger tie spacing. Further-

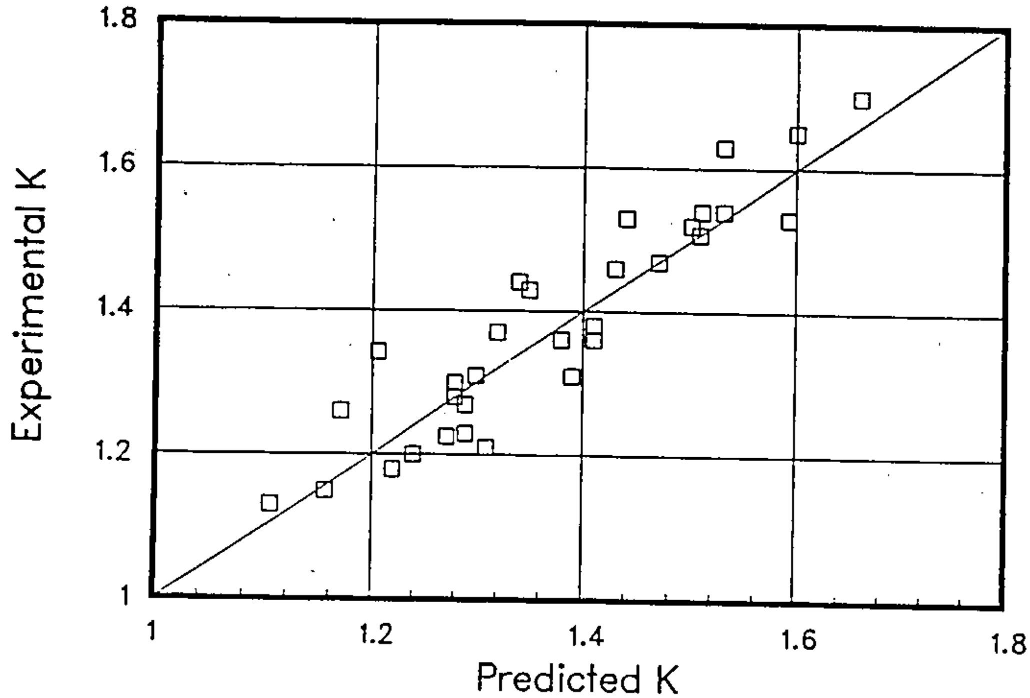

Figure 5.15: Experimental K vs. predicted K by Sheikh model

more, equation 5.44 was modified to be applicable to WWF as follows:

$$K = 1.0246 + 1.892\left\{\frac{\left(\rho_{equiv.}f'_{yequiv.}\right)^{0.5}}{(f'_c)^{1.15}}\ln\frac{B^2}{s_{equiv.}c}\right\} \tag{5.45}$$

Where c is the spacing of longitudinal wires.

5.3.1 Minimum Strain at Peak Stress (ϵ_1)

The strain corresponding to peak stress can be calculated from the equation proposed by Soliman and Yu and later used by Sheikh and Uzumeri. This equation was found to be suitable for both cases of concrete confined by

Column Designation Tested at University of Ottawa	Experimental K	Analytical K	
		Proposed	Sheikh and Uzumeri
3	1.22	1.32	1.27
6	1.32	1.25	1.20
7	1.15	1.11	1.10
15	1.15	1.15	1.16
16	1.31	1.35	1.30

Table 5.1: Comparison between experimental values obtained at the University of Ottawa and predicted values of K

lateral ties with or without WWF.

$$\epsilon_1 = f_{cc} \times 80 \times 10^{-6} \tag{5.46}$$

But

$$f_{cc} = K f'_c \tag{5.47}$$

Hence

$$\epsilon_1 = K f'_c \times 80 \times 10^{-6} \tag{5.48}$$

5.3.2 Maximum Strain at Peak Stress (ϵ_2)

The maximum longitudinal strain in concrete at peak stress is based on the equation proposed by Sargin et al. equation. The original equation

Column Designation Tested by Scott and Kent	Experimental K	Analytical K	
		Proposed	Sheikh and Uzumeri
2	1.53	1.55	1.59
6	1.50	1.46	1.50

Table 5.2: Comparison between experimental values obtained by Scott and Kent and predicted values of K

proposed by Sargin et al., for concentric loading, can be written as follows:

$$\epsilon_{oc} = \epsilon_{oo} \left\{ 1 + 0.154 \left(1 - 0.7 \frac{s}{B} \right) \frac{12.05 \rho_s f'_y}{\sqrt{f'_c}} \right\} \quad (5.49)$$

The above equation does not include the effect of longitudinal steel distribution. It was derived based on tests of laterally reinforced columns 125 x 125 x 510 mm in dimension, without longitudinal reinforcement. Sheikh and Uzumeri found that the equation proposed by Sargin et al. predicted the strain for columns with longitudinal steel spaced at a distance equal to the core dimension in Sargin's tests. The equation was later modified by Sheikh and Uzumeri to account for longitudinal steel distribution (see equation 5.20).

In the present program the core dimensions of the test specimens were approximately equal to those tested by Sargin et al. The original equation proposed by Sargin et al. and the modified equation by Sheikh and Uzumeri were used to predict the maximum strain at peak stress for columns tested in this program. Both equations predicted the strain fairly well in cases

Column Designation Tested by Sheikh and Uzumeri	Experimental K	Analytical K	
		Proposed	Sheikh and Uzumeri
1	1.18	1.23	1.22
2	1.26	1.18	1.17
3	1.21	1.32	1.31
4	1.20	1.25	1.24
5	1.65	1.62	1.60
6	1.53	1.46	1.44
7	1.28	1.27	1.28
8	1.37	1.36	1.32
9	1.23	1.27	1.29
10	1.31	1.42	1.39
11	1.27	1.28	1.29
12	1.46	1.47	1.43
13	1.30	1.29	1.28
14	1.38	1.40	1.41
15	1.47	1.52	1.47
16	1.36	1.40	1.38
17	1.36	1.41	1.41
18	1.70	1.69	1.66
19	1.43	1.33	1.35
20	1.52	1.52	1.50
21	1.54	1.53	1.53
22	1.44	1.32	1.34
23	1.54	1.55	1.51
24	1.63	1.54	1.53

Table 5.3: Comparisons between experimental values obtained by Sheikh and Uzumeri and predicted values of K

where concrete was confined by lateral ties spaced at d/4. However, in cases where ties were spaced at d/2, the equation suggested by Sargin et al. predicted the strain much better than the modified equation by Sheikh and Uzumeri.

The effect of WWF was introduced into the equation proposed by Sargin et al., as follows:

$$\frac{\epsilon_2}{\epsilon_{oo}} = 1 + 0.154\left(1 + 0.4\ln\frac{B^2}{s_{equiv.}C}\right)\frac{12.05\rho_{equiv.}f_{yequiv.}}{\sqrt{f'_c}} \tag{5.50}$$

Where c is the spacing of longitudinal wires.

5.3.3 Strain at 85% of Peak Stress (ϵ_{85})

The strain corresponding to 85% of peak stress can be calculated from the equation originally proposed by Kent and Park in 1971 and later modified by Sheikh and Uzumeri in 1978. The equation is given below:

$$\epsilon_{85} = 0.225\rho_s\sqrt{\frac{B}{s}} + \epsilon_2 \tag{5.51}$$

It was found that this equation is applicable to concrete confined by lateral ties with or without WWF. It is to be noted that $\rho_{equiv.}$ and $s_{equiv.}$ should be used instead of ρ_s and s in the above equation for the case of lateral ties with WWF.

5.3.4 Comparison of Experimental and Analytical Behavior Based on the Proposed Model

Figure 5.16 to 5.20 shows comparisons between the experimental and analytical stress strain relationships for concrete confined with WWF and ties. It is evident from these figures that the proposed model predicts the behavior fairly well. However, due to the limited test data available, the model does not include the effect of location of WWF with respect to ties and longitudinal reinforcement. This might explain the reason for the difference between experimental and predicted behavior of column pair 14.

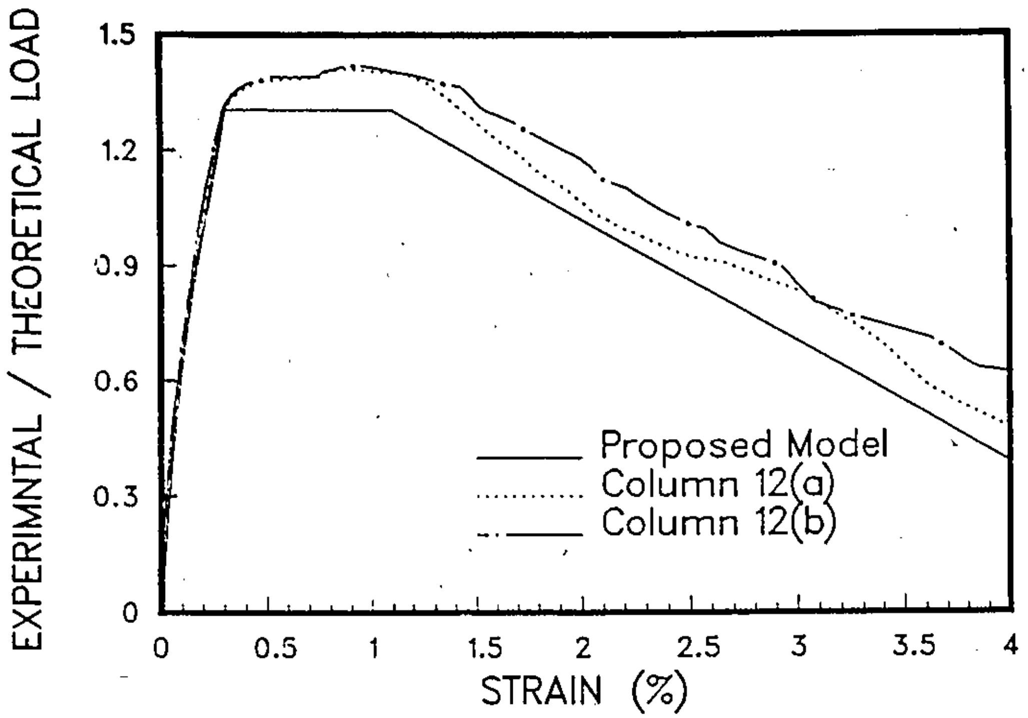

Figure 5.16: Comparison between experimental and analytical behavior for Columns 12(a) and 12(b)

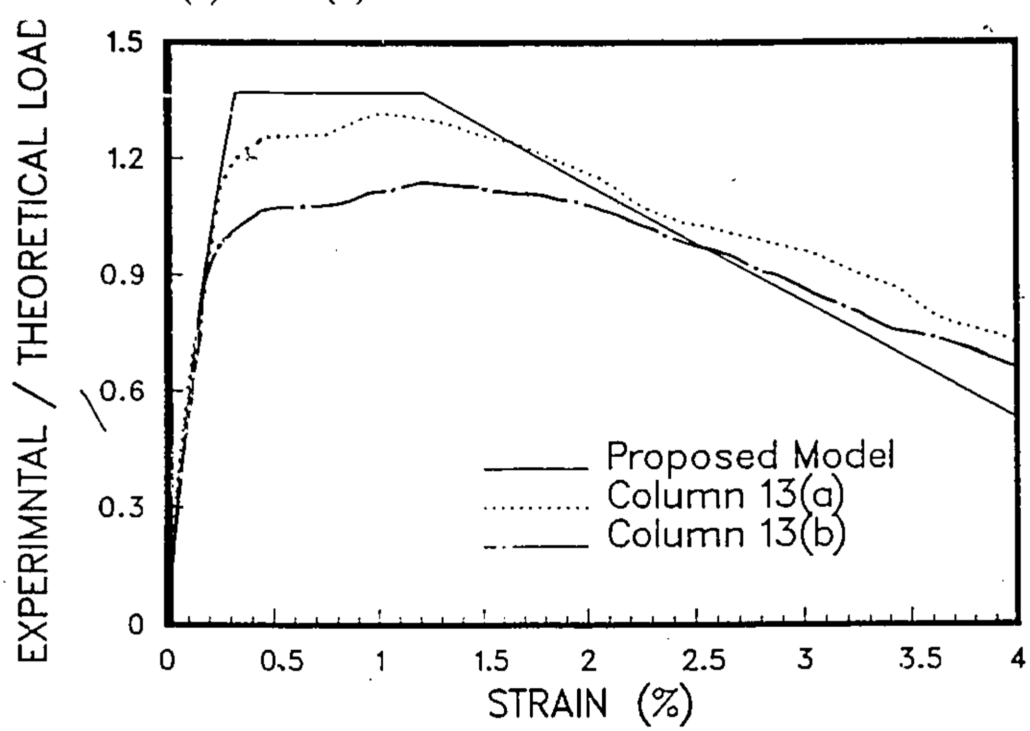

Figure 5.17: Comparison between experimental and analytical behavior for Columns 13(a) and 13(b)

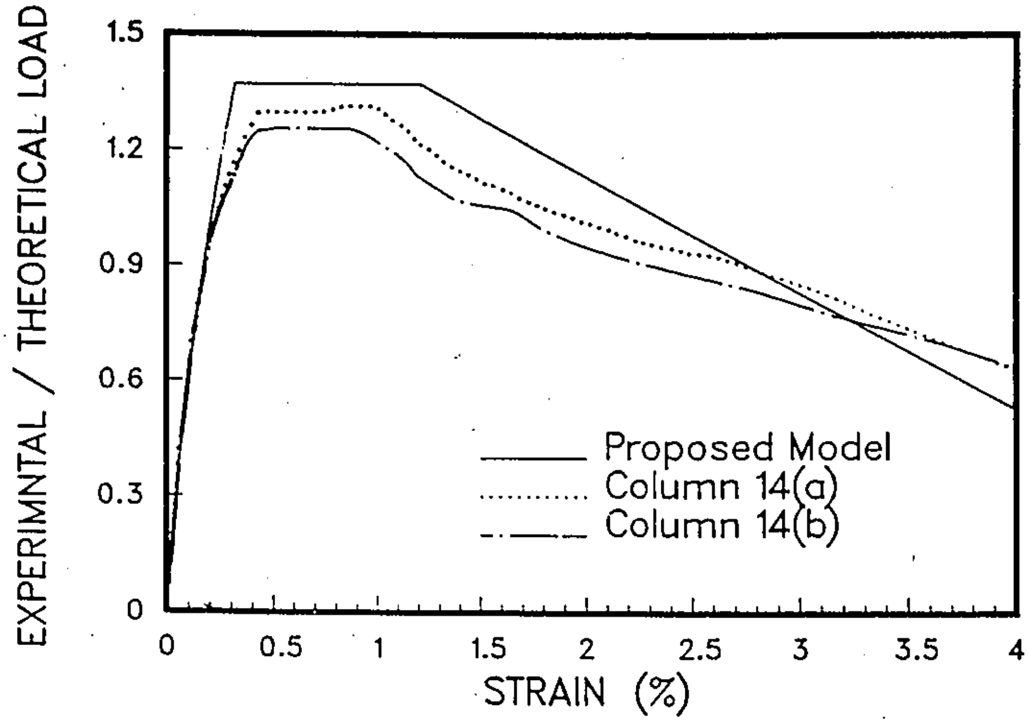

Figure 5.18: Comparison between experimental and analytical behavior for Columns 14(a) and 14(b)

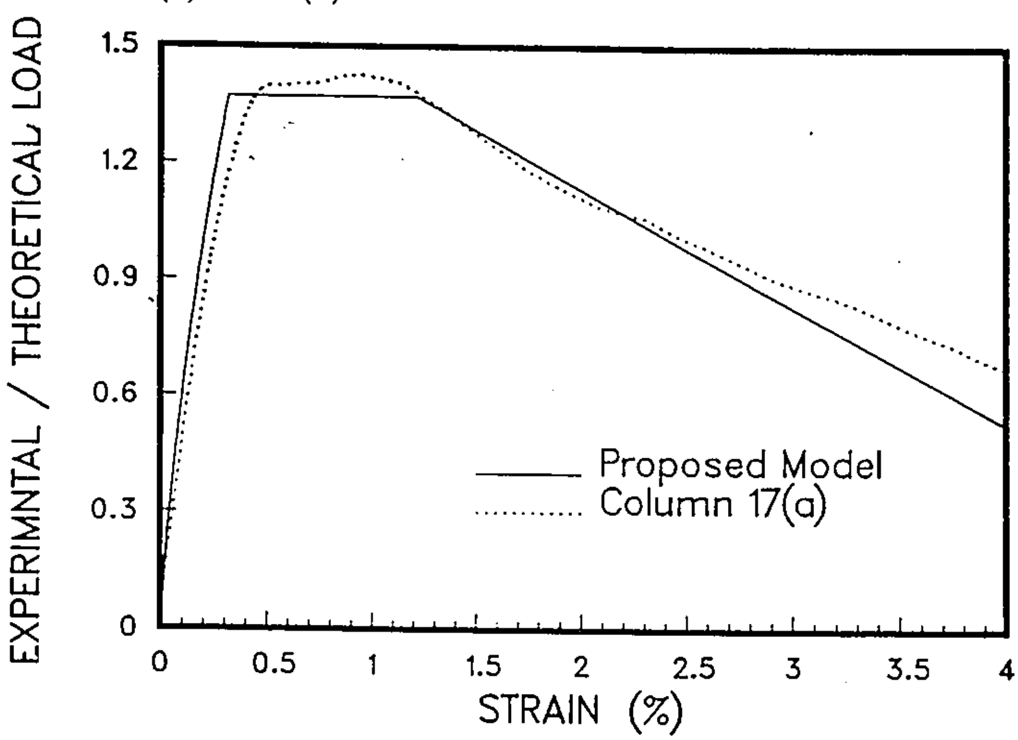

Figure 5.19: Comparison between experimental and analytical behavior for Column 17(a)

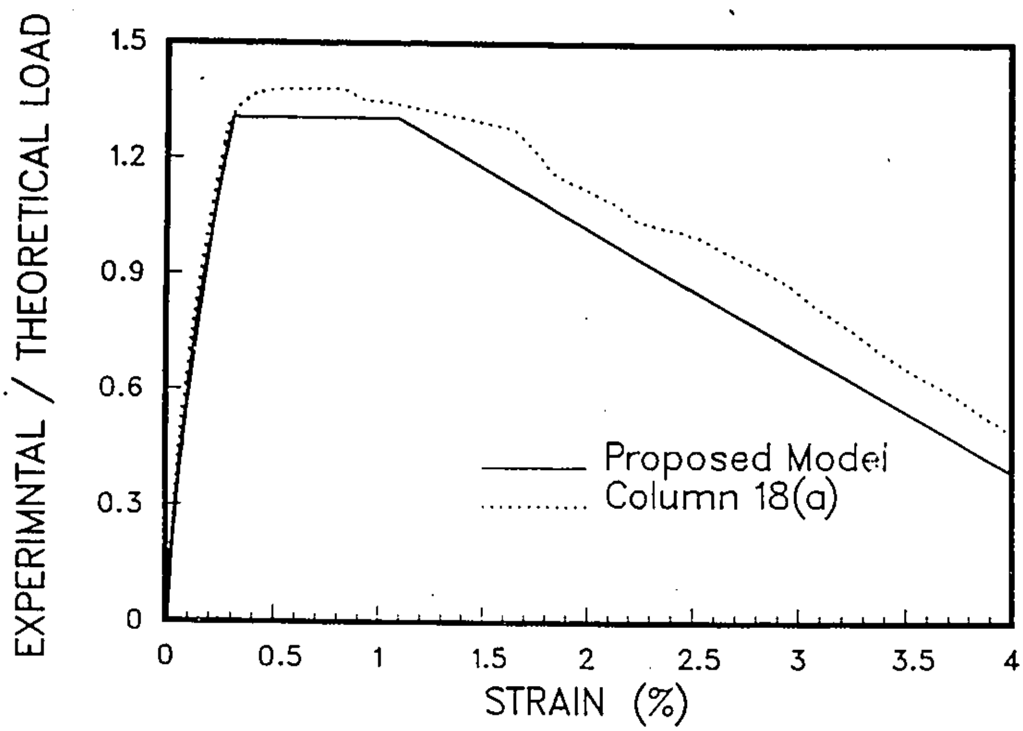

Figure 5.20: Comparison between experimental and analytical behavior for Column 18(a)

Chapter 6

Conclusions

Based on the results of the experimental and analytical investigations carried out in this research program, the following conclusions can be made:

1. The use of WWF for concrete confinement in reinforced concrete columns improves both strength and ductility. The load carrying capacity of concrete alone was observed to increase by up to 40%. These improvements were observed in columns laterally reinforced with ties having 135 degree hooks or 90 degree hooks welded at the ends. The improvement in response obtained by the use of WWF with ties was equivalent to that obtained by using twice as many ties (at one half the spacing) without the WWF.

2. WWF placed between the longitudinal and transverse steel showed less confinement efficiency than those placed inside the longitudinal and lateral reinforcement. The pressure applied by longitudinal bars on WWF limits its usefulness at high axial strain levels, rupturing the WWF.

3. Columns confined with WWF without lateral ties were observed to have brittle behavior regardless of the type of connector used to splice the WWF.

4. For approximately the same area of steel, finer mesh (12.7 X 12.7 mm X 16 gage) showed a better confinement efficiency than a coarser mesh (25.4 x 24.4 mm x 14 gage).

5. The conventional stress – strain relationship of longitudinal bars in the plastic region was found to be unrealistic. Bending of longitudinal bars was observed in the inelastic range prior to the expected buckling between the ties. The stage at which bending takes place seems to depend on the size of longitudinal bars, spacing and stiffness of ties.

6. Columns designed in accordance with the A23.3 - M84 CSA code requirements showed yielding of lateral ties at around the peak load. Hence it is reasonable to assume, for the purpose of modeling the behavior of confined concrete, that yielding of ties occurs at about the peak load.

7. Increasing the amount of lateral reinforcement and reducing tie spacing has significant effect on enhancement of both strength and duc-

tility.

8. Ties with 90 degree hooks showed poor behavior, compared to ties with 135 degree hooks. Opening of ties was observed shortly after reaching the peak load.

9. The behavior of tied columns without WWF, tested in this program, was compared with the predicted behavior by the Sheikh and Uzumeri and the Modified Kent and Park models. Good agreement was found between the experimental and predicted behavior for concrete confined with ties spaced at d/4. However, poor agreement was found for concrete confined with ties spaced at d/2.

10. In contrast to the findings of King [19] in 1946, analytical models for large scale columns were applied to predict the behavior of small scale columns tested in this program. The results did not indicate a significant scale effect.

11. Strength enhancement of confined concrete can be evaluated using the proposed equation. The advantage of this equation, in comparison to the other available equations, is that it is simple to use and also includes the influence of all the relevant parameters involved.

12. The mathematical model developed in this investigation provides a good agreement with the test results.

Appendix A

Experimental Data

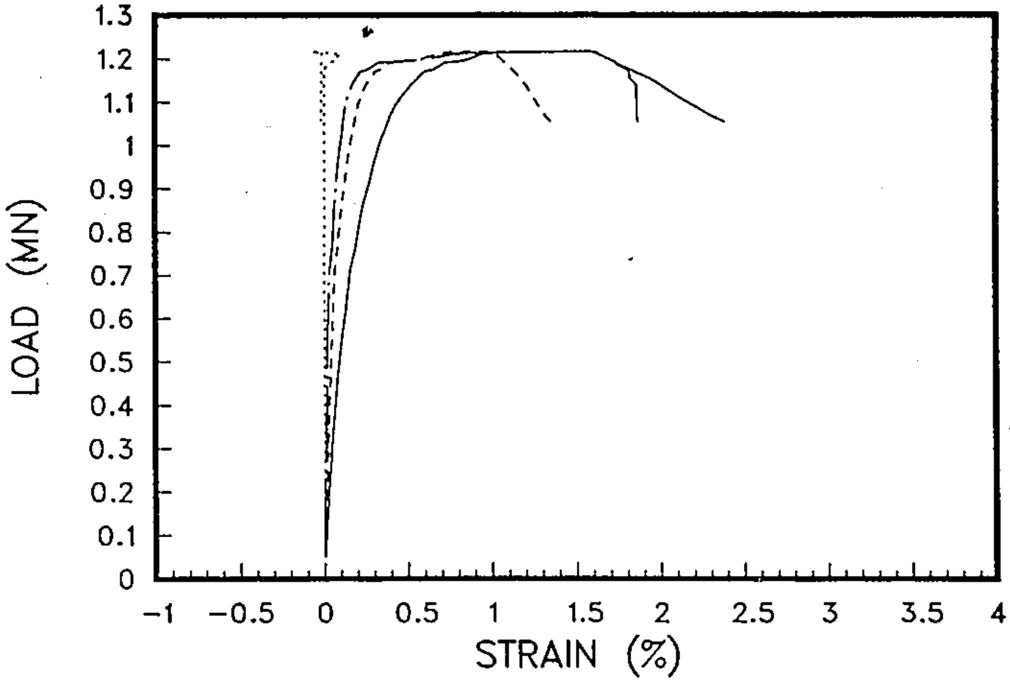

Figure A.1: column 1 (a)

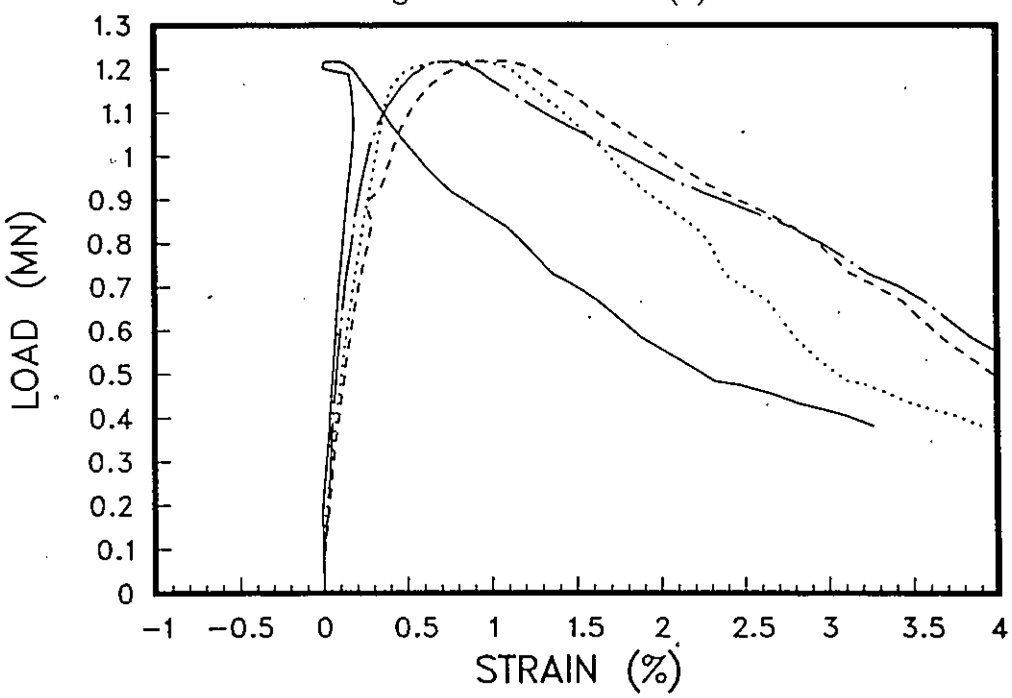

Figure A.2: column 1 (b)

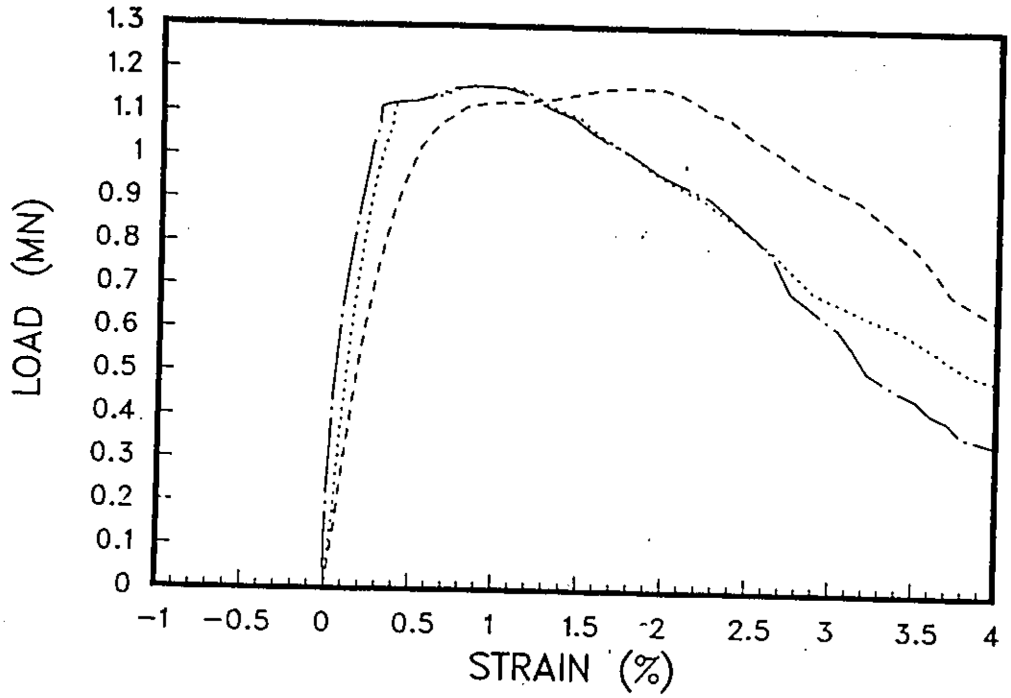

Figure A.3: column 2 (a)

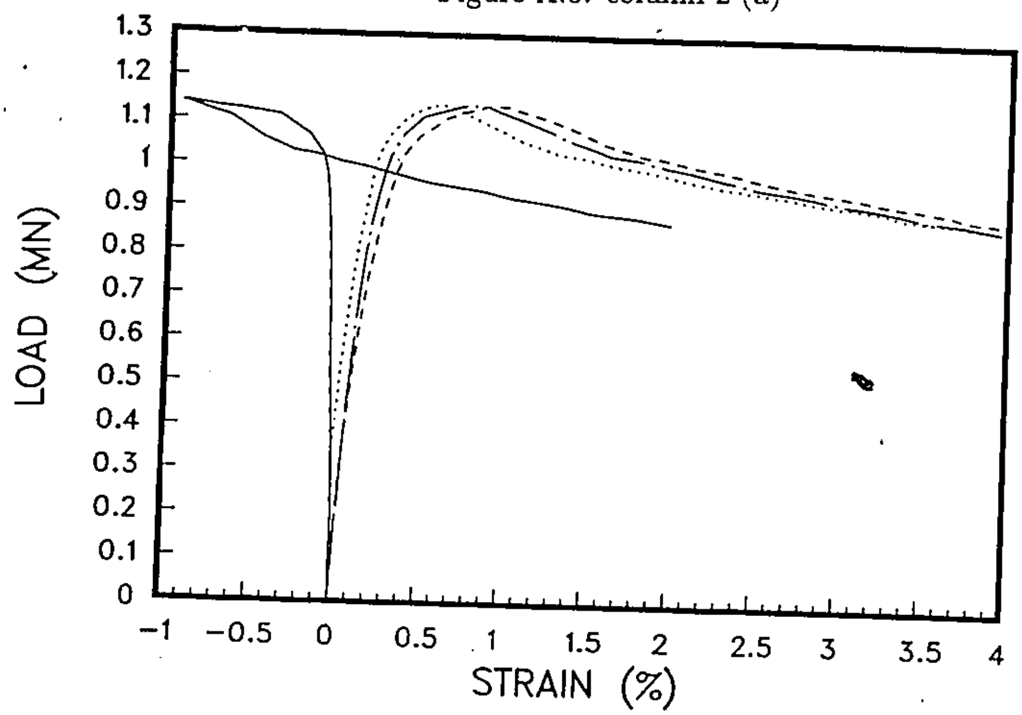

Figure A.4: column 2 (b)

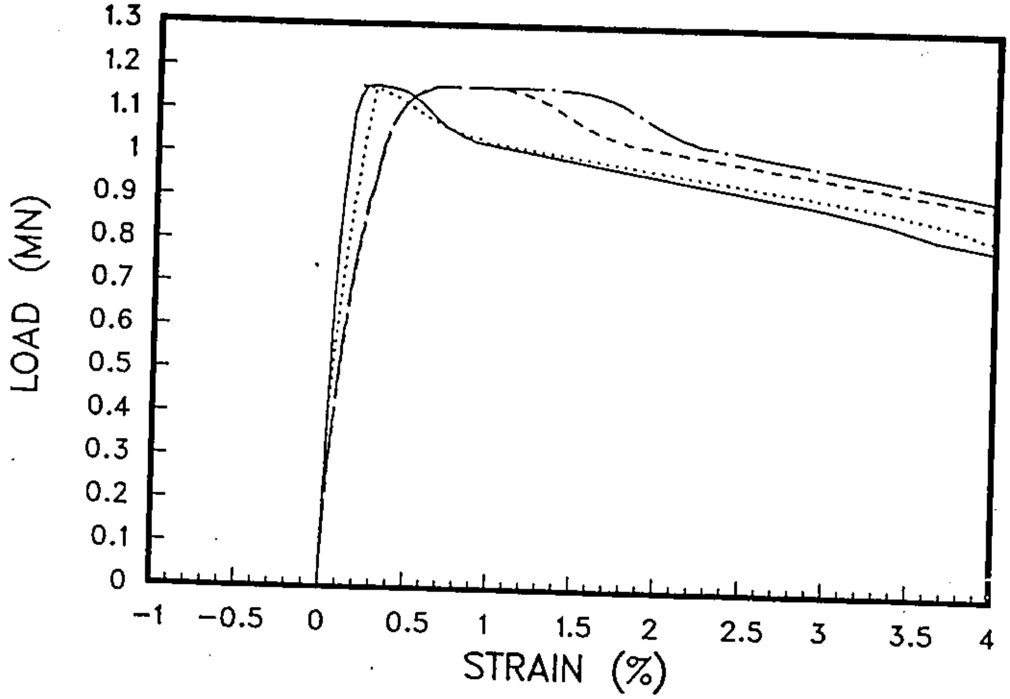

Figure A.5: column 3 (a)

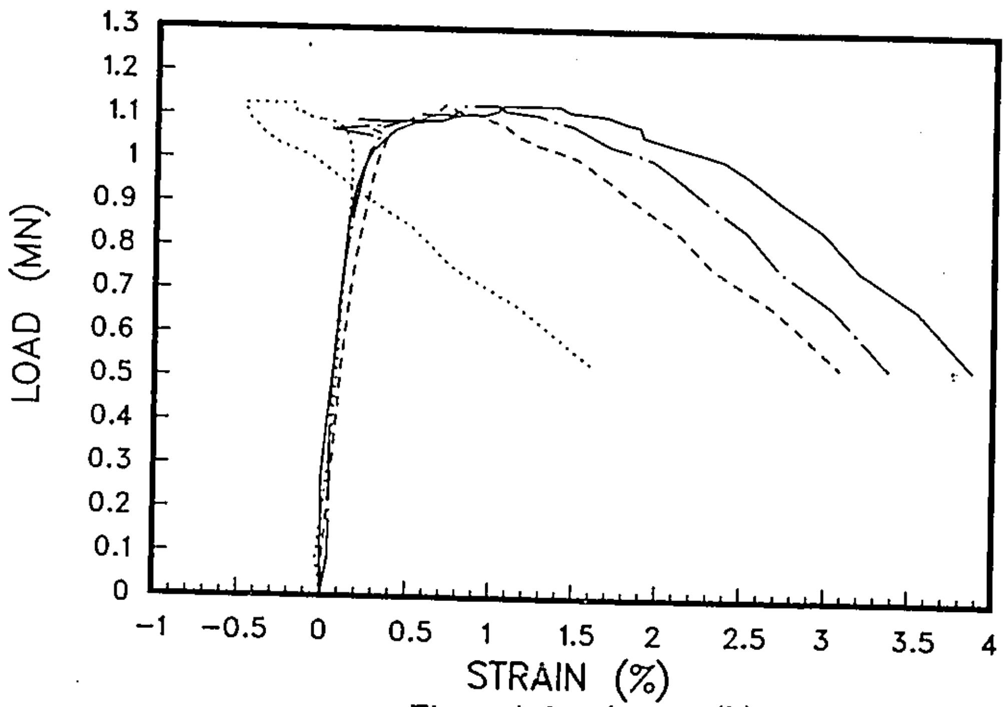

Figure A.6: column 3 (b)

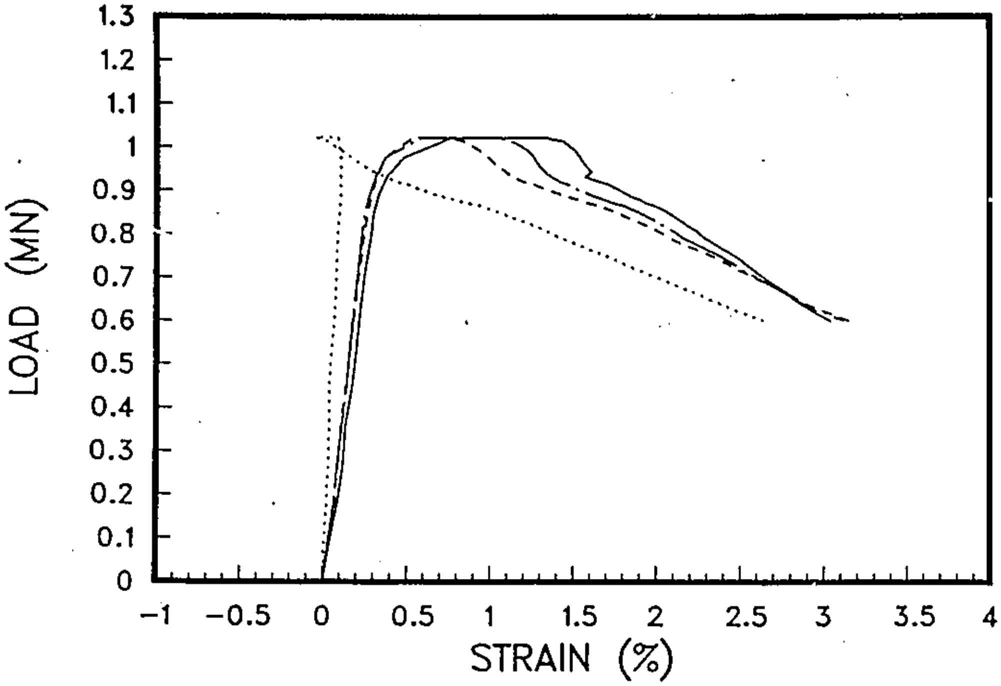

Figure A.7: column 4 (a)

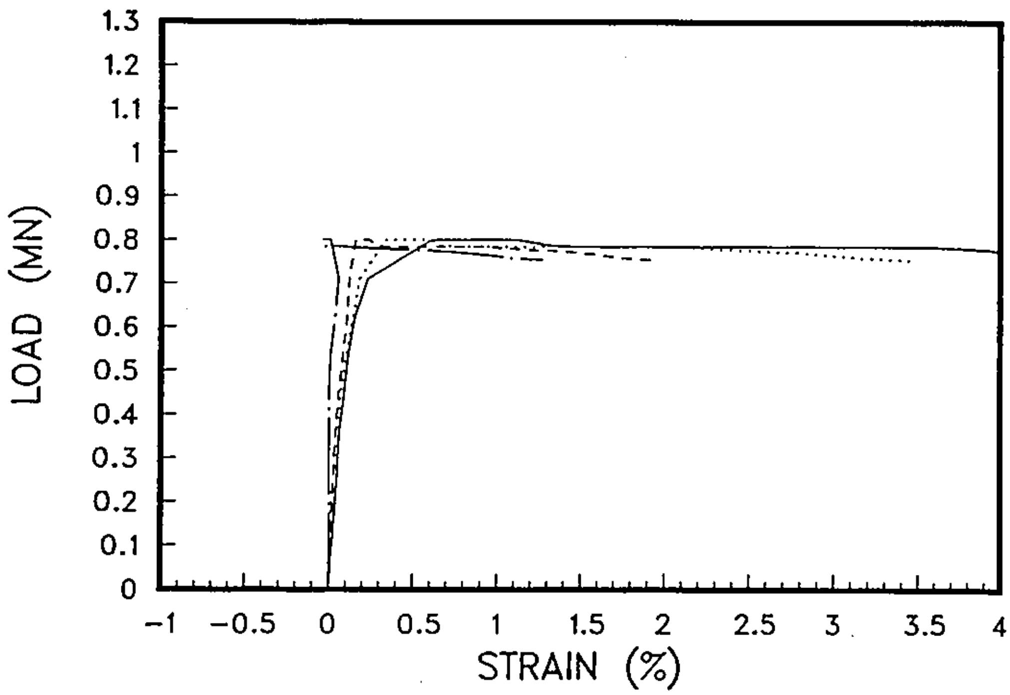

Figure A.8: column 4 (b)

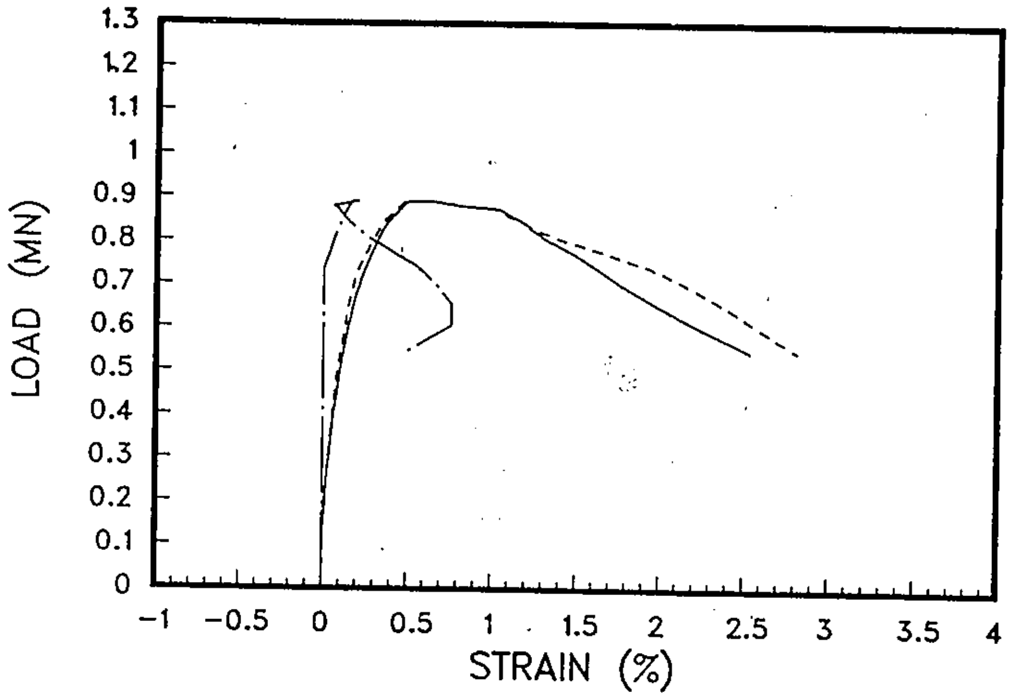

Figure A.9: column 5 (a)

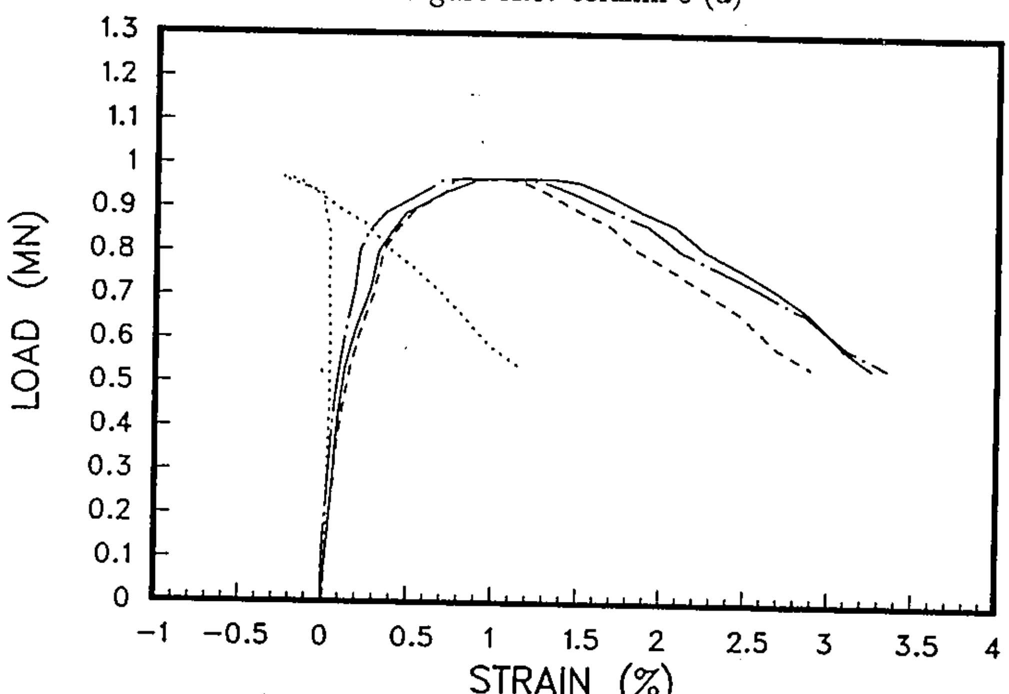

Figure A.10: column 5 (b)

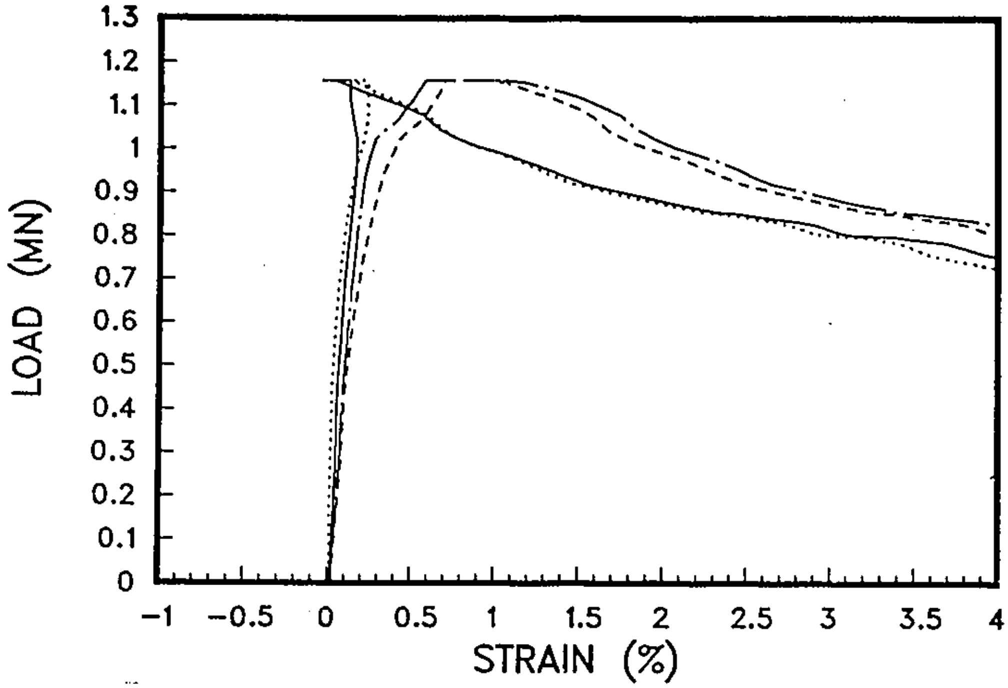

Figure A.11: column 6 (a)

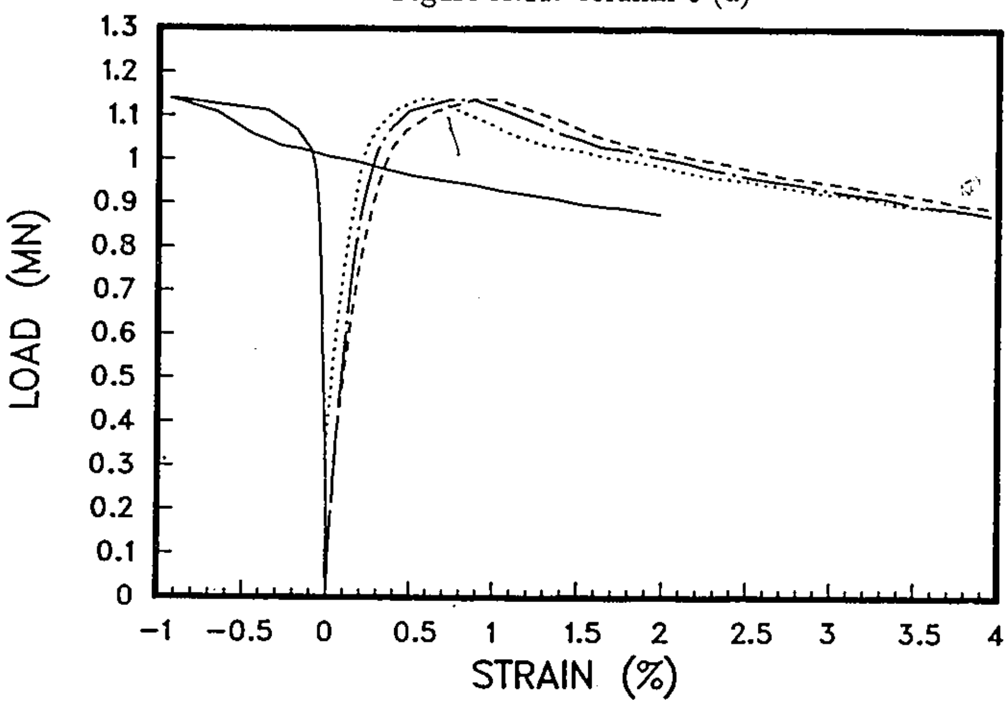

Figure A.12: column 6 (b)

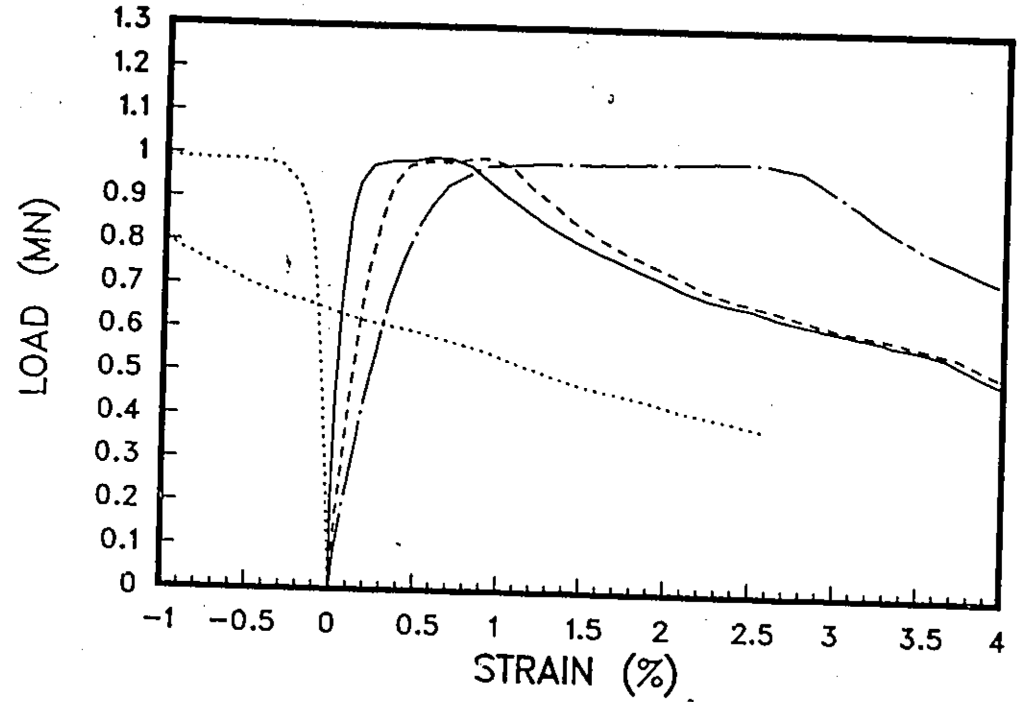

Figure A.13: column 7 (a)

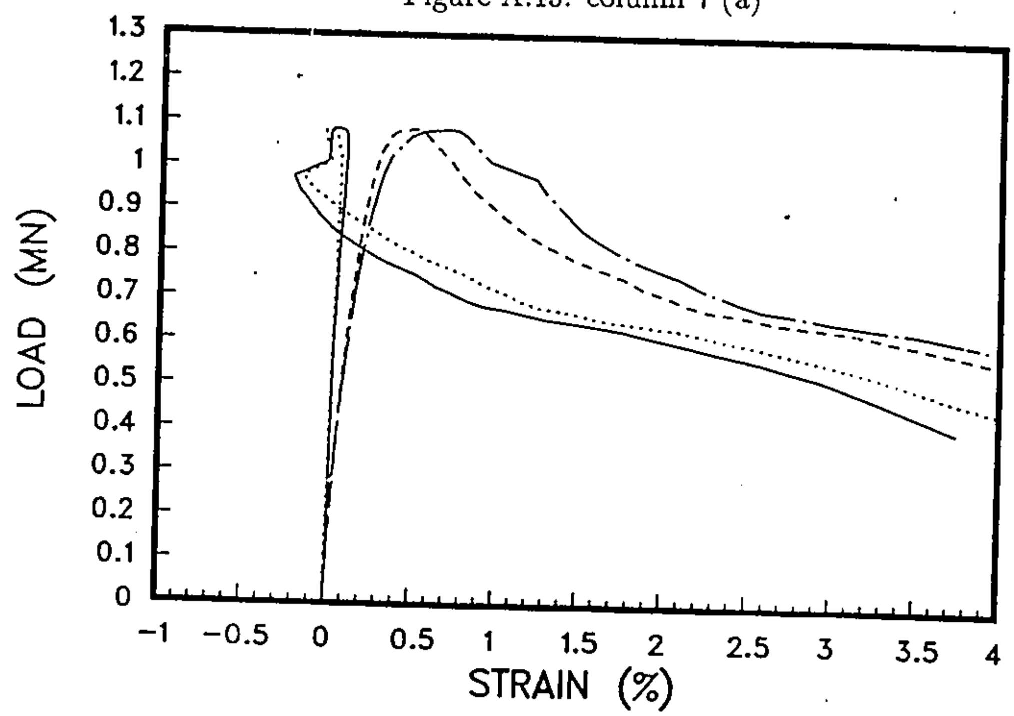

Figure A.14: column 7 (b)

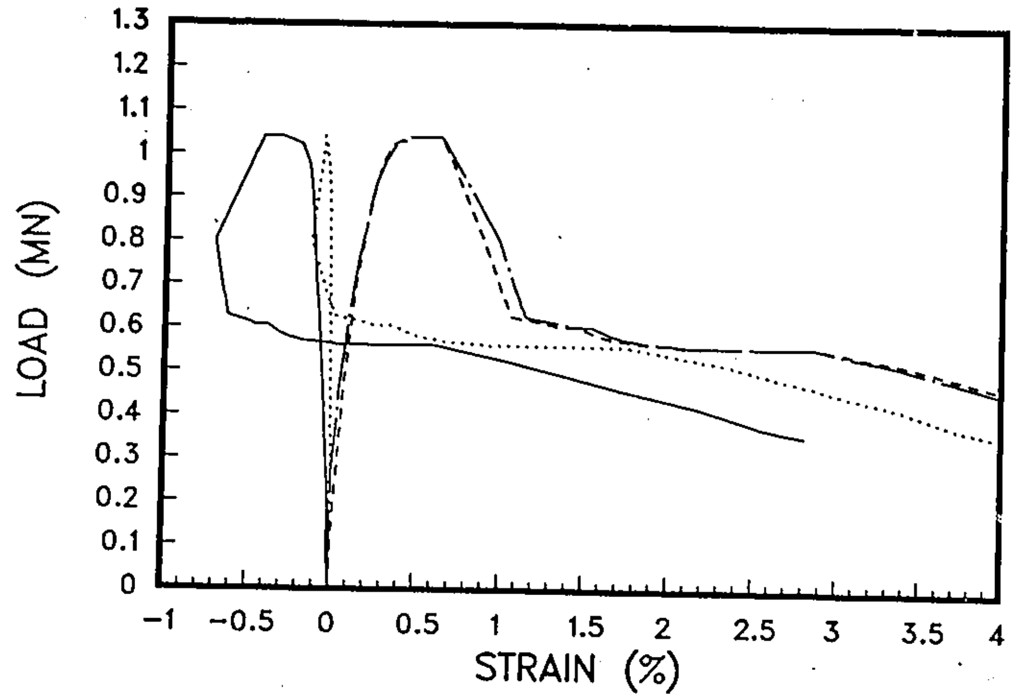

Figure A.15: column 8 (a)

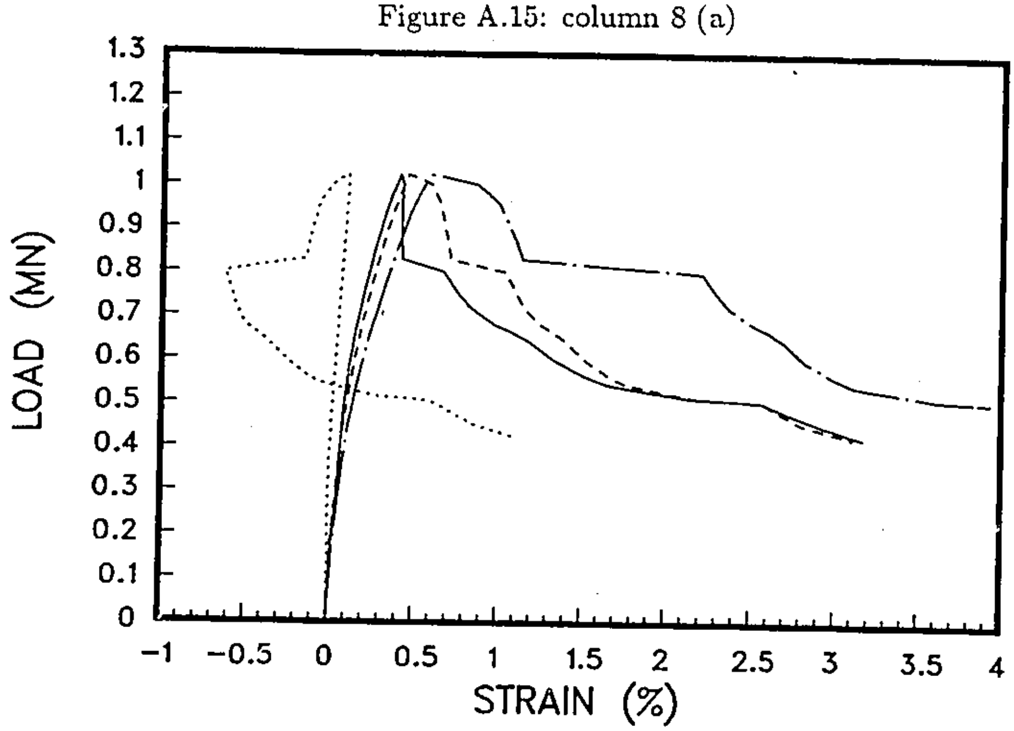

Figure A.16: column 8 (b)

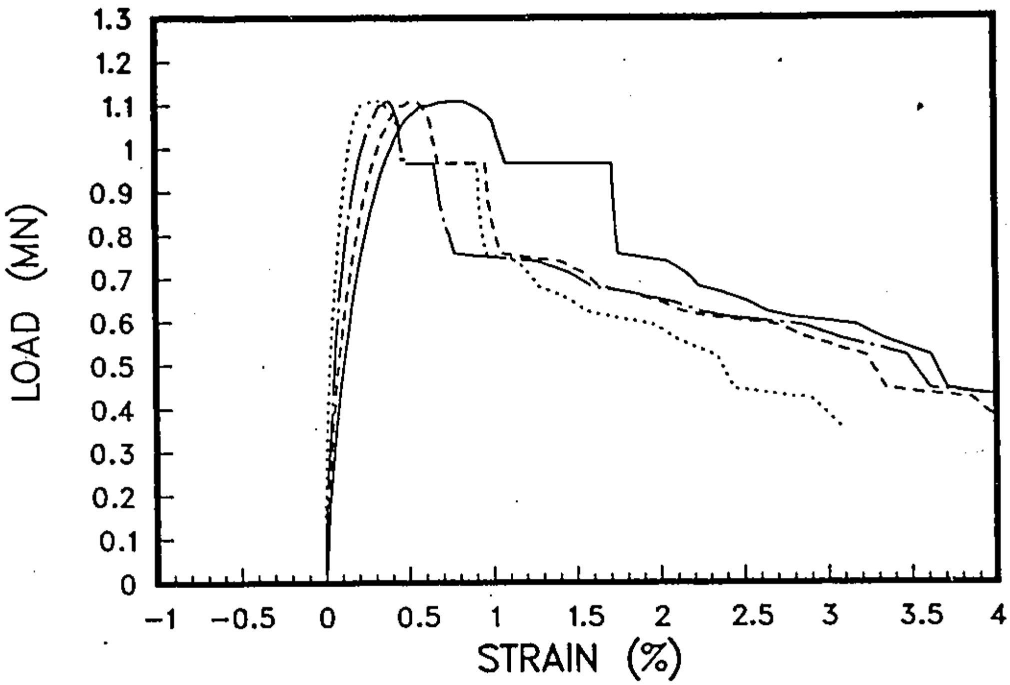

Figure A.17: column 9 (a)

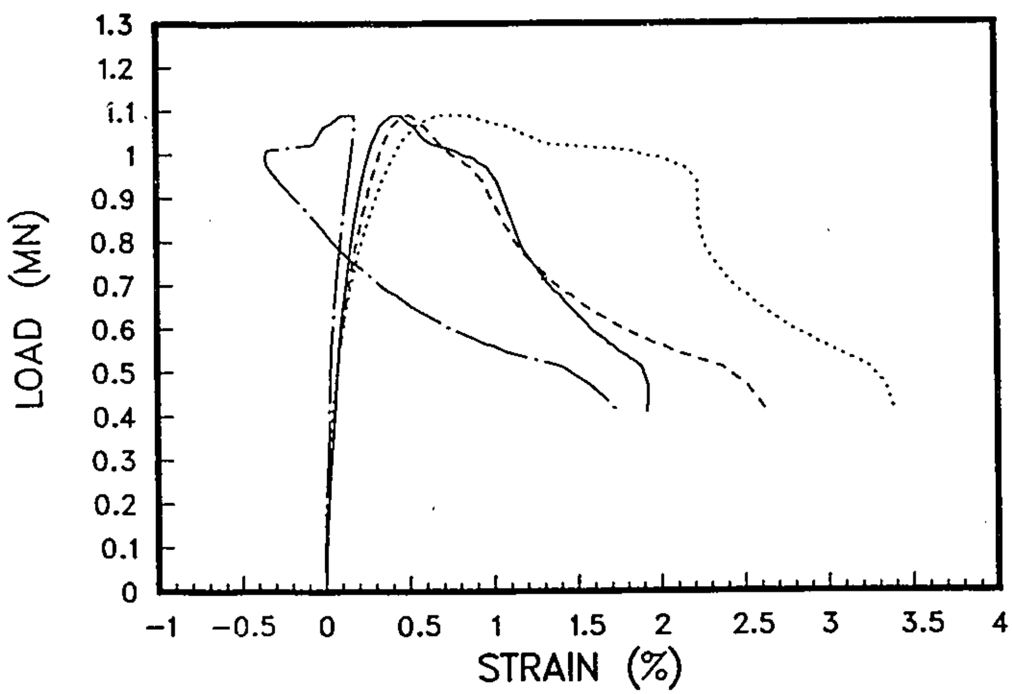

Figure A.18: column 9 (b)

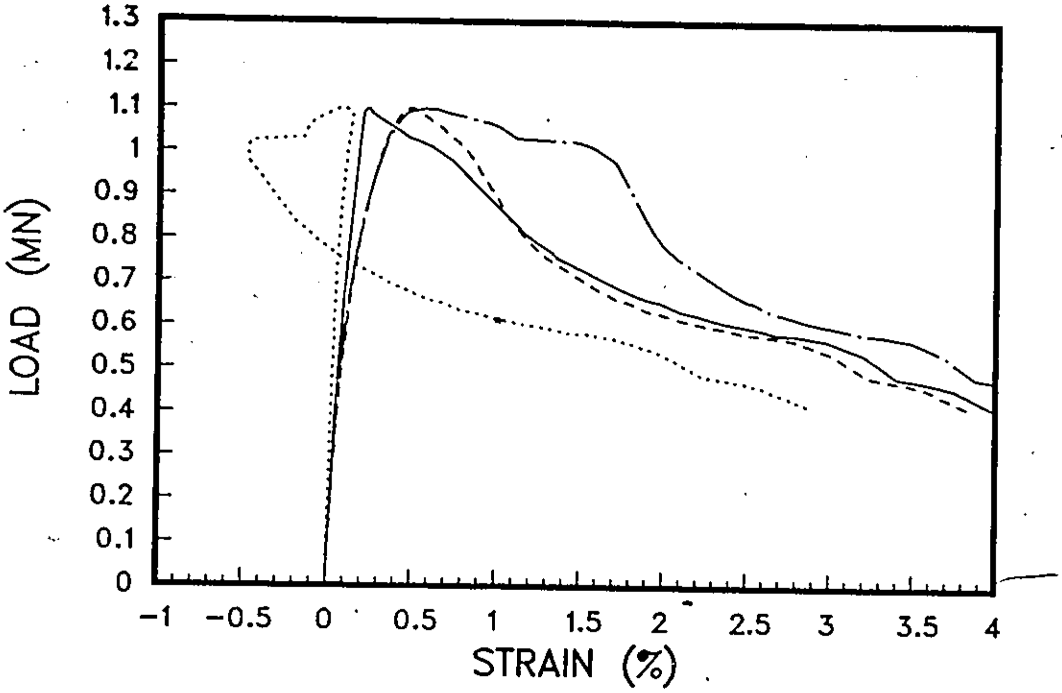

Figure A.19: column 10 (a)

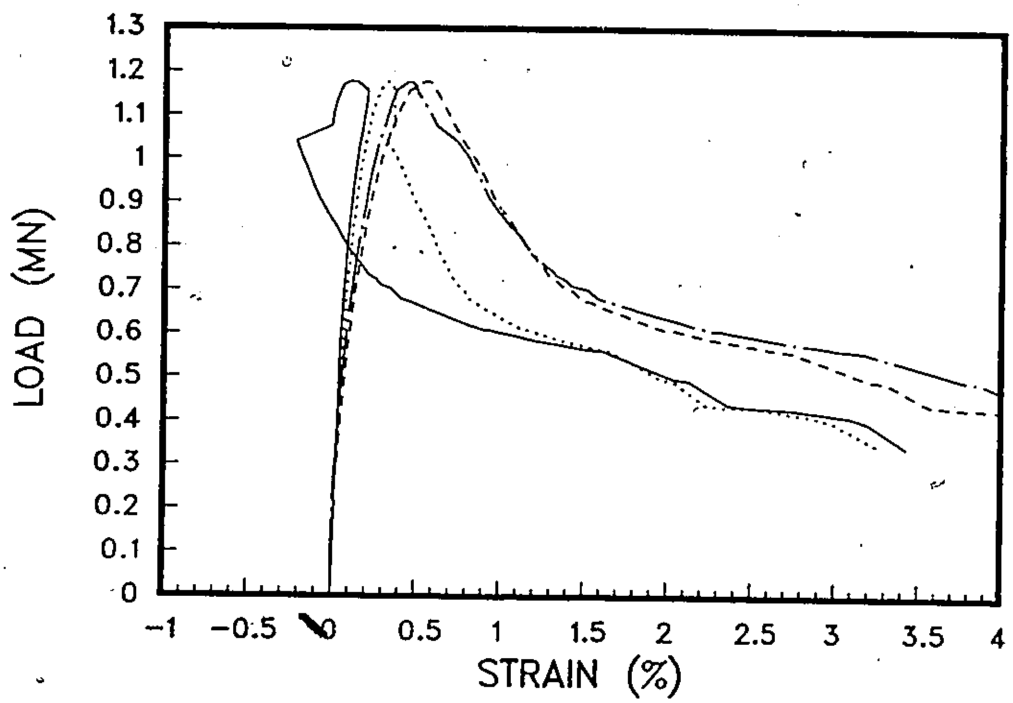

Figure A.20: column 10 (b)

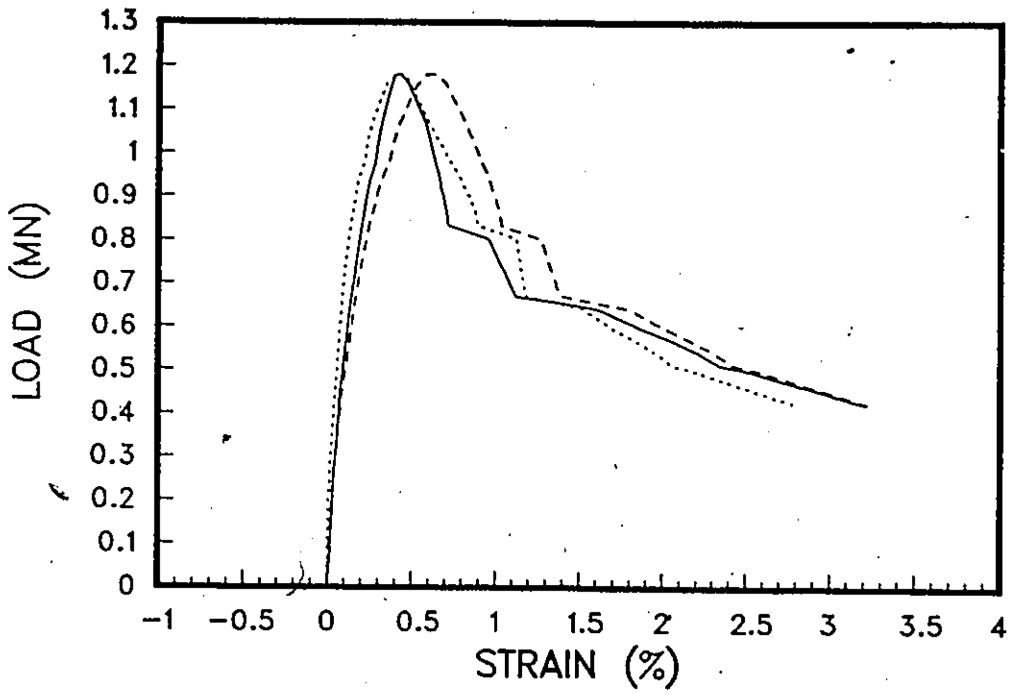

Figure A.21: column 11 (a)

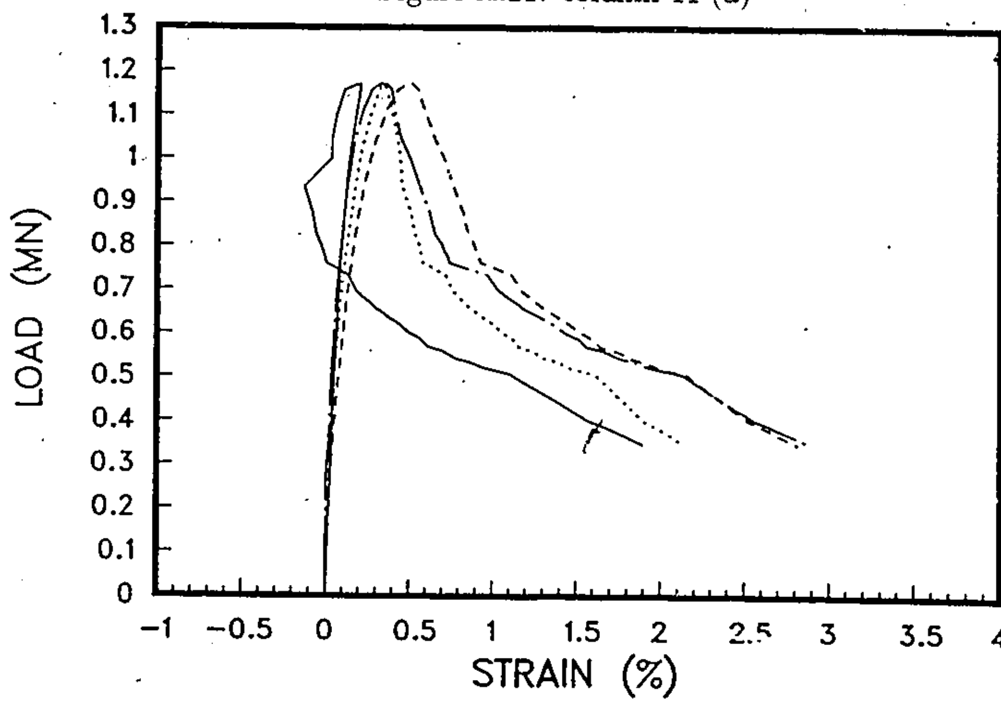

Figure A.22: column 11 (b)

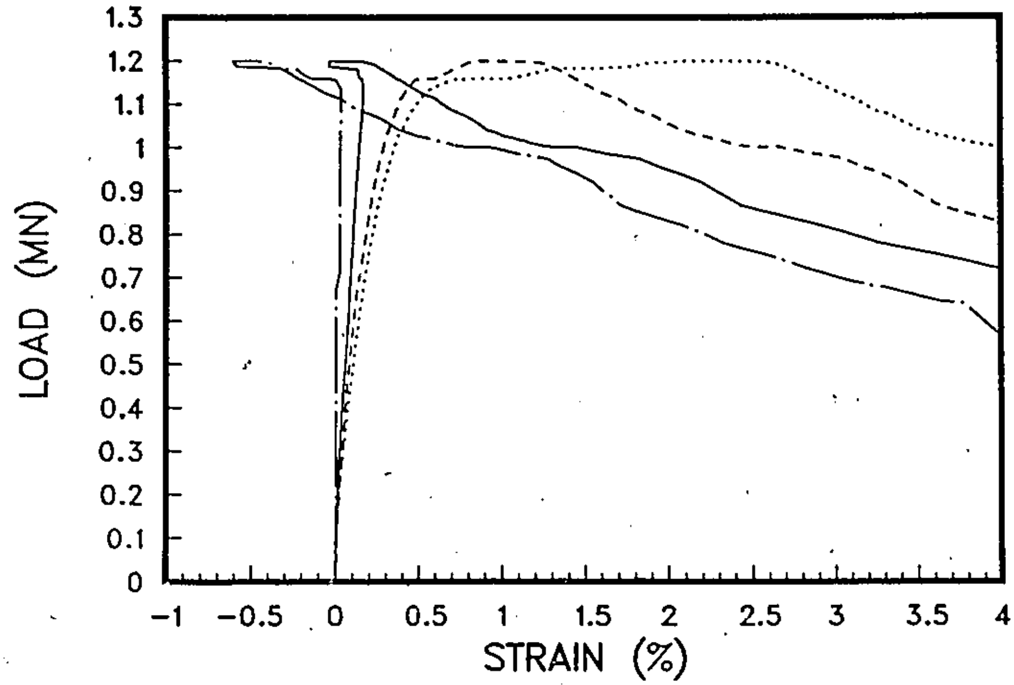

Figure A.23: column 12 (a)

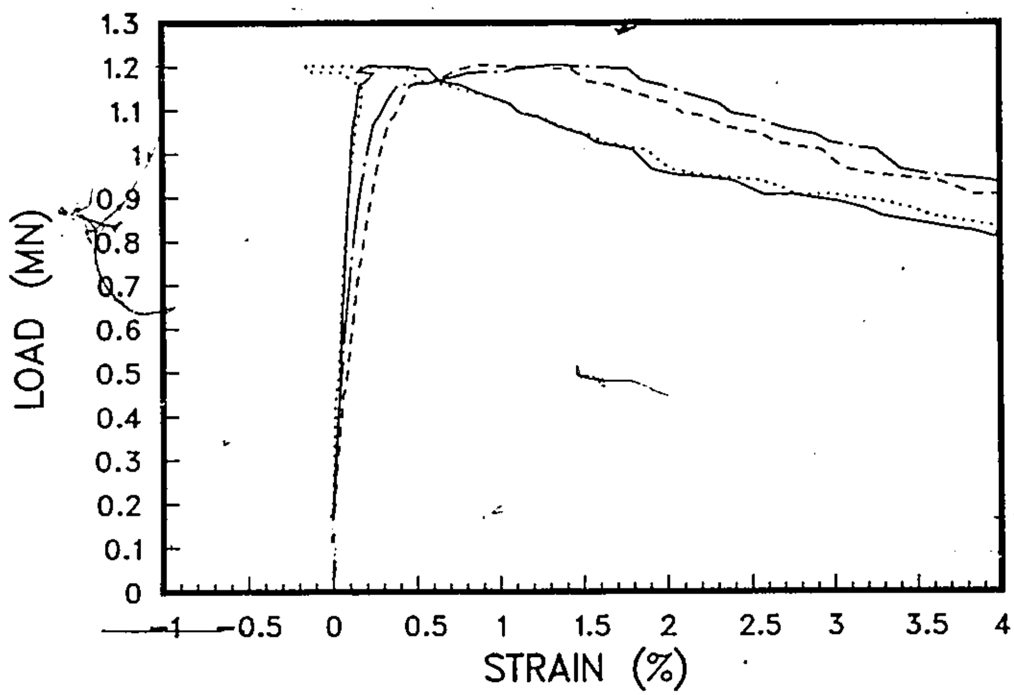

Figure A.24: column 12 (b)

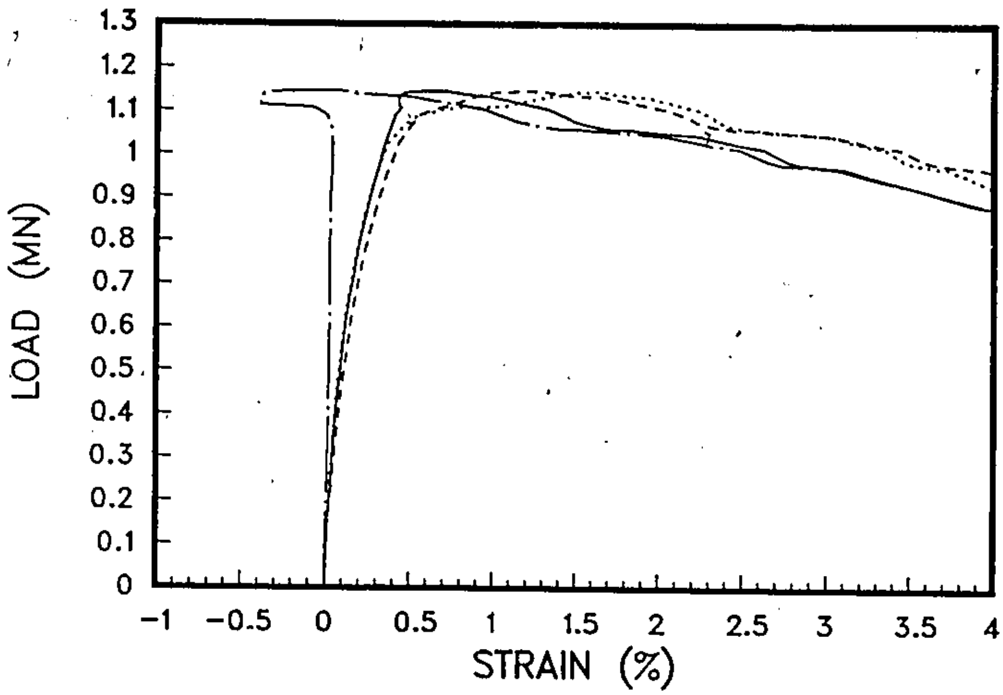

Figure A.25: column 13 (a)

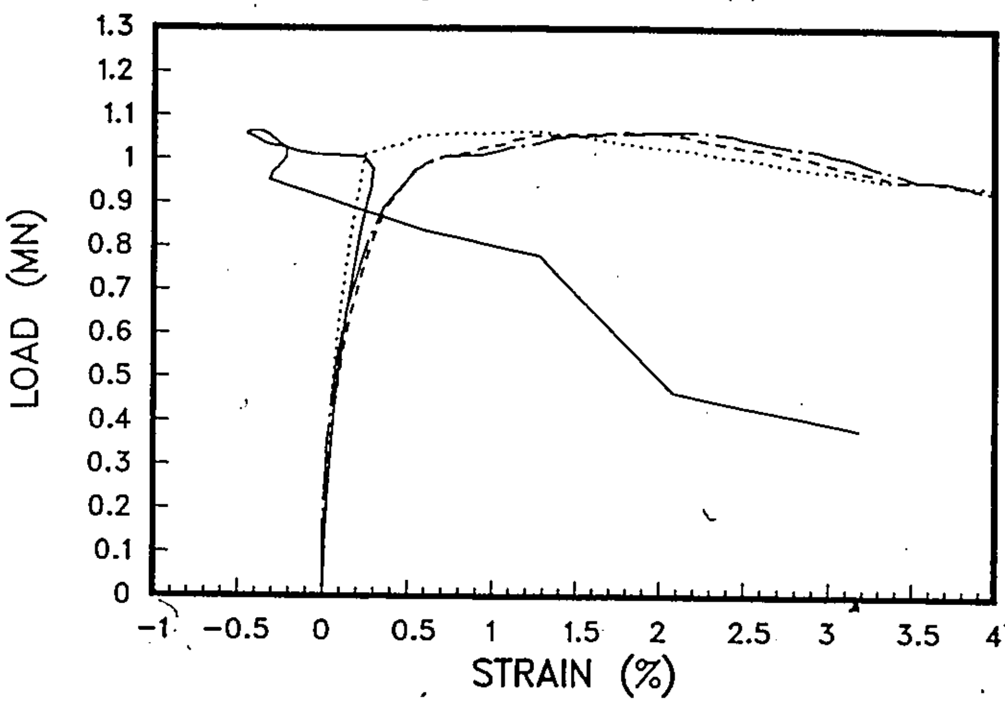

Figure A.26: column 13 (b)

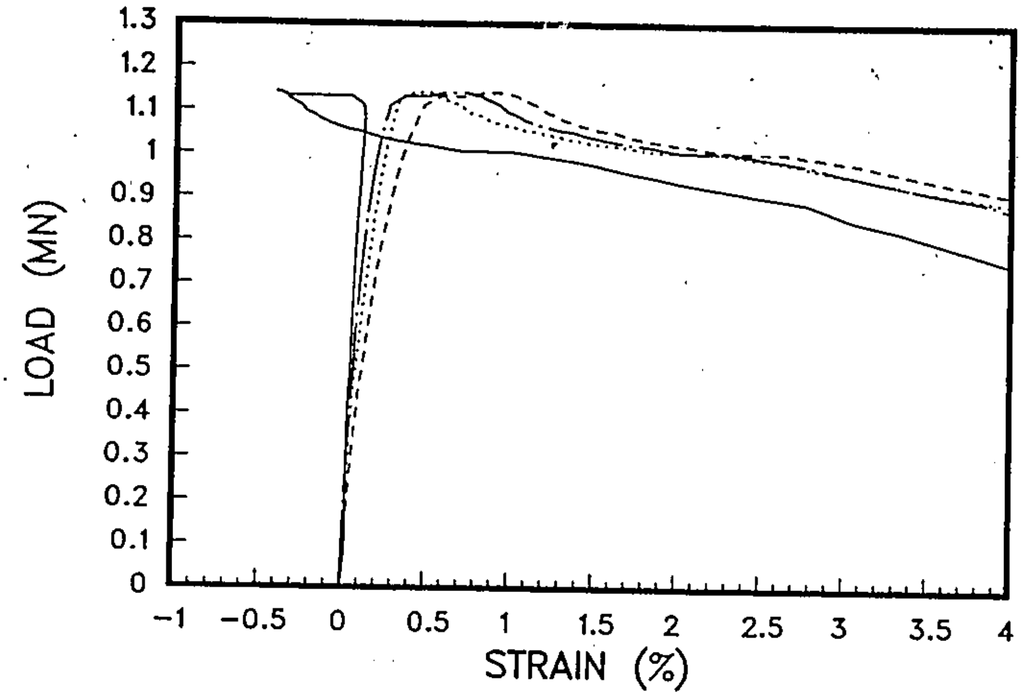

Figure A.27: column 14 (a)

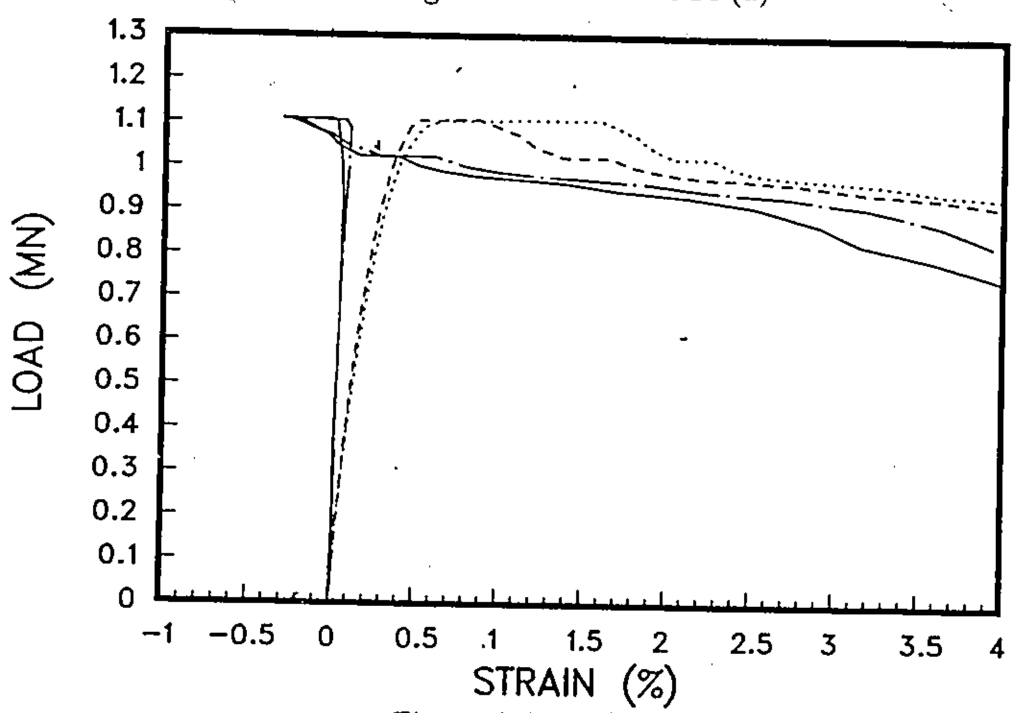

Figure A.28: column 14 (b)

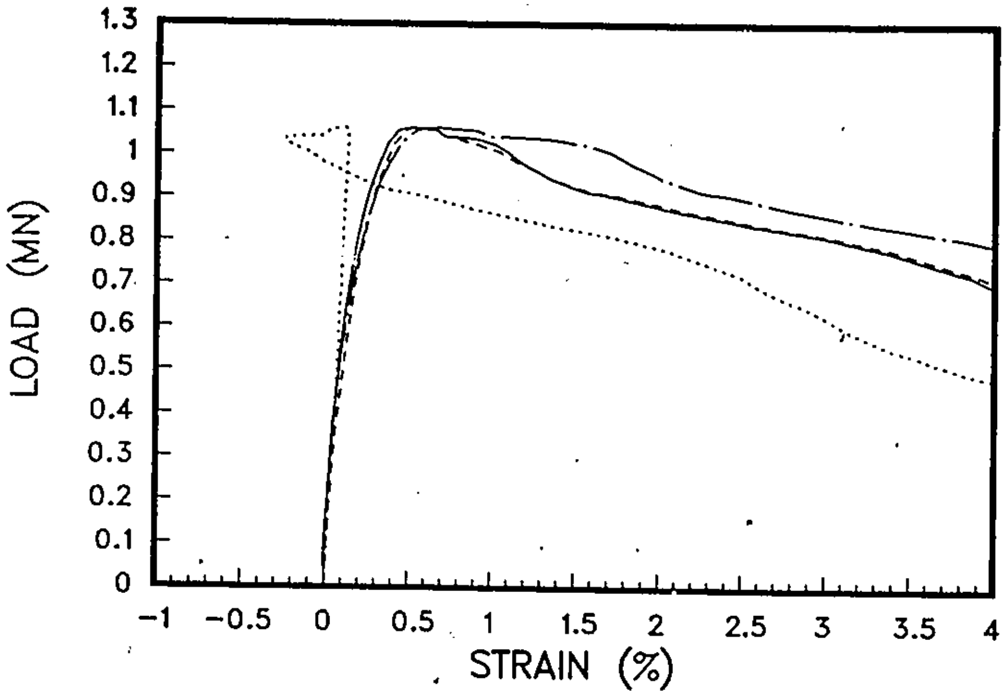

Figure A.29: column 15 (a)

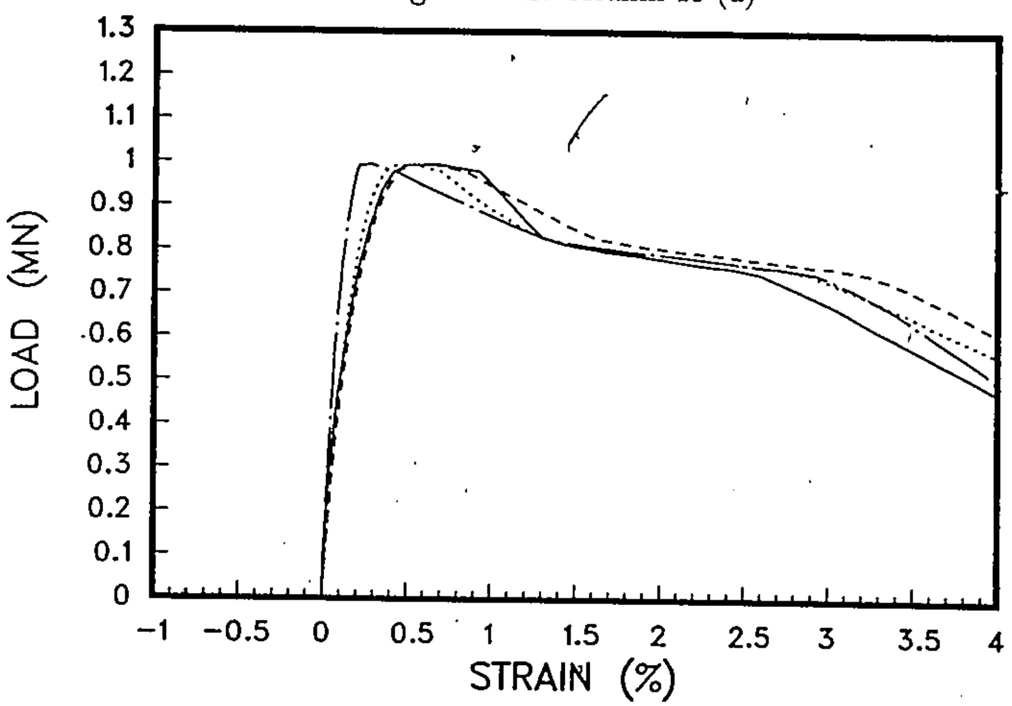

Figure A.30: column 15 (b)

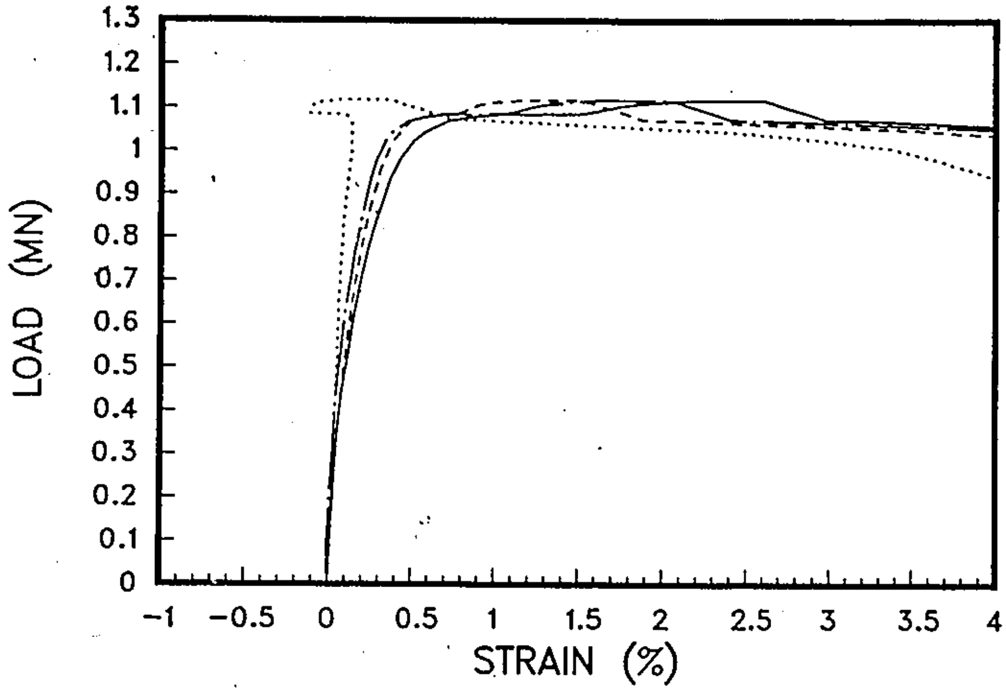

Figure A.31: column 16 (a)

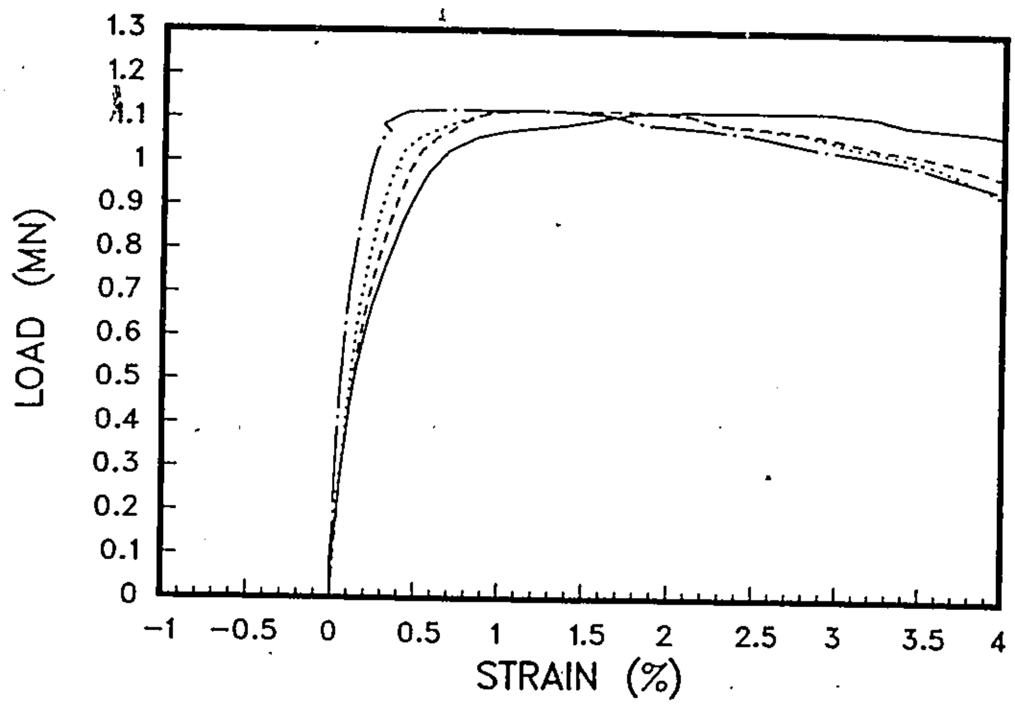

Figure A.32: column 16 (b)

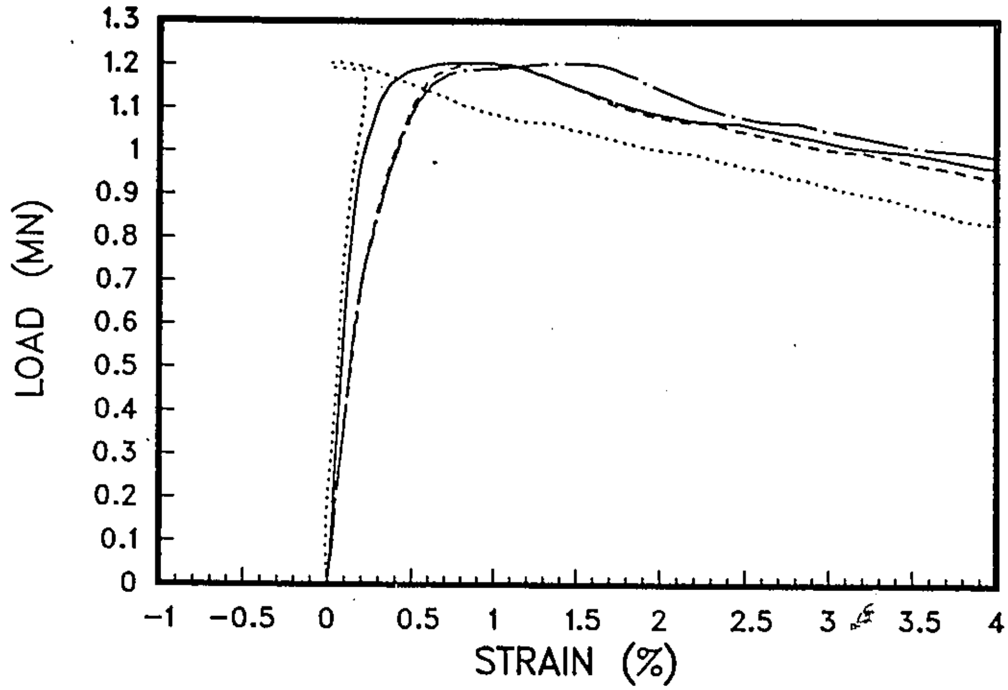

Figure A.33: column 17 (a)

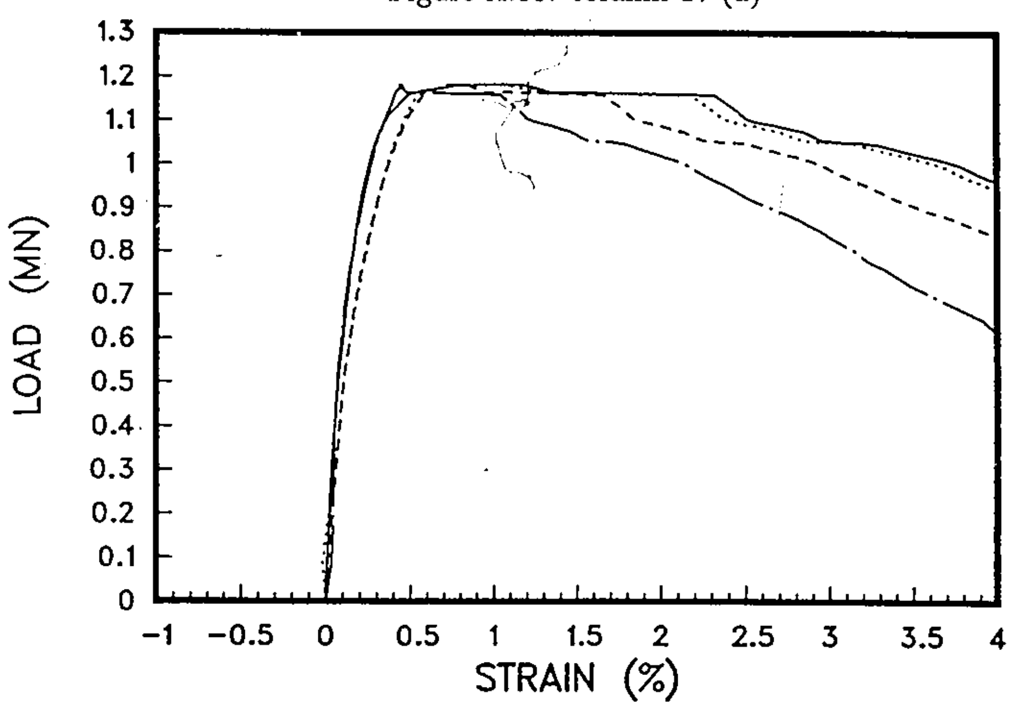

Figure A.34: column 18 (a)

Bibliography

[1] Sheikh, S. A. *Effectiveness of Rectangular Ties as Confinement Steel in Reinforced Concrete Columns.* thesis presented to the University of Toronto, in 1978, in partial fulfillment of the requirements for the degree of Doctor of Philosophy.

[2] Sheikh, S. A., Uzumeri, S. M. *Strength and Ductility of Tied Concrete Columns.* ASCE , vol.106, May 1980, pp. 1079– 1102.

[3] Scott, B. D., Park ,R., Priestley, M. J. N. *Stress - Strain Behavior of Concrete Confined by Overlapping Hoops at High and Low Strain Rates.*, ACI Journal, Jan. - Feb. 1982, pp.13–27 .

[4] Ozcebe, G., Saatcioglu, M. *Confinement of Concrete Columns for Seismic Loading.* ACI Journal vol. 84, No. 4, July–Aug. 1987, pp.308–315.

[5] Fafitis, A., Shah, S.P. *Prediction of Ultimate Behavior of Confined Columns Subjected to Large Deformation* ACI Journal, Vol.82, July –Aug. 1985, pp.423–433.

[6] Sheikh, S. A. *A Comparative Study of Confinement Models* ACI Journal, July–Aug. 1982, pp.296–305.

[7] Sheikh, S. A. *Analytical Model for Concrete Confinement in Tied Columns* ASCE, Vol.108, Dec. 1982, pp. 2703–2723.

[8] Park, R., Nigel, M.J., Gill, W. D. *Ductility of Square Confined Concrete Columns* ASCE, Vol. 108, 1982, pp. 929–951.

[9] Kent, D.C., Park, R. *Flexural Members With Confined Concrete.* ASCE, Vol.97, 1971, pp.1969–1990.

[10] Sheikh, S.A., Yen, C.C. *Flextural Behavior of Confined Concrete Columns* ACI Journal May–June 1986, No.3, Vol.83, pp.389–404.

[11] Park, R., Paulay, T. *Reinforced Concrete Structures.* John Wiley and Sons, Newyourk, Chichester, Brisbane, Toronto, Singapore, 1975.

[12] Sheikh, S.A., Yen C.C. *Flextural Behavior of Confined Concrete Columns Subjected to High Axial Load* Proceedings of Fifth Canadian Conference on Earthquake Engineering. July 1987.

[13] Chan, W.L. *The Ultimate Strength and Deformations of Plastic Hinges in Reinforced Concrete Frameworks* Magazine of Concrete Research, Vol.7, No.21, November 1955, pp. 121-132.

[14] Soliman, M.T.M., Yu, C.W. *The Flexural Stress-Strain Relationship of Concrete Confined by Rectangular Transverse Reinforcement* Magazine of Concrete Research, Vol.19, No.61, Dec.1967, pp.223-238.

[15] Sargin, M., Ghosh, S.K., Handa, V.K. *Effects of Lateral Reinforcement Upon the Strength and Deformation Properties of Concrete* Magazine of Concrete Research, Vol.23, 1971, pp. 99-110.

[16] Vallenas, J., Bertero, V.V., Popov, E.P. *Concrete Confined by Rectangular Hoops and Subjected to Axial Loads* Report No. UCB/EERC-77/13, Earthquake Engineering Research Center, College of Engineering, University of California, Berkeley, Aug. 1977, 114 pp.

[17] Karsan, I.D., Jirsa, J.O. *Behavior of Concrete Under compressive Loadings* Journal of Structural Division, ASCE, Vol.95, St12, Dec.1969, pp. 2543-2563

[18] Canadian Standards Association *Design of Concrete Structures for Buildings* National Standards of Canada, CAN3 - A23.3 - M84.

[19] King, J.W.H. *Further Notes on Reinforced Concrete Columns* The Structural Engineer, Vol.24, Nov. 1946, pp. 609-616